



KIT SCIENTIFIC REPORTS 7619

# Annual Report 2011

Institute for Pulsed Power and Microwave Technology  
Institut für Hochleistungsimpuls- und Mikrowellentechnik

John Jelonnek (ed.)



John Jelonnek (ed.)

**Annual Report 2011**

Institute for Pulsed Power and Microwave Technology  
Institut für Hochleistungsimpuls- und Mikrowellentechnik

Karlsruhe Institute of Technology  
**KIT SCIENTIFIC REPORTS 7619**

# Annual Report 2011

Institute for Pulsed Power and Microwave Technology  
Institut für Hochleistungsimpuls- und Mikrowellentechnik

edited by  
John Jelonnek

Report-Nr. KIT-SR 7619

### Impressum

Karlsruher Institut für Technologie (KIT)  
KIT Scientific Publishing  
Straße am Forum 2  
D-76131 Karlsruhe  
www.ksp.kit.edu

KIT – Universität des Landes Baden-Württemberg und  
nationales Forschungszentrum in der Helmholtz-Gemeinschaft



Diese Veröffentlichung ist im Internet unter folgender Creative Commons-Lizenz  
publiziert: <http://creativecommons.org/licenses/by-nc-nd/3.0/de/>

KIT Scientific Publishing 2012  
Print on Demand

ISSN 1869-9669

# Institute for Pulsed Power and Microwave Technology

## (Institut für Hochleistungsimpuls- und Mikrowellentechnik (IHM))

Director: Prof. Dr.-Ing. John Jelonnek

The Institute for Pulsed Power and Microwave Technology (IHM) is doing research in the areas of pulsed power technologies for material processing and biological applications as well as microwave technologies for plasma heating and material processing. It is doing research, development, academic education and, in collaboration with the KIT Division IMA and industrial partners, the technology transfer. Projects have been conducted within six HGF Programs: Renewable Energies (EE), FUSION, NUKLEAR, NANOMIKRO, Efficient Energy Conversion and Use (REUN) and Technology-Innovation and Society (TIG).

R&D work has been done in the following topics: fundamental theoretical and experimental research on the generation of intense electron beams, strong electromagnetic fields and their interaction with plants, materials and plasmas; application of these methods in the areas of generation of energy through controlled thermonuclear fusion in magnetically confined plasmas, in materials processing and in energy technology.

Research in both divisions of the IHM require the application of modern electron beam optics, high voltage technology and high voltage measurement techniques.

A short description of the R&D program of the IHM is as follows:

### **Pulsed Power Division:**

(Head: Dr. Georg Müller)

In environmental- and bio-technology the research and development is devoted to pulsed power technology with repetition rates up to 20 Hz, power in the Giga-Watt range and electric field strengths of  $10^5$ - $10^7$  V/m. The research is concerned with short pulse ( $\mu$ s) - and with ultra-short pulse (ns) treatment of biological cells (electroporation). The focus is related to large-scale applications, treatment of large volumes, to the realization of a high component life time and to the overall process integration. Main directions of work in this field are the electroporation of biological cells for extraction of cell contents (KEA process), the dewatering and drying of green biomass, the treatment of micro algae for further energetic use and sustainable reduction of bacteria in contaminated effluents. Another key research topic is related to the surface modification and corrosion protection of metals and alloys using high-energy, large-area pulsed electron beams (GESA process). The research is focused on electron beam physics, the interaction of electron beams with material surfaces and the corresponding material specific characterization investigations. The goal is to develop a corrosion barrier for improved compatibility of structural nuclear reactor materials in contact with heavy liquid metal coolants (Pb or PbBi) (Programs: EE, NUKLEAR, TIG).

- The commissioning of an annular gap photobioreactor has been completed. Due to media optimization an algae cell density of at least 5 g/l (dry mass) has been reproduced in monthly runs. The cell density and lipid status were monitored in time using photometric and fluorescent optical methods. It was shown that the maximum lipid content does not coincide with the highest cell density. Therefore, the development of a proper lipid diagnostic is a key issue for the energetic use of micro algae (Programs: EE, TIG).
- To measure the effectiveness of electroporation assisted extraction from micro algae fast photometric and

fluorescence optical tests were established. For quantitative measurement of intracellular lipids, the Nile-Red staining of the lipids and the coupled diagnostics was improved. Extraction results from initiated studies show that a combined process of pulse treatment, drying and ethanol as a solvent the lipid yield can be increased by a factor of 2-3. The protein content in the extracellular medium can also be doubled after electric pulse treatment (Program: EE).

- Basic studies on the influence of intracellular processes in plant cells using ultra-short (ns) pulsed electric fields (PEF) were performed. Previous results on electroporation assisted growth stimulation in fungi spawn have been confirmed by further experiments. Moreover, it was obtained that nsPEF-treatment also improves the development of rhizomorphic mycelium, which is responsible for the formation of fruiting bodies. First results indicate an increase of mushroom yield by a factor of 2 compared to the control (Program: EE, KIT-Shared Research Group).
- An effective long-term protection against corrosion in Pb and PbBi-cooled systems was confirmed at high temperatures (550 to 650 °C) by alloying aluminum into the steel surfaces or re-melting of FeCrAlY coatings by the GESA process. However, for selective formation of pure  $Al_2O_3$  at low temperatures of 400 to 500 °C, the Al and/or Cr content must be increased. At a concentration of 15 wt% Cr and 11 wt% Al, formation of thin alumina layers can be guaranteed over the entire temperature range (400-650 °C) (Program NUKLEAR).

### **High Power Microwave Division:**

(Head: Dr. Gerd Gantenbein)

Activities on high-power microwave technology are related to electron cyclotron resonance heating and current drive (ECRH&CD) of magnetically confined nuclear fusion plasmas and application of microwaves to materials.

- Collaboration in project PMW for planning, construction and testing of the 10 MW CW, 140 GHz electron cyclotron resonance heating (ECRH) system for the stellarator W7-X at IPP Greifswald. In particular, a 1 MW CW, 140 GHz gyrotron has been developed in cooperation with EPFL-CRPP Lausanne and Thales Electron Devices (TED), Paris. The first series tube delivered world record parameters in long-pulse operation with 0.92 MW at 30 min pulse lengths, an efficiency of nearly 45% and a mode purity of 97.5%. In 2010, series tube SN4R reached 1.02 MW. In 2011, FAT for SN6 has been nearly finalized, finalization date for 10 MW system is estimated for 2014. Additionally to the gyrotrons, the quasi-optical transmission system as well as the high-voltage modulator for the gyrotron has been developed in cooperation with IPF, University of Stuttgart. With the development of major components for the ECRH system KIT makes a significant contribution to W7-X (HGF program FUSION).
- Collaboration in EGYC consortium for development and testing of total 8 MW out of 24 MW CW ECRH system for ITER, Cadarache. In particular, 2 MW CW, 170 GHz gyrotrons with coaxial type cavity are under development. The project is coordinated by Fusion for Energy (F4E) and is

done within frame of HGF program FUSION. Institutional partners are CNR, Italy; EPFL-CRPP, Switzerland and HELLAS, Greek. Industrial partner is Thales Electron Devices (TED), Vélizy, France. In 2010 a pre-prototype tube of IHM for the European 2 MW, 170 GHz ITER gyrotron achieved a record output power of 2.2 MW at 30% efficiency (without depressed collector for energy recovery). In 2011, the industrial prototype has been manufactured and tested in collaboration with CRPP and TED at European test facility for ITER gyrotrons at Lausanne. A very promising output power of 2.2 MW at 45 % efficiency (w/o further optimization) has been achieved. Good beam quality has been verified. Unfortunately, tests have led to fatal defect of the tube at end of 2011. With regard to tight time schedule for ITER, 1 MW fall-back solution is under discussion again.

- Future fusion experiments will require frequency step-tunable gyrotrons mandatorily. A step-tunable 1 MW gyrotron (105-143 GHz), including edge-cooled microwave vacuum window made of synthetic diamond for future ECRH systems of large-scale tokamak experiments is under development and test therefore. In 2011, tests have been performed to examine the multi-frequency performance (HGF program FUSION).
- Experimental and theoretical studies on the plasma-wall interaction at the first wall and divertor of tokamak fusion reactors (HGF program FUSION) have been done.
- Sintering of advanced functional and structural ceramics, in particular of nanostructured ceramics and metal powders and process technology in nano-mineralogy by means of high power millimeter waves at a frequency of 30 GHz delivered by a gyrotron. In further experiments, fundamental new non-thermal microwave effects are validated (HGF program NANOMIKRO).
- System studies on microwave applicators for various applications at the ISM (Industrial, Scientific, Medical) frequencies 0.915 GHz, 2.45 GHz and 5.8 GHz, such as for energy-efficient production of aircraft components made of carbon fiber composites by microwave process technology at 2.45 GHz. The new HEPHAISTOS CA3 system with a payload capacity of 7000 l and a microwave power of 25 kW is already in routine operation. This will, in development with industry, offer various applications and processes on a service basis. With the new facilities of the 2.45 GHz HEPHAISTOS-line significantly shorter processing times at slightly improved material properties compared with the conventional production in autoclaves have been achieved (Programm REUN, TIG and IMA).

For the conduction of R&D in all of these theoretical and experimental fields the IHM is equipped with a workstation cluster and a large number of experimental installations: KEA, KEA-ZAR, three GESA machines, eight COSTA devices, one abrasion and one erosion teststand, two gyrotron test facilities with one common power supply and microwave-tight measurement chamber, one compact technology gyrotron (30 GHz, 15 kW, continuous wave (CW)), several 2.45 GHz applicators of the HEPHAISTOS series, one 0,915 GHz, 60 kW magnetron system and one und 5.8 GHz, 3 kW klystron installation.

In 2011, Prof. Manfred Thumm was teaching 4 courses (one at the International Department). PD Dr.-Ing. habil Lambert Feher and Dr.-Ing. Martin Sack each hold one lecture course at KIT.

At the end of 2011 the total IHM staff with regular positions amounted to 42 (21 academic staff members, 5 engineers and 17 technical staff member and others).

In addition 12 academic staff members and 11 technical staff members (and others) were financed by acquired third party budget.

In course of 2011 3 guest scientists, 8 PhD students (5 of KIT-Campus South, 3 of KIT-Campus North), 3 master students, 3 bachelor students, 6 internship students and 4 trainees in the mechanical and electronics workshops worked in the IHM.

### Strategical Events, Scientific Honors and Awards

By October 2011, Prof. Dr.-Ing. John Jelonnek started as successor of Prof. Dr. Dr. h. c. Manfred Thumm as Director of IHM. Prof. Dr.-Ing. John Jelonnek has been appointed Professor for High-Power Microwaves at the Institute of High Frequency Techniques and Electronics in the Faculty of Electrical Engineering and Information Technology of KIT..

At the 3<sup>rd</sup> Euro-Asian Pulsed Power Conference (EAPPC) at Korea in 2010, Dr. Georg Müller has been elected for the International Organizing Committee. He will be the General Chair of the next EAPPC in combination with the 19<sup>th</sup> International Conference on High-Power Particle Beams (BEAMS) in 2012 in Karlsruhe. Preparation of that conference did start in 2011 with high importance.

Prof. Manfred Thumm received “EPS Plasma Physics Innovation Prize 2011” for his outstanding contributions to the realization of high power gyrotrons for multi-megawatt long-pulse electron cyclotron heating and current drive in magnetic confinement nuclear plasma devices.

### Longlasting Co-operations with Industries, Universities and Research Institutes

- Basics of the interaction between electrical fields and cells (Bioelectrics) in the frame of the International Bioelectrics Consortium with Old Dominion University Norfolk, USA; Kumamoto University, Japan; University of Missouri Columbia, USA; Institute Gustave-Roussy and University of Paris XI, Villejuif, France; University of Toulouse, Toulouse, France, Leibnitz Institute for Plasma Science and Technology, Greifswald, Germany
- Desinfection of hospital wastewater by pulsed electric field treatment in cooperation with University of Mainz and Eisenmann AG
- Integration of the electroporation process for sugar production with SÜDZUCKER AG
- Development of protection against corrosion in liquid metal cooled reactor systems in the following EU-Proiectes: LEADER, GETMAT, MATTER, HELIMNET, ESFR (Partner: CEA, ENEA, SCK-CEN, CIEMAT)
- Development of core- and structure materials for liquid lead reactor cooling systems in collaboration with the Japanese Atomic Energy Agency (JAEA)
- Development of large area pulsed electron beam devices in collaboration with the Efremov Institute, St. Petersburg, Russia
- Experiments on liquid Pb and PbBi-cooling of reactor systems with the Institute for Physics and Power Engineering (IPPE), Obninsk, Russia
- Development, installation and test of the complete 10 MW, 140 GHz ECRH Systems for continuous wave operation at the stellarator Wendelstein W7-X in collaboration with the Max-Planck-Institute for Plasmaphysik (IPP) Greifswald and the Institute for Plasmaresearch (IPF) of the University of Stuttgart
- Development of the European ITER Gyrotrons in collaboration in the frame of the European Gyrotron



Consortiums EGYC and coordinated by Fusion for Energy (F4E). The other members of the Consortium are CRPP, EPFL Lausanne, Switzerland, CNR Milano, Italy, ENEA, Frascati, Italy, HELLAS-Assoc. EURATOM (NTUA/NKUA Athens), Greece. The industrial partner is the microwave tube company Thales Electron Devices (TED) in Paris, France

- Improvement of electron guns for gyrotrons and cavity interaction calculations in collaboration with the St. Petersburg Polytechnical University, Russia and the University of Latvia, Latvia
- Basic investigations of plasma-wall interaction in fusion reactors in collaboration with the State Research Center of Russian Federation Troitsk Institute for Innovation and Fusion Research (TRINITI), Troitsk, Russia and the Institute of Plasma Physics, Kharkov, Ukraine
- Fundamentals of application of gyrotrons for microwave materials processing in collaboration with the National Institute for Fusion Science (NIFS) in Toki, Japan and the University of Fukui, Japan
- Development of Microwave Systems of the HEPHAISTOS Series for materials processing with microwaves with the Company Vötsch Industrietechnik GmbH, Reiskirchen.



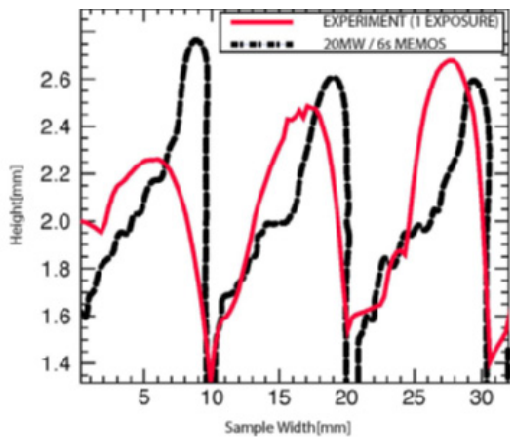
## HGF program: FUSION

### – Plasma Wall Interaction (PWI) –

(EFDA Task WP11-PWI-04-03-02: Modelling of cracked and molten divertor and first wall materials under high transient loads. Benchmark against experiments for ITER transient power load simulation)

In a fusion tokamak-reactor (ITER, DEMO) the transients such as edge localized mode (ELM) and off-normal plasma events: vertical displacements (VDE) and the disruptions, may produce runaway electrons (RE) and strong erosion (vaporization, melting and cracking) of the PFC materials (beryllium, tungsten, CFC). For modelling of armour material erosion, particularly a melt motion damage including heat transport into bulk materials, the incompressible fluid dynamics code MEMOS was applied. The validation of MEMOS by modelling experiments from plasma gun QSPA-T (TRINITI Troitsk, Russia) and from the tokamak TEXTOR has been continued as well as new calculations for ITER and DEMO carried out, being focused mainly for the magnitudes and the thresholds of melt splashing of Be and W under pulsed heat loads. Interpretation of experimental observation on tungsten brittle destruction (cracking) at the plasma gun QSPA-Kh-50 (IPP Kharkov, Ukraine) aiming further validation and improvements of models of thermomechanics code PEGASUS has been done.

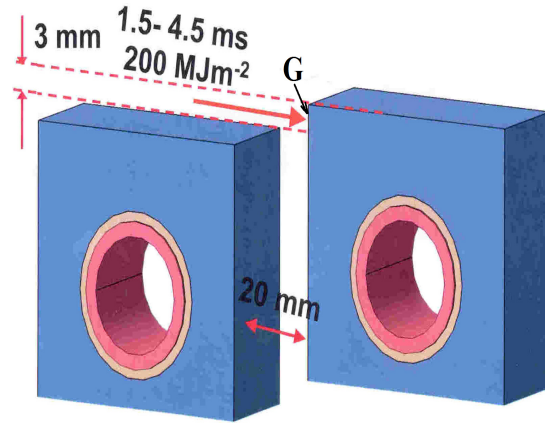
Experiments at the TEXTOR showed that the Ampere force generated by the thermo-emission electrons accelerates the melt layer and leads to a large scale melt motion damage (up to 1 mm per event). MEMOS simulations were performed for long-time plasma heat loads in a strong magnetic field. The model of space-charge limited thermo-emission current based on the modified Child-Langmuir expressions was implemented. The heat fluxes  $W = 18, 20, 22, 30 \text{ MW/m}^2$  of pulse duration  $\tau = 5$  and 6 s having rectangular space profile and time shape were applied to tungsten brushes of size 1 cm, thickness 3 mm, the distance between brushes 0.05 cm and radius of brush edge rounding 0.2 cm. It was also assumed that the back side of the target is passive-cooled by radiation. Results of carried out simulations are in a reasonable agreement with TEXTOR results (see figure).



MEMOS profiles vs. TEXTOR data. Comparison of the final erosion profile of W target;  $Q=20 \text{ MW/m}^2$ ,  $\tau=6 \text{ s}$ .

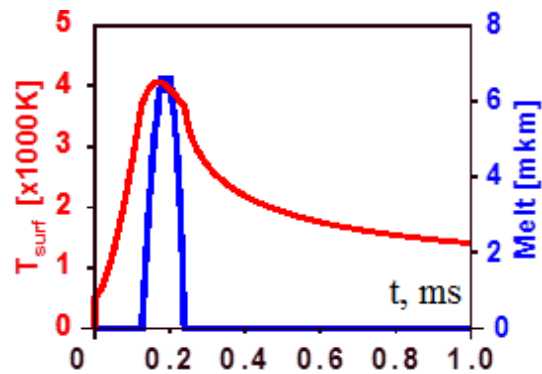
The consequences for W material damage as a result of plasma heat loads on vertical faces of misaligned leading edges between divertor cassettes due to downward VDE expected on ITER is investigated. Particular areas of concern are the edges present on either side of gaps between neighbouring divertor cassettes in the upper baffle region of the outer vertical target plates (see figure). Simulations with MEMOS of W melting are

performed. Melt layer damage is estimated for expected single plasma loads in the range  $Q=50\text{--}200 \text{ MJ/m}^2$ , with pulse durations between 0.5–3ms and edge misalignments up to several mm to cover the worst possible mechanical misalignment in the current divertor design. The principal finding is that the most significant contributors to damage on misaligned edges are the radiative vapour shielding coupled with strong melt motion.



Sketch of misaligned edge between monoblocks on sides of two neighbouring divertor cassettes.

Tungsten dust production rate due to ELM-like heat load was investigated in the quasi-stationary plasma accelerator QSPA Kh-50. At energy density  $Q = 0.75 \text{ MJ/m}^2$  (above melt threshold) the mass loss  $\mu \sim 5 \text{ } \mu\text{g/cm}^2/\text{pulse}$  after 200 plasma pulses. At  $Q = 0.45 \text{ MJ/m}^2$  (below melt threshold)  $\mu \sim 1.6 \text{ } \mu\text{g/cm}^2/\text{pulse}$  after 260 pulses. Since the erosion rate for the dust particles does not depend on the plasma density, for ITER it should be approximately the same as in the QSPA-Kh50 facility. Numerical analysis of experimental results with PEGASUS showed that for  $Q = 0.75 \text{ MJ/m}^2$  the main contribution to the dust production occurs after resolidification (see figure).



Calculated time dependences for the surface temperature and the melt layer depths for the QSPA-Kh50 shot with energy density of  $0.75 \text{ MJ/m}^2$ . The melt layer totally re-solidifies at 0.23 ms.

The dust is produced due to surface cracking under action of thermo-stress, which results in solid dust ejection. Resulting W influx into ITER plasma is estimated about  $\sim 5 \times 10^{18} \text{ W atoms}$  per one ELM of  $Q = 0.75 \text{ MJ/m}^2$  and  $\tau = 0.25 \text{ ms}$ . Corresponding radiation cooling power of produced W impurities is roughly estimated to be about 150-300 MW.

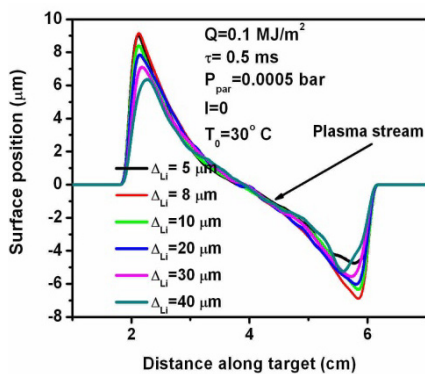
**(EFDA Task WP11-PWI-04-04-01:** Demonstration of liquid plasma-facing components behaviour under ELM-like load)

Behaviour of Li layer on various porous substrates is now under investigations at different tokamaks (FTU, NSTX). Experiments demonstrated that the 'lithization' of vessel surface leads e.g. to strong reduction of heavy impurities in the plasma and longer wall lifetime for high power heat loads. A heating system can increase the Li temperature above the melting point 450C, which forms a thin (from several microns to several tens microns) lithium film on the chamber wall. The impact of transients (ELMs) can result in contamination of plasma by Li ions owing to physical sputtering, melting and evaporation.

New numerical simulations for Li layer on W porous substrat were performed with the code MEMOS for the Li coating of 5-50  $\mu\text{m}$  thickness. The reference heat load  $Q=0.1 \text{ MJ/m}^2$  during the reference pulse of load time  $\tau=0.5 \text{ ms}$  was assumed, magnetic field  $B=5 \text{ T}$ , tangential pressure varied in the range  $2 \times 10^{-4}$  to  $.2 \times 10^{-3} \text{ bar}$ , electric current component normal to the target surface varied in the range  $5\text{--}50 \text{ A/cm}^2$ , initial surface temperature  $T_0=30 \text{ C}$  (assuming that Li can melt during the transient).

The evaporated mass is investigated in terms of evaporated layer thickness for the reference pulse duration and the heat load ranged between 0.1 and 0.4  $\text{MJ/m}^2$ . The applied force and the energy flux correspond to the rectangular pulse shape which recoils the ELM shape in experiments. It is shown that a significant evaporation starts at heat loads  $\geq 0.2 \text{ MJ/m}^2$ . For the reference heat load the vaporization is negligible, and the melt motion only causes the melt layer damage. In calculations the effects of tangential plasma pressure and the  $\mathbf{J} \times \mathbf{B}$  force on liquid Li motion were investigated as well as the dependence of the surface damage on the pulse shape.

The effect of different ELMs pulse shapes on the formation of a crater after melt removal by plasma pressure is also investigated. It is shown that for different thickness of Li layer that the craters caused by the tangential pressure gradient have similar depth (see figure).



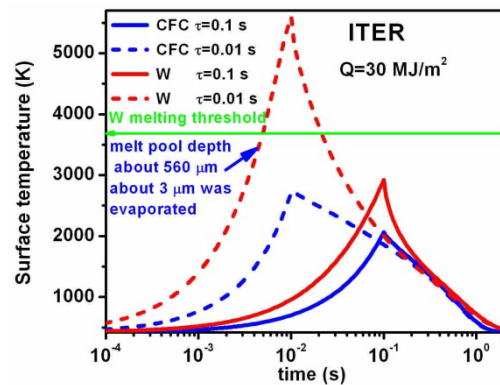
Crater shape caused by the tangential pressure for different thickness of Li layer after 3 ms from pulse trail. 'Real ELM' pulse shape. Capillary porous system is taken into account.

The rectangular pulse shape demonstrates somewhat higher surface damage in comparison with the "real ELM" pulse shape (which is triangular). In scenarios with  $\Delta_{\text{Li}} = 5 \mu\text{m}$  removed melted materials from the crater bottom is recovered by the capillary forces from the W porous matrix and the minimum thickness of liquid Li at the crater bottom remains about 0.4  $\mu\text{m}$ .

**(EFDA Task WP11-PWI-06-02-03:** Numerical modelling of heat deposition by runaway electrons and MGI validation simulations against JET)

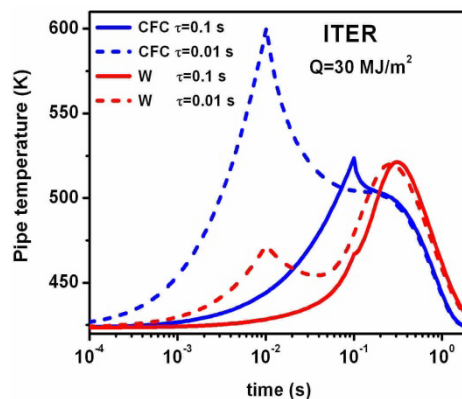
In ITER the disruptions can limit the lifetime of PFCs. During the thermal quench (TQ) of disruption relativistic runaway electrons (RE) can appear and damage the first wall (FW). Disruption mitigation by massive gas injection (MGI) of noble gases can also result in generation of RE. To estimate RE damage numerical simulations have been performed with the energy deposition Monte-Carlo code ENDEP and the melt motion code MEMOS.

The energy distribution of RE was assumed to be exponential as  $\exp(-E/E_0)$  or Gaussian function  $\exp(-(E/E_0)^2)$  with RE energy  $E$  and some given characteristic energies  $E_0 \sim 20 \text{ MeV}$ . Simulations demonstrated that in case of W, 20% of RE energy is converted into X-rays, but due to strong absorption inside bulk W only 0.5% of X-ray energy is released in the copper cooling pipe. For expected in ITER RE impact energy  $Q = 30 \text{ MJ/m}^2$  and pulse durations  $\tau = 10 \text{ ms} - 0.1 \text{ s}$ , W surface evaporates and can melt (see figure).



The evolution of the surface temperature for CFC and W during and after RE exposition times at 0.1-0.01s and RE energy of 30MJ/m².

Heat generation in W occurs in a subsurface layer  $\sim 10 \mu\text{m}$ , and in CFC  $\sim 1 \text{ mm}$ . At  $\tau = 0.1 \text{ s}$  W surface does not melt and CFC does not experience a brittle destruction. For  $\tau = 10 \text{ ms}$  and  $Q = 30 \text{ MJ/m}^2$ , W melting point is reached at  $\sim 0.4 \text{ ms}$ . The evolution of temperature at the Cu pipe for the CFC and W case in ITER for runaways of a power 30MW/m² lasting 0.1 and 0.01sec was also found (see figure).

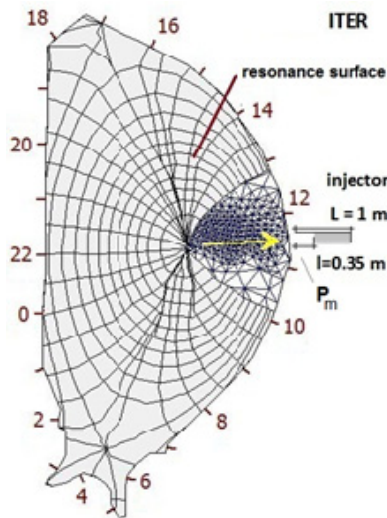


The evolution of temperature at the Cu pipe for the CFC and W case in ITER for runaways of a power 30MW/m² lasting 0.1 and 0.01sec (dashed lines).

For ITER and DEMO the RE energy deposition and erosion of W/EUROFER blanket module for the first wall is estimated. The simulations were performed for the RE deposition energy in the range of 30-100 MJ/m<sup>2</sup> over 0.05-1 s. It is shown that the minimum W thickness needed to prevent failure of the W/EUROFER bond (assumed to be the EUROFER creep point) is so large that armour surface melts. Therefore RE will pose a major lifetime problem in ITER and DEMO design.

Tokamak experiments demonstrated effective ionizations of injected atoms G (G = Ne, Ar, He) during MGI, the following MHD activity which causes the thermal quench (TQ) within a few ms, and a radiation flash. On the short time scale the ionization of G-atoms localized near the jet entry can result in drastic decrease of electron temperature  $T_e$  near the jet. This can significantly decrease the ionization rate resulting in deep jet penetration. For modelling of MGI the integrated tokamak code TOKES was applied.

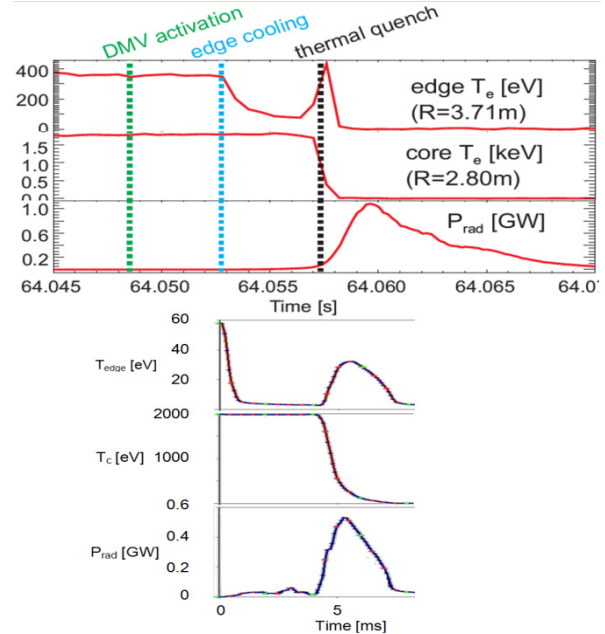
The modelling with the code TOKES has been focused upon further development of the code aiming two-dimensional MGI simulations with strongly varying plasma parameters in jet vicinity, where its triangular meshes for simulation of slow injected neutral have been drastically densified (see figure).



TOKES triangular and magnetic flux meshes. Positions of gas injector and the resonance surface of safety factor  $q=2$  are shown.

The plasma transport is calculated in confined region with closed magnetic surfaces as well as in the scrape-off layer (SOL) and in the private region of tokamak. TOKES radiation model was coupled with plasma thermal transport across deteriorated magnetic surfaces. First consequence of core instabilities appears to be small deteriorations of toroidal symmetry and thus slight overlapping of nested magnetic surfaces, which drastically increases electron cross-transport by thermal conductivity along entangled magnetic field lines (3D thermal transport) when jet reached the resonance magnetic surface. The heuristic coupling parameter which drives the thermal conductivity is the ratio of plasma energy to radiation loss energy. Preliminary predictive simulations for ITER have been performed, with the conclusion that after the radiation flash maximum wall temperature can exceed the beryllium melting point.

The code TOKES was successfully validated against two JET experiments on argon MGI. Experimental results on MGI of noble gas into various JET H-mode discharges have been analysed and two of them chosen for simulation. These are JPN76314 with ohmic heating only, plasma energy content  $W = 0.8$  MJ, and the discharge JPN77806 with  $W = 3.2$  MJ. In

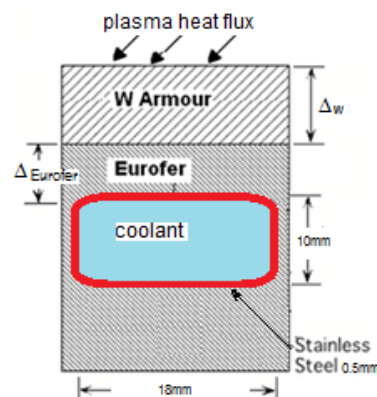


Comparison of time dependences for edge and core temperature and radiation power  $P_{rad}$  measured in JET pulse JPN76314 (upper panel) with the corresponding simulation (lower panel).

simulations the injected gas is ionized and plasma of the temperature  $T_{Ar} = 100-50$  eV expands with velocity of  $V_{||} = 2.5C_s \sim 5 \times 10^6$  cm/s making one toroidal turn during  $\sim 0.5$  ms, which soon provides toroidal symmetry. The comparisons of simulated and experimental centre temperature and radiation power indicate that the simulation satisfactory reproduces main processes of TQ (the figure above).

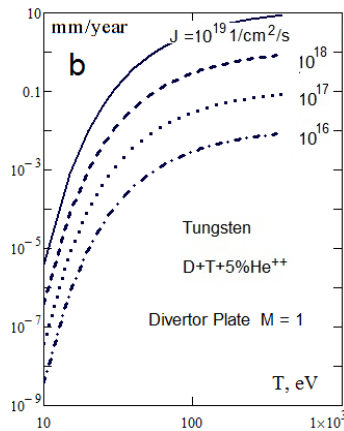
(EFDA Task WP11-DAS-PLS-P02-01: Review of problems for steady-state DEMO reactor operation)

It is still under consideration whether the next Demonstration Power Plant (DEMO) will be designed as a steady-state machine or based on a pulsed operation like ITER. The pulsed operation introduces additional mechanical and thermal cyclic loads which would increasingly impact on the structural materials therefore the steady DEMO would be preferable however the impact of transients and off-normal events must be addressed. We estimated steady-state design plasma impacts of heat and plasma particles on the first wall (FW) and consequent bulk plasma contamination associated with sputtering erosion. The sputtering of FW and baffle surfaces could mainly occur due to the impacts of hot neutral atoms coming due to charge-exchange in the pedestal region. The sandwich type blanket first wall module is considered (see fig.).



Sandwich type blanket first wall module used for calculation of DEMO plasma impact.

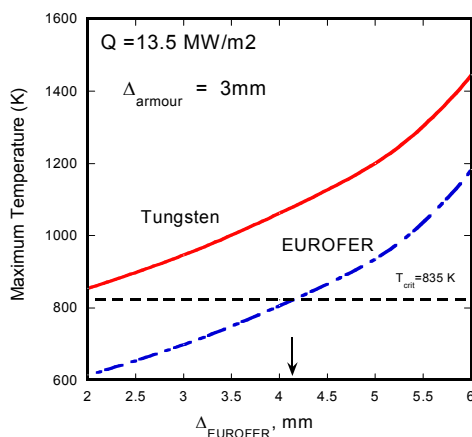
It is shown that at neutral temperatures  $\leq 100$  eV the sputtering of W is negligible. For neutrals undergoing the charge-exchange collisions in the pedestal region strong erosion can be expected (it can be much more than  $10^{14}$ - $10^{15}$  atom/cm<sup>2</sup>/s, see figure).



The thickness of tungsten divertor plate sputtered during one year of continuous operation by various particle fluxes of D/T/5%He of incident ions.

The most intensive W release is due to the impacts of charge-exchange neutrals, probably from baffles. However, due to low W sputtering yield even for high pedestal temperatures the impurity concentrations in plasma core will remain below the fatal values for W impurities  $\sim 5 \times 10^{-5}$  under steady-state operation and normal conditions. The sputtering erosion can reach 1 mm/year.

Calculations using MEMOS show that under steady state operation and ITER like coolant conditions the interlayer temperature is weakly dependent on the W armour thickness in the range of incoming heat fluxes. The maximum W armour thickness is limited by the maximum allowable temperature of EUROFER under maximum steady-state loads. The armour surface temperature increases with the armour thickness increase and for reference case of  $\sim 3$ mm remains well below the tungsten melting point. For reference conditions ( $\Delta w \sim 3$ mm,  $\Delta_{EUROFER} \sim 4$ mm) the maximum heat flux which does not cause intolerable thermal stresses in structural material (it occurs at  $T > 835$  K) is about  $\sim 13.5$  MW/m<sup>2</sup> (see figure).



Maximum temperature of W and EUROFER vs EUROFER thickness.

In the case of off-normal event ('hot' vertical displacement) the energy deposition of plasma into the W armour causes surface melting and evaporation. The accommodation of VDE power requires thicker W armour to maintain the maximum heat flux and temperature in the material structure at acceptable level. It is shown that the presence of vaporized layer and a

macroscopic molten layer is unavoidable for expected exposition times and power loads.

The runaways (RE) deposit their energy rather deep into W armour. For deposition energies  $Q \geq 50$  MJ/m<sup>2</sup> during times  $\tau \leq 0.1$  s the minimum armor thickness required to prevent EUROFER from thermal destruction is  $\geq 1.4$  cm. However, this size of layers doesn't prevent the W surface from melting. At higher RE energy deposition rates ( $\geq 100$  MJ/m<sup>2</sup> in 0.1 s), the required armor thickness to prevent creeping destruction is even larger so that the bulk of the armor layer will melt and evaporate.

Hence although W/EUROFER bound is compatible with high neutron fluencies, the loss of creep strength at relatively low temperature represents the main drawback of EUROFER as a structural material. Our estimations of erosion of the FW by charge-exchange neutrals and the divertor plates by incoming ions show also the importance of angular dependence of sputtering yield and, particularly, the effect of sheath potential.

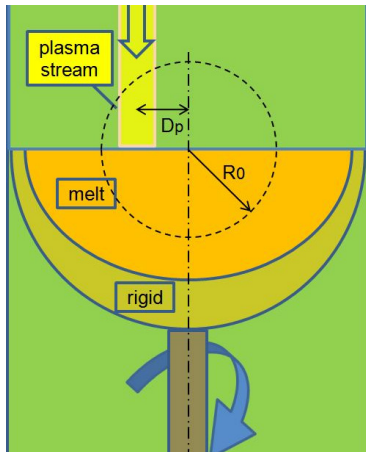
(EFDA Task WP11-PEX-01-ACT3-01: Preliminary studies of alternative concepts for heat removal in future fusion reactors based on moving or liquid targets or hybrid systems of it)

Large localized plasma heat flux exhaust is one of most critical problems for DEMO because without reradiation of  $\alpha$ -fusion energy by burning plasma the divertor must accommodate the power. For the electric power  $P_{net} = 1$  GW, operation availability  $A = 0.5$  and the heat-electricity transformation efficiency  $\eta = 0.3$  the power to be exhausted follows as  $P_{exh} = (P_{net}/(5A\eta)) \approx 1.3$  GW. As a reference case we consider DEMO with major radius  $R_p = 8$  m and the plasma stream width  $w_s = 5$  cm. Then the localized heat flux is estimated as  $Q_{exh} = P_{exh}/(2(2\pi R)w_s) \approx 260$  MW/m<sup>2</sup>. It is to note that for present technology the accepted steady heat flux is limited to 5 MW/m<sup>2</sup> thus tilting of divertor plate in order to spread the power requires the angle of 1 grad, which seems unrealistic. One concept to mitigate the heat flux can be based on movable targets which are regularly removed from the exposed area and simultaneously replaced. Those ideas have been proposed previously. So far the only moving surfaces used in a tokamak were a rotating limiter tested on the Princeton Large Tokamak (PLT) and a gallium droplet limiter tested on Russian tokamak T-3M.

We will assess some alternative concepts based on replacing the conventional actively cooled divertor plates by a set of moving divertor targets with passive (radiative) or remote cooling. The estimations are very preliminary and can need revisions. In first concept an array of rotating W discs of small thickness is considered as divertor targets which experience the power flux of incident plasma. Thin plasma stream locally hits the discs and due to rotation the absorbed heat is homogeneously redistributed over the disc volume. The cooling is due to radiation losses from hot disc surface. The radiation losses are estimated by Stefan-Boltzmann formula which in the case of tungsten for the surface temperature  $T_s = 3000$  K gives  $q_{rad} \approx 1.4$  MW/m<sup>2</sup>. Then, for the value of exhausted power per toroidal length  $P_{exh}/2(2\pi R) = 13$  MW/m the required radius of disk is about  $R_d \approx 3$  m, which is too large to be appropriate.

The radius of plasma facing surface can be reduced in another design based on a spinning segment of spheroid, which resembles half-egg spinning about its vertical axis (see figure on next page).

Our estimations show acceptable size of the spherical target 0.5 – 1 m. However, high vapour pressure of W surface  $p_{sat} \sim 0.36$  bar for expected temperatures  $T_s \sim 5500$  K will strongly contaminate plasma. Large  $p_{sat}$  is serious obstacle for applying radiation cooling of the target. However, the target can be isolated from confined plasma by using the cooling chamber with rather narrow slot for plasma incoming to the target. Only unimpeded W vapour flow near the plasma has chance to get into the gap. It can be shown that impurities near the target can



Concept of divertor plate as a rotating spheroid with partially melted W surface layer.

be effectively entrained by the plasma stream and brought back to the target. Some part of W atoms can penetrate into the SOL and plasma bulk. Detailed 3D calculations are required to assess the impurity behaviour in the main plasma. The main drawback of the model is an accidental contact of plasma stream with the slot edge with consequent thermal erosion and strong contamination.

## – Microwave Heating for W7-X (PMW) –

### Introduction

Electron cyclotron resonance heating (ECRH) and current drive (ECCD) are the standard methods for localised heating and current drive in future fusion experiments. Thus ECRH will be the basic day-one heating system for the stellarator W7-X which is currently under final construction at IPP Greifswald. It is expected that the ECRH system for W7-X will be finalized in 2014. In its first stage W7-X will be equipped with a 10 MW ECRH system operating at 140 GHz in continuous wave (CW).

The complete ECRH system is coordinated by the project "Projekt Mikrowellenheizung für W7-X (PMW)". PMW has been established by KIT together with IPP and several EU partners in 1998. The responsibility of PMW covers the design, development, construction, installation and system tests of all components required for stationary plasma heating on site at IPP Greifswald. PMW coordinates the contribution from Institut für Plasmaforschung (IPF) of the University of Stuttgart (IPF) too. IPF is responsible for the microwave transmission system and part of the HV-system. IPF coordinates the team at IPP Greifswald, which is responsible for the in-vessel components and for the in-house auxiliary systems. PMW benefits from the collaboration with Centre de Recherche de Physique des Plasmas (CRPP) Lausanne, Commissariat à l'Énergie Atomique (CEA), Cadarache and Thales Electron Devices (TED), Vélizy.

A contract between CRPP Lausanne, FZK Karlsruhe and TED, Vélizy, had been settled to develop and build the series gyrotrons. First step in this collaboration was the development of a prototype gyrotron for W7-X with an output power of 1 MW CW at 140 GHz.

Seven series gyrotrons have been ordered from industrial partner Thales Electron Devices (TED), Vélizy. First operation and long pulse conditioning of these gyrotrons is being performed at the teststand at KIT. Pulses up to 180 s duration at full power are possible (factory acceptance test, FAT) whereas 30 minutes shots at full power are possible at IPP (necessary for site acceptance test, SAT). Including the pre-prototype tube, the prototype tube and the 140 GHz CPI-tube, in total 10 gyrotrons

will be available for W7-X in final state. To operate these gyrotrons, in addition to the Oxford Instruments and Accel magnets, eight superconducting magnet systems have been manufactured at Cryomagnetics Inc., Oak Ridge, USA.

In 2010 and 2011 the completion of the project made significant progress. Most of the components of the transmission system, HV-systems and in-vessel-components have been ordered, manufactured, delivered and are ready for operation at IPP Greifswald. A part of the existing ECRH system has been already used to test new concepts and components for ECRH. Some delay arose in the project during the last 1-2 years due to unexpected difficulties in the production of the series gyrotrons.

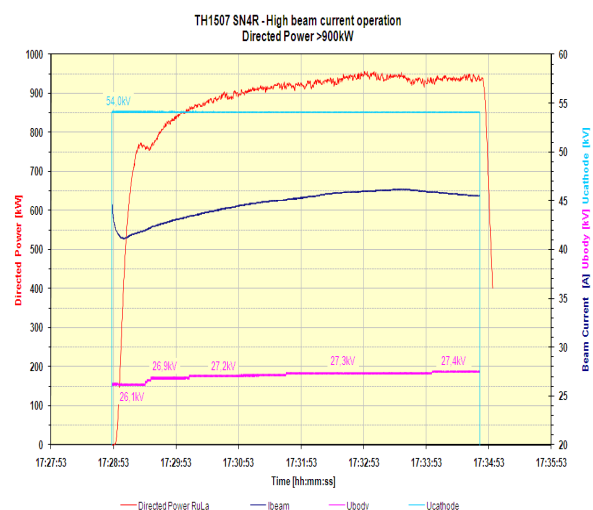
### Series Gyrotrons

In 2005, the first TED series gyrotron SN1 had been tested successfully at FZK and IPP (920 kW/1800 s). It fulfilled all specifications during the acceptance test, no specific limitations were observed. In order to keep the warranty SN1 has been sealed, one prototype gyrotron is routinely used for experiments.

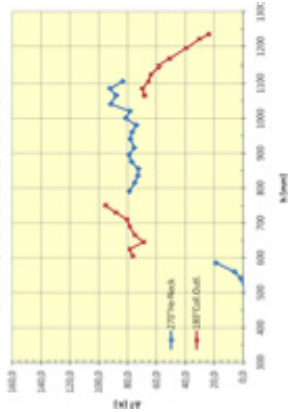
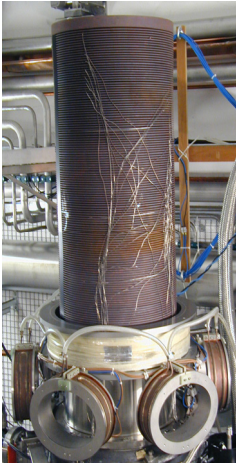
Series gyrotrons following SN1 did show a more or less different behavior with respect to parasitic oscillations excited in the beam tunnel region. These oscillations resulted in an excessive heating of the beam tunnel components, in particular of the absorbing ceramic rings. The gyrotrons re-opened after operation showed significant damages due to overheating at the ceramic rings and the brazing of the rings. A possible solution was proposed and successfully tested by KIT. As the main difference to the usual beam tunnel this design features corrugations in the copper rings which handicap the excitation of parasitic modes.

The first W7-X gyrotron (SN4R) which is equipped with an improved beam tunnel was delivered and tested at KIT in 2010. During the tests at KIT no parasitic oscillations originating from the beam tunnel region were observed. In early 2011 this tube was delivered to IPP for final Site Acceptance Tests (SAT). This gyrotron produced 1.02 MW directed RF power at the output window (0.95 MW in the absorber load) with an efficiency of 42%. The pulse length was limited to 353 s due to arcing in the absorber load (see figure below).

At IPP an advanced beam sweeping system at the collector was used additionally. It is a combination of the usual vertical field sweeping (VFSS) and a new transversal field sweeping system (TFSS). It results in a strong decrease of the peak temperature at the collector and a more homogeneous distribution of the thermal loading. Due to this sweeping system it was possible to operate SN4R at a higher beam current with increased output power (see figure next page).

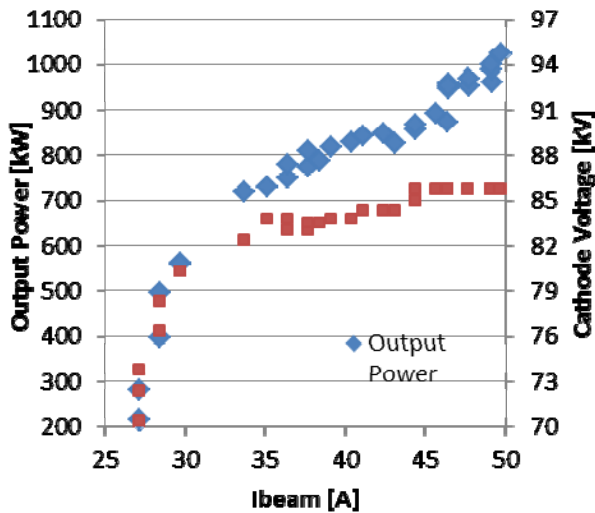


Output power, beam current and operating voltages of series gyrotron SN4R, measured at IPP Greifswald.



Collector and transversal field sweeping system (left), temperature distribution of the loaded collector along the axis of SN4R (right).

SN6 has been taken into short pulse operation at KIT. First tests demonstrated an output power of 1.024 MW at 50 A (see figure). The Gaussian beam content of the RF output beam has been measured with an IR system, the analysis of the profiles gave a TEM00 content of 97%. Further conditioning and long pulse tests is continued in 2012.



Output power and cathode voltage versus beam current for series gyrotron SN6, measured during first short pulse tests at KIT.

### Transmission Line System

The transmission line system consists of single-beam waveguide (SBWG) and multi-beam waveguide (MBWG) elements. For each gyrotron, a beam conditioning assembly of five single-beam mirrors is used. Two of these mirrors match the gyrotron output to a Gaussian beam with the correct beam parameters, two others are used to set the appropriate polarization needed for optimum absorption of the radiation in the plasma. A fifth mirror directs the beam to a plane mirror array, the beam combining optics, which is situated at the input plane of a multi-beam wave guide. This MBWG is designed to transmit up to seven beams (five 140 GHz beams, one 70 GHz beam, and one channel connected to the N-port launchers via a switch) from the gyrotron area (entrance plane) to the stellarator hall (exit plane). To transmit the power of all gyrotrons, two symmetrically arranged MBWGs are used. At the output planes of the MBWGs, two mirror arrays (beam distribution optic, BDO) separate the beams again and distribute them via two other

mirrors and CVD-diamond vacuum barrier windows to individually movable antennas (launchers) in the torus.

The manufacturing and installation of the components of the basic transmission system has been completed. Cooling tube manifolds to supply the mirrors and stray radiation absorbers mounted in the towers in front of the stellarator are being prepared for installation early next year.

In 2011, gyrotron SN4R was installed in Greifswald, and beam characterization and the subsequent design and manufacturing of the surfaces of the two matching mirrors for this tube has been performed. SN6 is presently under test at KIT Karlsruhe, where the beam parameters are being measured.

Further remaining work includes diagnostics and power measurement of the gyrotron beams. The receivers attributed to the directional couplers on the mirrors M14 and related alignment control are in fabrication.

The water-cooled version of the "long load" was put into operation and tested successfully.



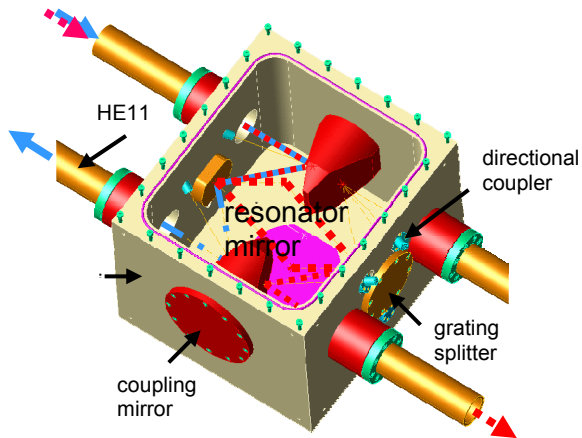
Input section of the long load, showing matching horn, and the absorbing waveguide with cooling connection.

This load (see Figure above) consists of a 23 m long stainless steel tube with a water jacket, which is tapered down towards the end. The inner diameter is reduced from 56 mm at the beam input down to 38 mm at the load end in three steps in order to match the power absorption of the waveguide to the power loss along the guide. A non-linear horn (diameter 80 – 56 mm) at the input avoids spill-over of the Gaussian input beam at the waveguide entrance. The calculated absorption of the waveguide is 80 %. The remaining power is dumped in a standard calorimetric load, which is designed for 1 MW power in repetitive short-pulse operation. This load can be operated in CW mode at lower power. The present tests have demonstrated a CW capability of at least 140 kW. High-power test of the long load in combination with the calorimeter and the Maquette gyrotron showed that the absorption of the stainless-steel waveguide is somewhat dependent on the power level as well as on the input polarization within a range of 74 .....82 %. This is explained by the increase of damping with increasing wall temperature in the waveguide, as well as by finite precision in the alignment of the whole system. The power level used for the test was up to 820 kW, short-pulse, and 650 kW at 60 s, limited by the output power of the Maquette tube. Further tests are planned in the frame of acceptance of the next series gyrotron.

In the past years, the ECRH system at IPP -Greifswald was used as a test bed for novel components, e.g. for test of high-power diplexers. These devices are developed for use as a combiner for the power of two gyrotrons as well as a fast directional switch (FADIS) between two outputs, and therefore are of potential interest for ITER. Based on the experience gained from the tests, very compact diplexers have been designed and built. The diplexer MC IIIb is compatible with the corrugated waveguides system used at ASDEX Upgrade, and is



intended to be used there for in-line ECE experiments. For this purpose, a new resonator mirror drive was built by TNO in Delft, and the diagnostics for the drive control was upgraded and simplified. Commissioning at ASDEX Upgrade is planned for next year. An evacuated version (MQ IV) compatible with the ITER system is being designed at present (see figure). Provided that funding for the manufacturing is available, high-power tests on the ITER test system at JAEA, Naka are foreseen.



*Diplexer MQ IV compatible with the ECRH system on ITER (waveguide diameter 63.5 mm, distance of adjacent guides 300 mm). The top plate with the mirror drive and the absorber tubes is removed to reveal the resonator geometry and the beam path shown in red dotted (resonant channel) and blue dash-dotted lines (non-resonant channel).*

#### In-vessel components

The four refurbished ECRH-plug-in launchers have successfully passed the official vacuum leak test for W7-X in-vessel components. They also demonstrated the robustness and reliability of their motor drive mechanism in mechanical cycling tests of the front steering mirrors in the MISTRAL-chamber in vacuum.

For two of the N-ports of W7-X, "remote-steering" (RS) launchers are foreseen. This is due to the fact, that front steering launchers as used in the A and E ports will not fit into these narrow ports. The remote-steering properties are based on multi-mode interference in a square waveguide leading to imaging effects: For a proper length of the waveguide, a microwave beam at the input of the waveguide (with a defined direction set by a mirror system outside of the plasma vacuum) will exit the waveguide (near the plasma) in the same direction. For W7-X, the vacuum window, a vacuum valve as well as a mitre bend must be incorporated into the 4.6 m long waveguide, as shown in the conceptual design (see figure).

In 2011, the N-port engineering design activity was frozen. The project is waiting for the final approval of a BMBF application on support for developing and constructing two remote-steering launchers. This application (collaboration of IPP with IPF and two industrial partners) was filed in 2011, with the expectation to start early 2012.

Basic research on the optimization of remote-steering antennas was continued at IPF Stuttgart.

In the frame of a diploma thesis, investigations on the influence of a mitre bend and gap in the waveguide were performed on a slightly scaled antenna mock-up made from square corrugated waveguide. The results show that both elements can be included in the launcher without remarkably reducing the performance in the reachable steering range of  $-12^\circ < \varphi < 12^\circ$ .

In parallel, the IPF-FD3D full-wave code has been adapted to the problem of finding the waveguide dispersion relation for arbitrarily deformed waveguide cross sections. A waveguide cross-section with outward bulges resulting in an increased angular steering range has been identified. The PROFUSION code was extended to calculate the remote-steering qualities of the deformed waveguide.

A first mock-up for investigations of deformed waveguide cross-sections was built, and measurements are underway.

The final design of electron cyclotron absorption (ECA) diagnostics, which measures the transmitted ECRH power, the beam position and polarization was completed. A prototype waveguide bundle was successfully test-assembled in the W7-X vacuum chamber. A minor rerouting of the waveguides in the plasma vessel had become necessary due to collisions with other in-vessel components. The design is officially approved as collision free now and the production drawings were completed. The counter part of the plasma vessel waveguide bundles are the four B-port inserts with vacuum interfaces for the waveguides. Vacuum leak tests of the first B-port insert showed, that some of the mica vacuum interface windows were damaged by a superelevated compacting pressure. Therefore, the waveguide vacuum interfaces have been slightly modified. They were reassembled into the B-port plug-in and are presently leak-tested.

The microwave material test chamber, which measures the material properties at 140 GHz with low-power stray radiation, was upgraded within a Bachelor thesis in co-operation with the Humboldt University Berlin. A detailed investigation of the radiation field inside the sphere helped to improve the measurement accuracy significantly. This small chamber is also used to calibrate the stray radiation detectors for the MISTRAL chamber and for W7-X.

The stray radiation in W7-X will also be monitored by so called "sniffer" probes, which are highly over-moded spherical resonators. It is planned to install at least one probe in every W7-X module. The probes have been characterized in collaboration with the Eindhoven University of Technology (TU/e). The detailed design for their integration into W7-X plasma vessel is ongoing.

## - ITER ECRH Advanced Source Development -

### Coaxial Cavity Gyrotron, Backup Design and Test Facility

The development of a 2 MW, CW, 170 GHz coaxial cavity gyrotron for ITER is pursued within the European Gyrotron Consortium (EGYC, consisting of CRPP, Switzerland; KIT, Germany; HELLAS, Greece; CNR; Italy), which acts as scientific partner for F4E, and in cooperation with ISSP, Latvia. The goal of the development is the supply of sources for 170 GHz ECH & CD at ITER providing 8 MW CW power, to cover the EU contingent on ECH & CD sources in ITER. In contrast to other contributors to ECH & CD on ITER, the EU plans to provide sources with 2 MW RF power per unit (ITER minimum specification: 1 MW) for reduced cost and space requirements, to be able to double the system power if requested and to establish the - essentially more powerful - coaxial technology.

While the industrial gyrotron prototype, build by Thales Electron Devices (TED, France), is tested at CRPP, KIT provides support to the development through component design, scientific investigations and collaboration as well as low and high power tests at KIT. The latter are done with KIT's modular pre-prototype gyrotron (see figure). In particular, KIT is solely responsible for the design of cavity, uptaper and mode converter system, and, with the position change of Dr. Ioannis Pagonakis from CRPP to KIT, also for the electron gun and other aspects of the electron optical system up to the collector. KIT also

supports the experimental phases at CRPP in the frame of mobility missions.

In parallel to the coaxial 2 MW gyrotron activities, a 1 MW conventional cavity design was prepared in 2010 as fallback solution. Since the coaxial ITER gyrotron project is strongly delayed due to an unexpected repair cycle of the prototype, the strategic decision about keeping the 2 MW design or switching to a conventional 1 MW design is under strong discussion and will be taken early in 2012.

#### **Status of work at the beginning of 2011**

The refurbishment of the industrial prototype for the ITER gyrotron was started in 2009 and aimed at delivery to CRPP Lausanne in summer 2010. Due to various delays, the delivery date had to be shifted first to end March 2011 – finally, the delivery took place end September. The first problem was a leaky brazing at the ceramic collector insulator during the final bake-out of the tube.

To fill this gap of experiments, the KIT pre-prototype was equipped with the old 165 GHz-gun, after the 170 GHz-gun also failed due to a crack in a gun insulator. In former short-pulse experiments with the new KIT dimpled-wall launcher, an internal stray radiation of 7% was measured. The next hot experiments with a different launcher-antenna designed by IAP Nizhny Novgorod were set up to determine the change of stray radiation level due to the launcher exchange.

Since it was obvious that on the one hand the KIT electron guns reached the end of their life time, on the other hand an increase of pulse length was highly desirable for more scientific insight and for a better support to the long pulse experiment with the industrial prototype at CRPP, the so-called modular project was started. It is reminded that in 2009 the pre-prototype produced a world-record power of 2.2 MW at 170 GHz with good efficiency, which was a major step and calls now for validation at longer pulses. The modular project should transform the short pulse pre-prototype into a modular medium-pulse and, if possible, into a pre-tested long-pulse tube.

Regarding theory and simulation, first steps for a further improvement of the quasi-optical system through phase correcting mirrors or smoothing of the launcher structure have been made, initiated within the dissertation of Dr. Matthias Beringer on a 4 MW coaxial gyrotron, which was finalized end 2010. A different dissertation on simulation code improvement was started, aiming at a better interaction description through realistic magnetic field modelling. The simulation work on GRT-034 regarding the influence of stray-magnetic fields in the ITER environment was also started, in strong collaboration with CRPP.

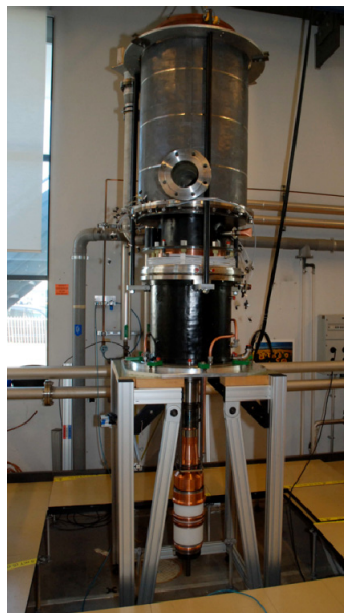
The investigations on parasitic oscillations were, after the successful redesign of the beam tunnels of the coaxial gyrotron and the conventional tubes at KIT, extending to investigations on dynamic ACI and the possible influence of tolerances and misalignments on parasitic oscillations.

#### **Achievements in 2011**

##### **High power tests with the industrial prototype at CRPP**

After a large number of unexpected delays caused by smaller damages and process problems, the modified and refurbished first industrial prototype was finally delivered end September to CRPP. The experiments there until 9th of December were strongly supported by all EGYC associations, including continuous presence of KIT experts at the experiment.

The experiment first had to prove that the site acceptance test criteria were fulfilled, such that the tube could be accepted by the customer F4E. After this, F4E would take over the ownership from the manufacturer TED, and the actual RF experiments could be started. Before going in details, it should be said that this was basically done very successfully, but the tube broke on 9th of December after a first four days of rapidly improving RF operation, which fortunately reached a performance close to the specification.



*Coaxial 2.2 MW 170 GHz short pulse pre-prototype gyrotron at KIT (left); the refurbished industrial long pulse prototype at delivery end September 2011 (mid); and the same prototype, installed at the CRPP test stand inside the ASG magnet (right).*

The first observation was quite disappointing, since the gyrotron arrived with a leak that developed during transport. The leak could be sealed by a special resin, as shown in the following figure, but the tube fell back to an unbaked condition, which made long pulse operation questionable. Despite this problem, the vacuum could be regained and quickly improved; during all subsequent experiments the vacuum behaviour was clearly better than that of an unbaked tube, which raised hopes on long pulse operation, but this was finally disabled by the terminating accident.

The achievements of the site acceptance test and the short phase of RF experiments are in overview:

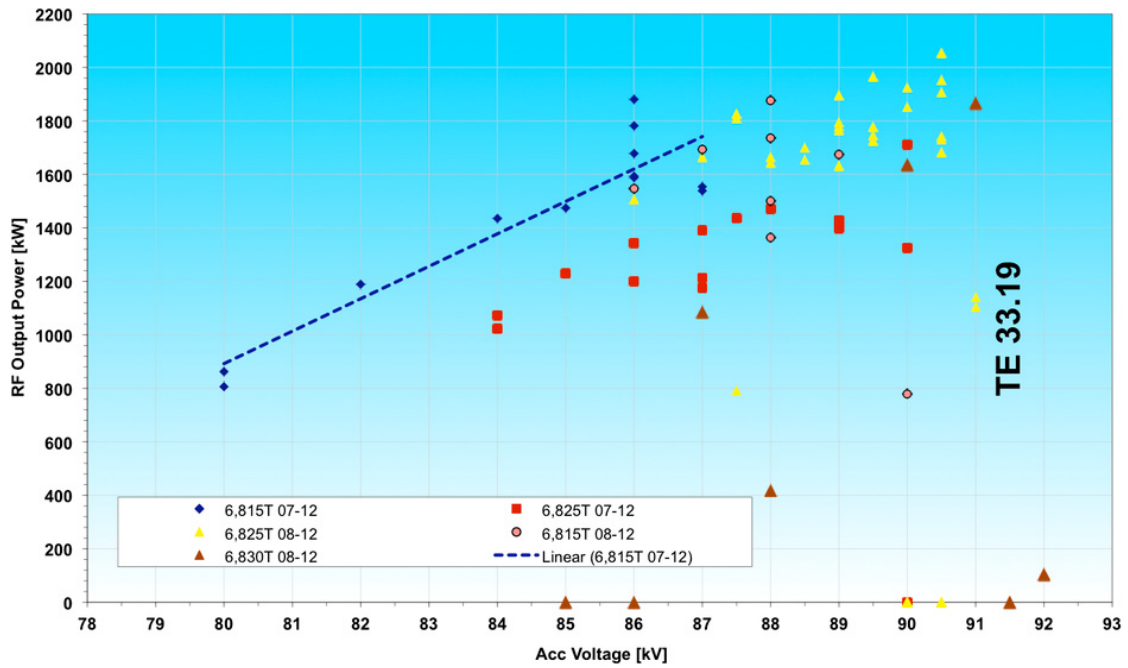
- The SAT acceptance tests were successfully completed at the end of November:
  - The gun design changes have been validated. The tube stood the high voltage without any problem without and with magnetic field - in strong contrast to the first design - and permitted the operation at nominal parameters.
  - Good alignment of the inner rod was could be done (0.06mm accuracy), and the overall tube position in the magnet could also be verified.
  - The conditioning time needed to reach high power operation was surprisingly short, especially if the leak is taken into account.
- RF tests started on December 5<sup>th</sup>:
  - The tube showed excellent potentialities: Within four days, it was possible to reach nominal parameters (90 kV, 75 A) and extract 2 MW of output power with an efficiency of 45% on the right mode. Pulse lengths were limited to ca. 1 ms pulses. It should be noted that no particular optimization other than the magnetic field value was done, in particular the depression voltage was arbitrarily set to 30.5kV – at the nominal 35 kV, the efficiency would have exceeded 48%. Further optimization appeared easily possible. See both figures on next page.
  - No low frequency oscillations were observed. The new beam tunnel concept was again (after the pre-prototype measurement) validated at short pulse on this tube.
  - The microwave beam symmetry was measured with thermal paper and found to be very good, and in agreement with experiments and simulations made at KIT (see figure on page 15).
  - One strange observation is that the mode's starting currents were unexpectedly high.
- An internal ceramic RF absorber failed on December 9<sup>th</sup> during an accidental (but not uncommon) operation under wrong mode rotation, putting an early end to the experimental phase. It is under discussion if the mode jump is indicating a reduced stability region.

The short reminder of the year was dedicated to post-evaluation of the event and the measurements, as well as on discussions of the implications. This will be continued in 2012, the possible consequences and conclusions are not established at the end of 2011.



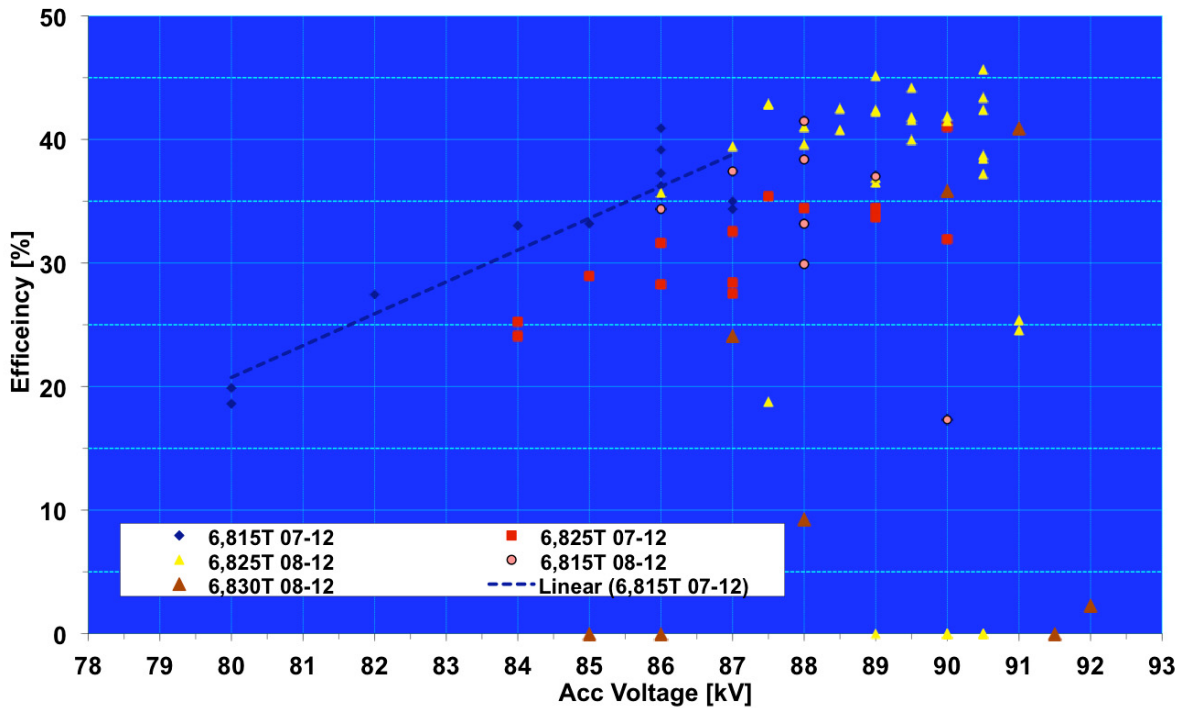
*C. Lievin (TED) fixing the vacuum leak.*

TH1508R-Output Power VS Acc Voltage

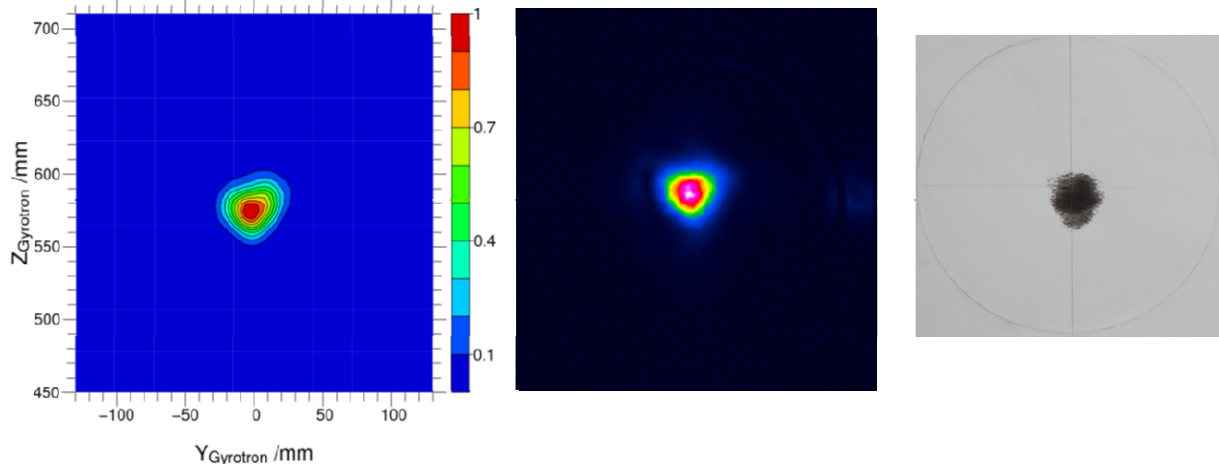


Measured RF output power of the industrial prototype for different magnetic field settings.

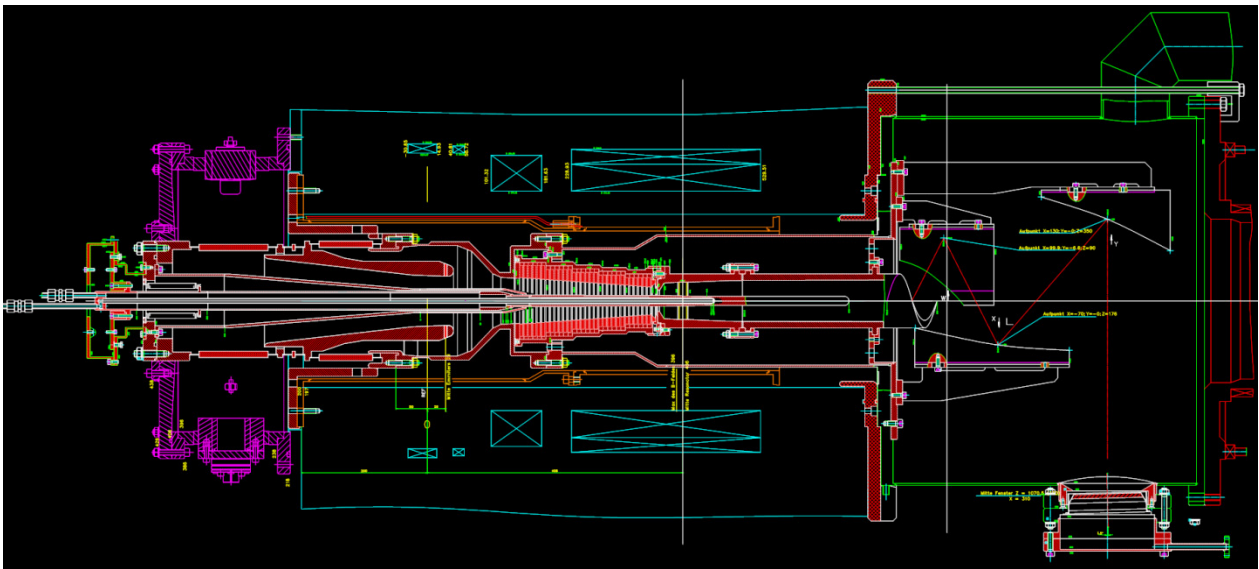
TH1508R-Efficiency VS Acc Voltage



Measured total efficiency of the industrial prototype for different magnetic field settings. Note that due to the short experimental time the efficiency was not optimized.



The RF output beam pattern of  $TE_{34,19}$  in simulation (left, linear scale), thermal camera measurement at the KIT-pre-prototype (mid) and in thermal paper measurement at the refurbished prototype (right) shows very good agreement and beam alignment at the RF window.



Sketch of the KIT pre-prototype gyrotron with small gyrotron body inside the magnet (rotated; up is right side). The brown shape is the cooled NC coil inside the magnet (blue), and the red thick material at the upper magnet end is a new isolating spacer that shifts the gyrotron in the right position and also enables depressed collector operation with high voltage standoff.

### High power tests at KIT and redesigns of the pre-prototype

Since no high power experiments during 2010 could be done, the plans for these experiments were shifted to 2011. After several problems were solved, it was possible to operate the pre-prototype again in short pulses with the 165 GHz gun. This gun is unfortunately not suitable for application of the additional normal conducting coil, which would be necessary for 2 MW operation, so only some 1 MW working points from former tests could be reproduced. The major result of these investigations was that the stray radiation could be reduced from 7% to 5.5% by employing the IAP launcher. This result motivates the further work on smoothed KIT rippled-wall launchers. During the course of the experiment, it became impossible to operate the gyrotron with the old gun, so the experiments were stopped after that result.

In order to regain the capability for hot experiments, the modular project was taken further. First, the aim was to use the refurbished KIT 170 GHz-gun in June to do a fast validation experiment relevant for the redesigned electron gun of the

industrial prototype. This experiment appeared to be of strategic relevance, since the decision on keeping or dropping the 2 MW concept was, and is still, under investigation through the TAP expert group on gyrotrons for F4E – this group was set up to elaborate a recommendation for TAP on the 2 MW program. After both the gun delivery and the decision point was delayed until end of the year, no further high power tests were done at KIT in 2011. The next tests are scheduled in February 2012. The preparation activities for these tests were running throughout the year, starting with design, manufacturing and test of a cooled normal-conducting (NC) coil for CW operation of the KIT Oxford instruments magnet, as required for 2 MW operation – the tests in 2009 were done with a pulsed uncooled NC coil. Mid of the year, after the gun delivery was delayed, the decision was taken to modify the pre-prototype already in the first step by equipping it with a small shaft that fits the cooled NC coil (see figure 6). These mechanical modifications, together with other mechanical adaptations and improvements, lasted until end of 2011 and will be finalized for the first tests.

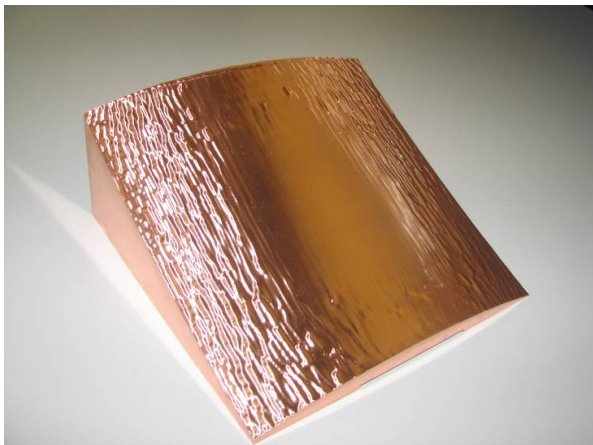
### Quasi-optical systems for ITER gyrotrons

The pre-prototype experiments mentioned above have shown clearly that the level of stray radiation created by the rippled-wall launcher and its quasi-optical system needs to be reduced. In addition, it was desired to increase the fundamental Gaussian mode content of the RF output beam further above 96%. Two approaches were pursued, first to equip the existing "first version" launcher with phase correcting mirrors (see figure) to increase the Gaussian Content, and second to refine the launcher design by smoothing its surface to achieve both lower stray radiation and higher Gaussian content, even with smooth mirrors. Both approaches required some code work and investigations on the best filtering methods for smoothing without degrading performance. Finally, both approaches succeeded and resulted in design improvements: While the phase correcting mirrors approach could increase the Gaussian content even to 99%, as shown in simulation (in cold tests 97% has been measured), the smoothed launcher approach reached around 97% in simulation with a significant reduction of stray radiation. The hardware for both designs is now available, cold measurements of the smoothed launcher are scheduled at the beginning of 2012, and both system variants will be tested in high power tests during 2012, too.

In addition, some redesign work for the 1 MW ITER backup design was started, since a check of the manufacturer TED showed that the first design would not fit the foreseen housing.

Finally, the dissertation of Jens Flamm on efficient simulations of tapered launchers was nearly finished by the end of the year, resulting in a new analysis code that can directly consider the small taper angles of real world launchers – until now, this could only be done in slow analysis codes like SURF3D.

Last not least, it should be mentioned that the KIT quasi-optical millimetre-wave VNWA had to be upgraded from outdated software and operating systems to make these measurements possible. In addition, the RF backward-wave tube sources had to be replaced by solid state devices, which in return called for new mixers to maintain system sensitivity. All these redesign and upgrade works were being done and are continued by trying to bring the backward wave tubes into operation again, for even increased system dynamic.



Phase correcting mirror for improved Gaussian RF beam content.

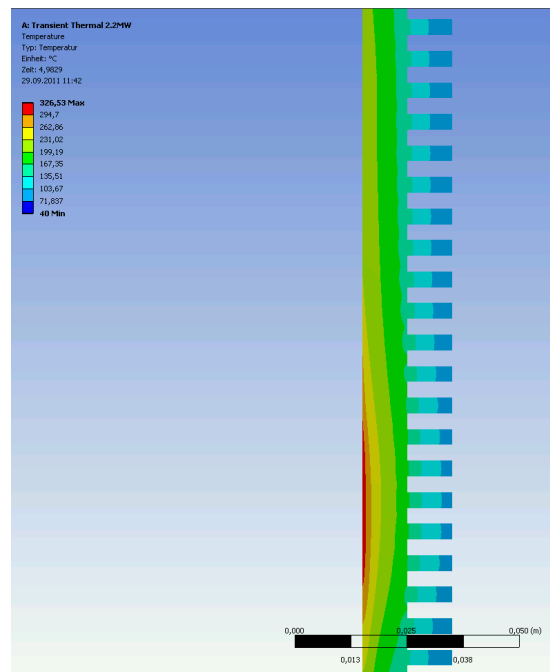
### Investigation of the ITER stray magnetic field on gyrotron operation

In the context of the F4E GRT-034 Task No. 1, the effect of the ITER stray magnetic field (SMF) on the operation of the European gyrotron has been studied. The SMF include the magnetic field generated by neighboring gyrotrons, the ITER tokamak and also fields generated by the ferromagnetic

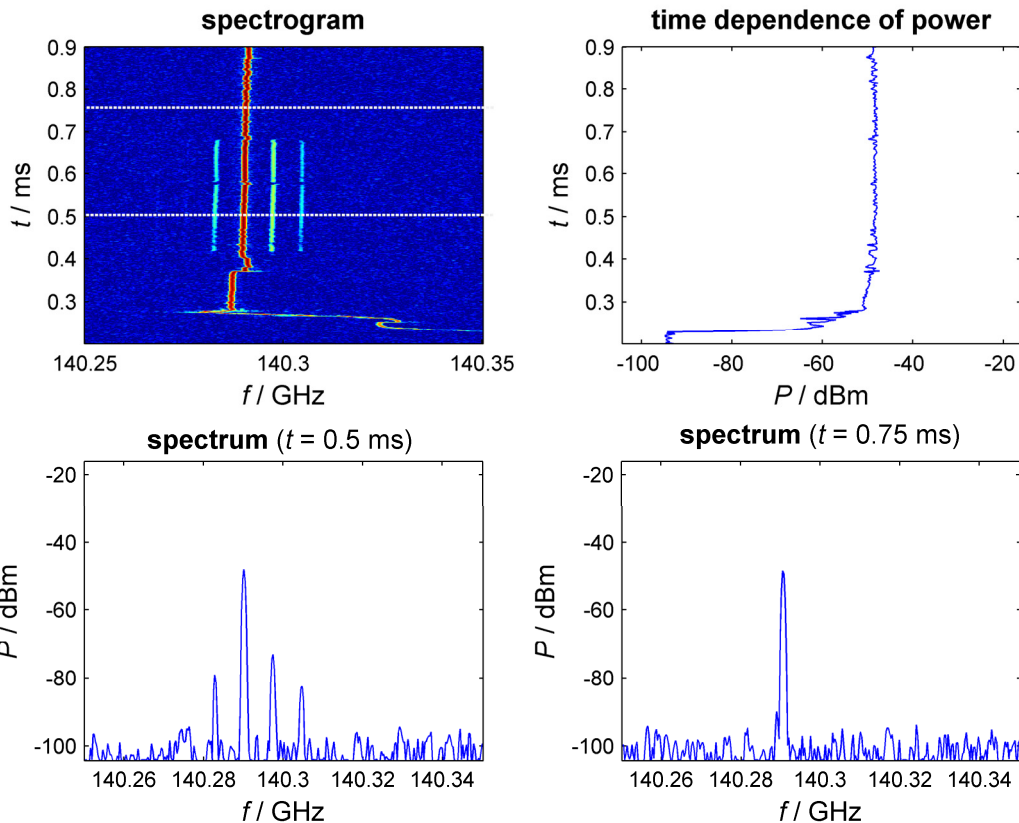
structural materials used in the ECRH building. The 3D self-consistent electrostatic code ARIADNE has been used for the evaluation of the stray magnetic field effect on the electron beam in the cavity and the collector region. It is shown that the beam parameters at the cavity of the gyrotron are not significantly affected by the SMF. On the other hand, the magnetic field lines in the collector region are significantly deformed in the presence of the SMF. A part of the electron beam is guided to the non-appropriately cooled part of the collector surface, while the electron beam power is distributed in a significantly smaller area of the collector walls. In order to address the problem, the use of an advanced transverse sweeping system is proposed which would allow to compensate the stray magnetic field and to improve the collector operation. A manuscript dedicated to this study with title "Study of the ITER SMF Effect on the EU 170 GHz 2 MW Coaxial Cavity Gyrotron" has been submitted to the journal IEEE Transaction of Plasmas Science.

### Investigation of the modulation capability of the ITER gyrotron

In the framework of the F4E GRT-034 Task No. 2, the power modulation capabilities of the 2MW, 170 GHz gyrotron for ITER have been addressed. One of the critical parts of the tube is the collector, which will experience an increased load in the case of modulated operation of the gyrotron (where the averaged efficiency will be decreased). One of the main results obtained from the transient thermomechanical analysis with ANSYS show that the less efficient modulation with the body power supply will raise the peak temperature and therefore the thermomechanical stress inside the collector wall beyond critical values and therefore should be avoided. As a consequence, the more efficient modulation with the main power supply should be preferred. Nevertheless, even in this case the peak temperature and stress will be slightly increased compared to the nominal operation point. Therefore more investigations are needed to optimize the collector surface shape or to increase the sweeping frequency.



Snapshot of the temperature distribution in the collector wall during nominal operation (obtained with ANSYS).



Measurement example of spectrum versus time at the SN6 W7-X gyrotron. It can be seen in the waterfall plot (top left) that, after a startup process, a modulation appears and vanishes again. The example is just shown in small band, the actual measurement bandwidth expands over two separate ranges of 2 GHz each.

#### Theoretical and experimental investigations on parasitic oscillations and related effects:

#### Simulation code improvement, ACI investigations and measurement system development

Triggered by the investigations on beam tunnel oscillations started in 2009, there is a growing interest on parasitic oscillations and their implications. While the beam tunnel oscillation problem appears solved, the search for parasitic frequencies in experiment resulted in a number of observations of high interest for further research. This coincided with observations of dynamic after cavity interaction (ACI) processes in simulation that led to similar RF spectra and had a clear influence on performance. For this reason, the activities on code improvement, particular ACI investigations as well as improving spectral millimetre wave measurement systems and applying them at gyrotron experiments were and are continuing.

Code improvement is done in the frame of a dissertation, aiming at incorporating enhanced numerical models for non-uniform magnetic fields in interaction simulations. The older code versions were assuming a constant magnetic field only or a simplified model, which is suitable inside the resonator, but increasingly loses dependability outside, in locations where the parasitic oscillations are generated. First versions of the new code are being tested; one simulation example featured a surprisingly good coincidence between simulated and parasitic frequencies.

In a broader view, investigations on the influence of numerically induced reflections on ACI and their reduction are ongoing, in strong collaboration with colleagues from HELLAS and CRPP.

First results show a strong influence of numerical reflections on ACI, but it is also found that when these influences are removed, strong dynamic ACI can still appear. All these code improvement activities are continued, aiming at creating a simulation tool that can reliably predict the appearance of parasitic oscillations and support their suppression by design.

On the experimental side, the next spectral measurement system is being developed as a part of another dissertation work. With the system developed in 2009, it became possible to display millimetre wave spectra in large bandwidth with high dynamic resolution, as long as the oscillations remained stationary enough over a millisecond range. The new system is utilizing fast digital oscilloscopes, receiving a downmixed time domain signal with bandwidths exceeding 2 GHz. This permits the calculation of instantaneous spectra, and with a special dual-receiver technique, undesired mixing signals can be safely excluded while actually increasing the usable bandwidth. The system is under development, with the particular problem of having to acquire large amounts of data very quickly and over long time ranges. A measured example is shown in figure 9. This high dynamic and wide band measurement technique is essential for investigations on parasitic oscillations, especially when the aim is to check by measurement that no such oscillation appears. Here it can be said that in the coaxial pre-prototype, after being equipped with the corrugated beam tunnel, it could be shown through such measurement systems that no parasitic RF oscillations were generated. While this result appears of little interest seen from the measurement technique side, it is very hard to obtain and at the same time an important performance feature of the gyrotron. Other gyrotrons, which are also under investigation, are still creating parasitic oscillation spectra, thus justifying the further development of the measurement systems.

## Conclusions and prospects

The unfortunate conditions for the coaxial gyrotrons during 2011 can unfortunately only partly be balanced by the impressive list of successes during the four days RF experiment phase of the industrial prototype. A significant part of 2012 will be dedicated to the post-evaluation of the measurements and of the damage event. Still it should not be overlooked that even the short measurement campaign represents a quantum leap for the industrial prototype: For the first time, a coaxial industrial prototype was operated reaching the high design power of 2MW at high efficiency of 45% and at good beam quality, without any parasitic oscillations.

A usual experimental program would now immediately call for a redesign and a next prototype. Since the damage comes under high time pressure and also otherwise difficult times for fusion technologies, the first thing that will happen now is a re-evaluation of project plans. It is currently open if the 1 MW backup design project will be re-activated. In any case, KIT will prepare for such an event.

Another parallel opportunity to go on with coaxial gyrotron developments is the modular project, which actually was set up to be a substitute in exactly such a damage case as experienced. This project will in any case start through the next pre-prototype tests scheduled in February, right after the refurbished gun was delivered. This experimental phase concentrates on component tests in short pulse, and the most important component to be redesigned and validated is the RF absorber scheme at the mirror box. In addition, this experiment will be operated with depressed collector, opening another chance to quickly determine efficiency limits in short pulse. Other components to be tested during the year are the new quasi-optical systems and several different beam tunnels.

The test stand will need further modifications in view of upcoming longer pulse tests. These activities will go on through the whole year. The same is true for the efforts on code improvement and measurement systems mentioned above.

## – IHM Advanced Gyrotron Research –

### Studies on electron beam diagnostic systems

One of the big unknowns in experimental gyrotron diagnostic is still the electron energy distribution at the absorption in the collector. Even though the distribution can be simulated with many tools today, a measurement in full operation is impossible yet. On the other hand, the energy distribution is one of electron beam features that determines the possible energy recovery, on the other hand measuring their after interaction would give valuable insight into the interaction mechanisms, as well as a good tool for code validation.

One possibility for creating a diagnostic tool for energy distribution is to measure the X-ray spectra that are emitted as bremsstrahlung at the collector. One of the problems is to find a solution to reconstruct the electron's energy distribution through de-convolution. Other problems are sensitivity and possible error sources through shielding. With such a diagnostic in hand, an important tool would be available for further optimisation of gyrotron efficiencies and simulation codes.

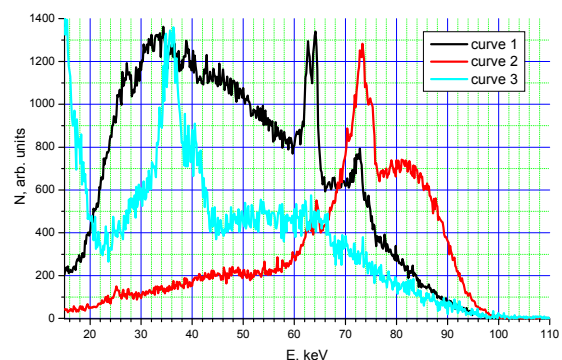
## Status of work at the beginning of 2011 and achievements in 2011

The X-ray electron beam diagnostic is currently developed within a collaboration between KIT and the St. Petersburg State Polytechnical University (SPbSPU), Russia. In 2010, an extensive theoretical study on the calculation of electron energy distributions from bremsstrahlung was accomplished. The result was that a very good reconstruction of energy distributions is possible if the radiation is measured through materials and walls which don't absorb strongly, like the ceramic isolators on the gyrotron or additional windows, for example at the collector.

In 2011, an X-ray spectrometer "AmpTek X-123CdTe" was purchased and sent to St. Petersburg for first experimental tests. Unfortunately the transfer caused customs problems in Russia which delayed the whole project by several months and made it impossible to continue the measurements on a KIT gyrotron at the end of the year. Nevertheless, experimental measurements could be done with a "Introvolt 120" X-ray source. Several spectra were investigated (see figure). It was found that the calculation of electron energies from measured data required a modification of the software developed in 2010, to take into account distortions and characteristic lines and to pre-process the measured data accordingly. With all these modifications, it was possible to reconstruct test spectra created by running the source sequentially at different voltages. Using such measurements, the influence of the pre-processing parameters was studied in detail (figure 11). After these tests finished successfully, a shielding box for the spectrometer was designed to reduce the influence of both external electromagnetic influences as well as the strong static magnetic field at the gyrotron.

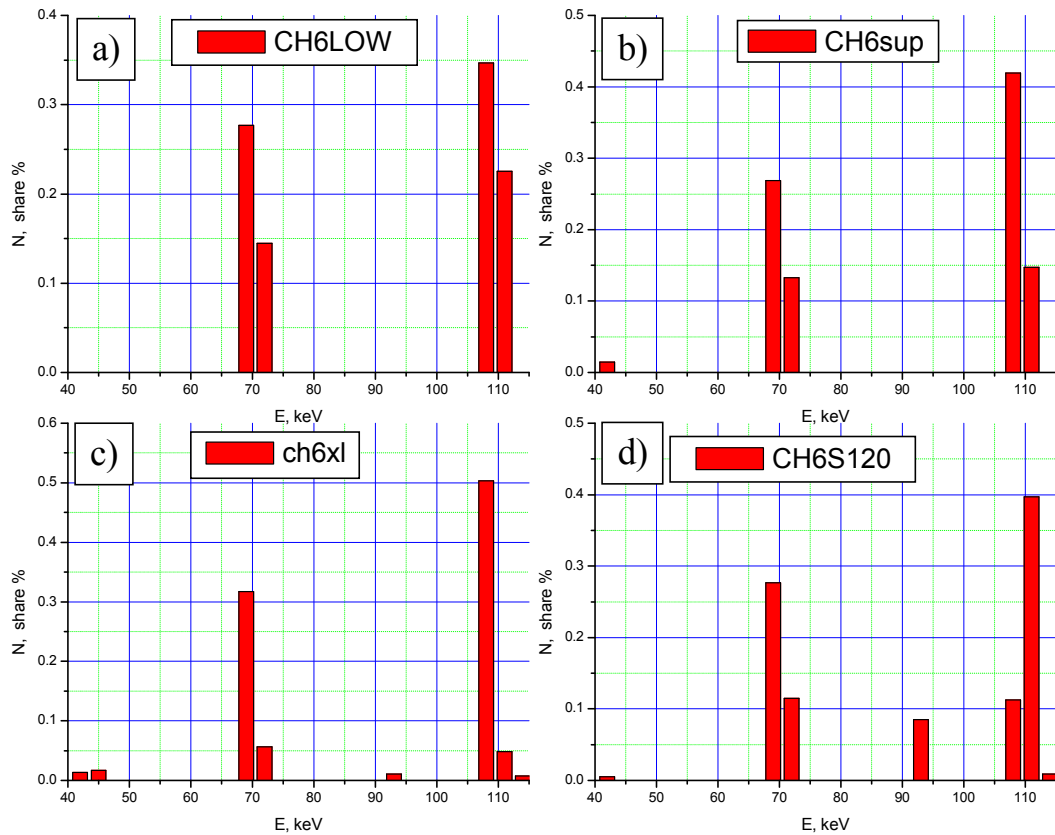
## Conclusions and prospects

The experimental tests foreseen at KIT could not be done due to the lack of a suitable gyrotron experiment. Through the experimental preparation with the "Introvolt 120" X-ray source and the corresponding code modifications, the necessary experience was gathered to continue with measurements on a gyrotron at KIT. For this, it is planned to equip the step-tunable gyrotron with a dedicated collector that features a top window for measurements. The shielding box for the spectrometer was already built.



*Photon spectra of different types measured with X-ray tube with tungsten target at  $U = 100$  kV – for different conditions of X-ray generation and propagation to spectrometer sensor.*



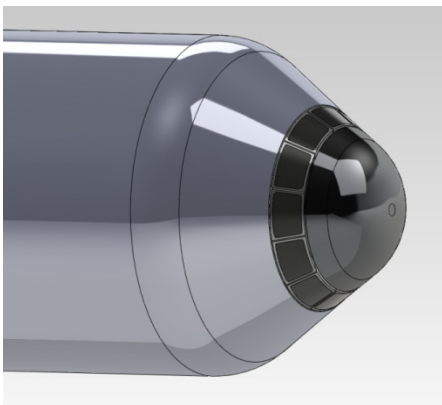


Electron energy distributions reconstructed from X-ray spectrum for X-ray operation regime "100 s at 110 kV + 75 s at 70 kV" with usual basis (energy points are  $eU = 33, 36, \dots, 120$  keV, step 3 keV) and different weight functions on energy discretization intervals and steps:

- the usual weight function  $W = E^2$ ;
- the same weight function divided by 3 in an interval near characteristic radiation lines;
- the same weight function divided by 10 in an interval near characteristic radiation lines;
- weight function is equal to basic function for the highest energy  $W = A_{120}(E)$ .

### Design of a low power gyrotron for the test of a new emitter concept

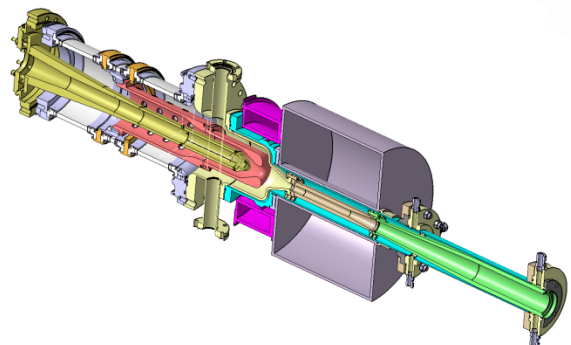
The design phase of a 28 GHz, 15 kW gyrotron for the test of a new segmented emitter is nearly finished. The new emitter type is based on small individual emitter rods, heated in the rear part of the segment. The goal of this project is to combine several segments to a ring-shaped structure to replace the conventional emitter ring. This concept allows to influence the emission current of each emitter segment and therefore enables the experimentalist to control the azimuthal homogeneity of the emission, which is not possible in the case of conventional ring-shaped emitters.



Drawing of the cathode section with segmented emitter.

This work is done in collaboration with Calabazas Creek Research (USA) which will design and build the cathode part of the tube in two variants, one equipped with the new segmented emitter (see Fig. left part) and one with a conventional ring-shaped emitter for comparison measurements.

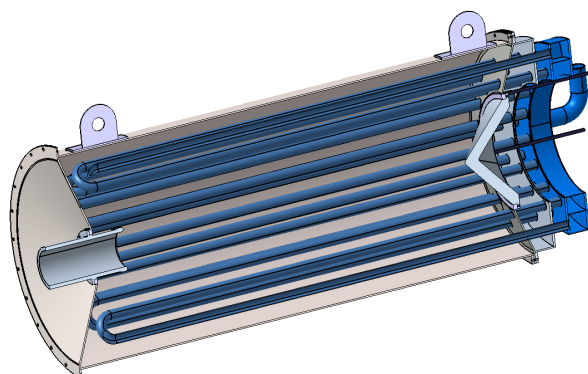
All other parts of the gyrotron are under development at IHM and reached now the final design phase (see Fig. right part), including the electron beam optics, cooling, material selection and UHV technology. First brazing tests with relevant materials have been performed at the IHM mechanical workshop.



Drawing of the complete test gyrotron.



The stainless steel microwave load prepared for the second measurement in 2011.



### Design and test of a high power stainless steel microwave load

Conventional high power microwave loads usually use a ceramics coating to absorb the RF power. Unfortunately this concept has the drawback that local hot-spots may appear on the load surface that will cause ablation of the coating. To avoid this problem, we designed a load manufactured solely from stainless steel and increased the overall absorbing area of the device with additional U-shaped stainless steel pipes. Since experiments in 2010 without active cooling of the load showed promising results, we equipped the inner pipe structure with water cooling (leaving the outer structure still without active cooling). The results obtained with this set-up allowed RF pulses of 550 kW for 30 s and 780 kW for 20 s, respectively, indicating a significant performance increase compared to the measurements of 2010.

## Step-Tunable Gyrotron Development

### Introduction

In recent years electron cyclotron resonance heating and current drive (ECRH and ECCD) has been established as a successful instrument in magnetically confined fusion plasmas. Gyrotrons are the unique devices which meet the extraordinary requirements of those applications: output power in the MW range, 100 – 200 GHz output frequency, and pulse length of several seconds up to continuous wave (CW). Due to its excellent coupling to the plasma and the very good localization of the absorbed RF power, ECRH is applied in present day machines and is also foreseen in large forthcoming fusion project: it will be the main heating system for the stellarator W7-X which is currently under construction and it will play a major role in the ITER tokamak. In particular advanced tokamaks are operated in a plasma regime where MHD instabilities may limit the performance are present. To a large extent the stability in a tokamak is influenced by the distribution of the internal plasma currents which can be manipulated by the injection of RF waves. The location of the absorption of RF waves with the angular frequency  $\omega$  is dependent on the resonance condition  $k_z v_z = \omega_c$  ( $k_z$ : z-component of the wave number,  $v_z$ : electron velocity along z-axis). Thus, by changing the wave frequency  $\omega$  the absorption can be moved to any radial position where the local cyclotron frequency of the electrons  $\omega_c$  holds for the expression above.

Industrial gyrotrons in the relevant frequency range with an output power of about 1 MW are usually designed for a fixed frequency. However, frequency tunable gyrotrons are not a standard product since these broadband tubes require additional optimization of major components of the gyrotron like the electron beam forming optics, cavity, quasi-optical mode converter and output window.

For experiments on plasma stabilization at ASDEX Upgrade (IPP Garching) with advanced ECRH and ECCD, multi-frequency tunable (105 – 143 GHz) 1-MW long-pulse gyrotrons are highly needed.

### Experiments with modified profile of resonator.

According to our program established in 2010 it was decided to modify the profile of the up-taper in the resonator in order to suppress the effect of After Cavity Interaction (ACI) of the spent electron beam with a traveling EM wave. The ACI effect was observed in numerical simulations and was believed to be the possible reason for low mode purity of the RF beam at the output window, and reduced efficiency of the gyrotron.

The machining of the new resonator was performed at the IHM workshop in order to reduce the costs. The profile of the produced resonator was measured and it was found within the range of acceptable tolerances.

Experiments with a new resonator started in August and continued till October 2011. During that period various comparative measurements have been performed allowing conclusions on the influence of the up-taper geometry on the performance of the gyrotron, based on the assumption that parasitic frequencies are excited in the up-taper. Experimental measurements showed that at usual operation condition a specific parasitic oscillation was still present with each excited cavity mode (at different frequencies). A detailed study of the dependency of the frequency of parasitic oscillations on cathode voltage and magnetic field was performed.

The power measurements were made for several cavity modes at different frequencies for comparison with the original resonator and, in addition, at higher frequency range four modes with radial number 9 were studied.

With the short pulse experiment It was found that for a number of modes, which have the matching caustic radius, it was possible to obtain nearly one megawatt power at nominal beam current and a efficiency of about 26 %. Though according to the calculations of the electron beam properties the pitch factor (ratio of perpendicular to parallel electron velocity) is larger than a nominal one. Operation of the gyrotron at higher power was followed by the appearance of both high frequency parasitics and low frequency electron beam instability in the range of few tens megahertz.

In the following table the list of measured modes is reproduced with achieved power and beam properties used during operation.

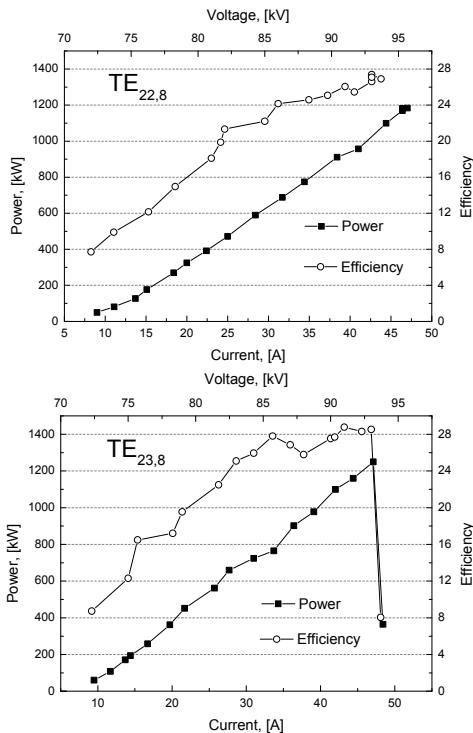
Mode	Freq. [GHz]	Uc, [kV]	Ib, [A]	P, [kW]	Eff., [%]
TE <sub>19,7</sub>	119,5	93,0	41,1	880	23,0
TE <sub>20,7</sub>	124,1	91,7	41,0	890	23,6
TE <sub>22,7</sub>	130,9	90,0	40,0	900	25,0
TE <sub>22,8</sub>	140,0	91,7	41,0	960	25,5
TE <sub>23,8</sub>	143,3	90,3	39,1	980	27,5
TE <sub>24,9</sub>	155,9	91,7	41,1	980	26,0
TE <sub>25,9</sub>	159,2	91,0	40,4	1000	27,2
TE <sub>26,9</sub>	162,5	89,7	40,4	990	27,3
TE <sub>27,9</sub>	165,9	90,0	40,4	950	26,1

Mode	Freq. [GHz]	Uc, [kV]	Ib, [A]	P, [kW]	Eff., [%]
TE <sub>19,7</sub>	119,5	93,0	41,1	880	23,0
TE <sub>20,7</sub>	124,1	91,7	41,0	890	23,6
TE <sub>22,7</sub>	130,9	90,0	40,0	900	25,0
TE <sub>22,8</sub>	140,0	91,7	41,0	960	25,5
TE <sub>23,8</sub>	143,3	90,3	39,1	980	27,5
TE <sub>24,9</sub>	155,9	91,7	41,1	980	26,0
TE <sub>25,9</sub>	159,2	91,0	40,4	1000	27,2
TE <sub>26,9</sub>	162,5	89,7	40,4	990	27,3
TE <sub>27,9</sub>	165,9	90,0	40,4	950	26,1

Frequency, power and efficiency of measured modes at nominal parameters of operation.

In the table the efficiency of short pulse operation is calculated without taking into account the effect of voltage depression. In a long pulse operation one could expect higher efficiency to be obtained.

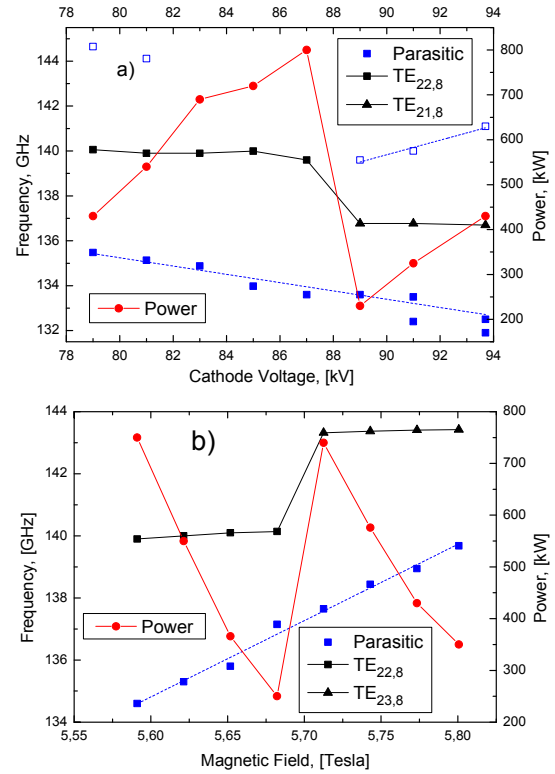


Output power in dependence of the beam current for the modes TE<sub>22,8</sub> and TE<sub>23,8</sub>.

The frequency dependency of parasitic modes on the cathode voltage and magnetic field was studied. The results of the measurements are plotted in the following figure (a) and (b). Parasitic oscillation demonstrates gradual dependence both on the beam voltage/energy and magnetic field amplitude. The change of the working mode in the cavity from TE<sub>22,8</sub> to

TE<sub>23,8</sub> nearly does not affect the frequency of the parasitics. From this we may conclude that parasitic and gyrotron oscillations are not strongly coupled and the parasitics may occur at different sections of the resonator or even in the downtaper of the beam tunnel section. In addition, in contrast to the gyro mode the parasitics show a stronger dependence on the magnetic field and the cathode voltage change which is characteristic for BWO type interaction.

At the moment the origin of this oscillation is still the subject of investigation.



Frequency of resonator and parasitic modes in dependence of the voltage (a) and magnetic field (b).

A special study was performed to investigate the influence of beam disposition on the RF field profile pattern measured by IR-camera. The Gaussian content detected for the main mode TE<sub>22,8</sub> is at the value 79% instead of 93% expected from calculations of the Quasi Optical System (QOS). Such a low value of Gaussian content was stably reproduced at different positions of the electron beam in the cavity and various regimes of operation by the same mode of oscillation. In principle, in the case of multimode oscillation the power of each mode must be sensitive to the operation. Therefore, the beam pattern must strongly vary, which was not the case. A new type of QOS having higher efficiency is developed (see below).

#### New quasi-optical mode converter.

A new type of quasi-optical mode converter for the step-tunable gyrotron was developed with the use of an improved code for the launcher and mirrors synthesis. The improvements of the code reduce the stray radiation from the launcher and, therefore, thermal loading on inner construction parts of gyrotron. Generally the Gaussian content is higher for the main operating modes.

Mode	Frequency [GHz]	FGMC [%]
TE <sub>17,6</sub>	104.9	97.8
TE <sub>18,6</sub>	108.2	96.8
TE <sub>19,6</sub>	111.5	94.7
TE <sub>19,7</sub>	120.8	97.8
TE <sub>20,7</sub>	124.1	98.9
TE <sub>21,7</sub>	127.4	98.2
TE <sub>21,8</sub>	136.7	93.2
TE <sub>22,8</sub>	140.0	95.6
TE <sub>23,8</sub>	143.3	97.4

*Calculated Fundamental Gaussian Mode Content at the last Brillouin zone of the launcher for 9 modes.*

The Fundamental Gaussian Mode Content (FGMC) of the field calculated at the last section of the launcher is presented in the above table. The launcher will be used together with a quasi-elliptical mirror and two new toroidal mirrors.

#### **CVD-diamond Brewster window**

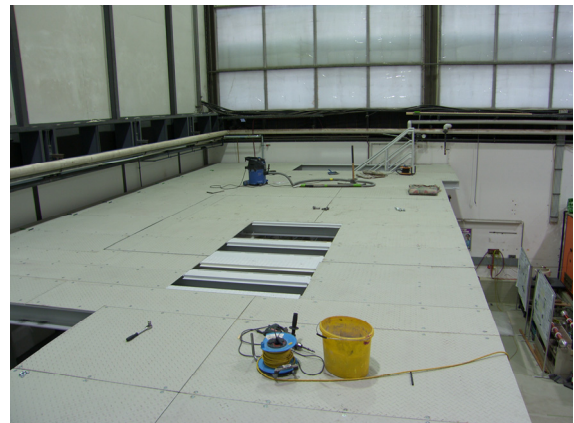
The efficient operation for a large number of operating modes at different frequencies is only possible by using a broadband synthetic diamond Brewster window fabricated by chemical vapor deposition (CVD). Due to the large Brewster angle of 67.2° deg, the diameter of the disk has also to be rather large in order to have sufficient aperture for the RF beam. One disk

with a thickness of 1.7 mm and a diameter of 140 mm was developed by Element Six and already delivered. This disk can be used for the elliptic shape of a Brewster window with an effective aperture of 50 mm.

Because of the ellipticity, the stresses during the brazing procedure are different from circular disks. These stresses were calculated to be increased by a factor of 1.3. After successful preliminary brazing tests at TED with a quartz disk and a small diamond disk the brazing of the 140 mm diamond disk was finished at TED. This disk will be introduced into housing, experiments with the gyrotron are foreseen.

#### **– Launcher Handling Test Facility (LHT) –**

After a successful period of thermohydraulic/IR measurements of structural components for the ITER ECRH Upper Port Plug (UPP) Launcher (Prototyping and Testing) a extension of the test facility was planned and executed in 2011 and continued in 2012. The extension consists on a large platform over the full width of the IHM experimental hall to build a first floor for access of the test stand from above. The control unit office will be built in a special room/box on that platform containing operation PCs and electronics. The construction of a huge vacuum vessel for outgassing measurements with a rail system to move the heavy structural components into vacuum was finished end of 2011. The start of new experiments is foreseen for May 2012. To be more independent on other experiments in the experimental hall, the electrical power connections are rebuild with higher power and separated from the other experiments of IHM.



*Pictures from the construction phase of the new LHT platform.*

## Involved Staff:

### KIT/IHM

K. Baumann  
Dr. B. Bazylev  
K. Boscher  
Dr. G. Dammertz  
Dr. J. Flamm (KIT, CS)  
Dr. G. Gantenbein  
Dr. H. Hunger  
Dr. Yu. Igitkhanov  
Dr. S. Illy  
Prof. J. Jelonnek  
Dr. J. Jin  
Dr. S. Kern  
Dr. I. Landman  
R. Lang  
W. Leonhardt  
M. Losert  
D. Mellein  
A. Meier (KIT, IAM-AWP)  
S. Miksch  
A. Papenfuß  
Dr. S. Petchanyi  
Dr. B. Piosczyk  
Dr. A. Samartsev  
Theo A. Scherer  
(KIT, IAM-AWP)  
A. Schlaich (KIT CS)  
D. Schmid  
Dr. R. Schneider  
W. Spiess  
Dr. D. Strauss  
(KIT, IAW-AWP)  
J. Szczesny  
Prof. M. Thumm  
J. Weggen

### Humboldt Universität Berlin:

Prof. G. Fußmann  
R. Brose

### Eindhoven University of Technology:

J.W. Osterbeek, S. Paquay

### IPF

(University of Stuttgart)

H. Höhnle  
Dr. W. Kasperek  
H. Kumric  
C. Lechte  
**R. Munk**  
F. Müller  
Dr. B. Plaum  
P. Salzmann  
K.H. Schlüter  
U. Stroth  
**A. Zeitler**

### M. Bohner

**H. Dadgostar,**  
**X. Glad**  
**J. C. Ruiz**  
(Diploma/Master students)

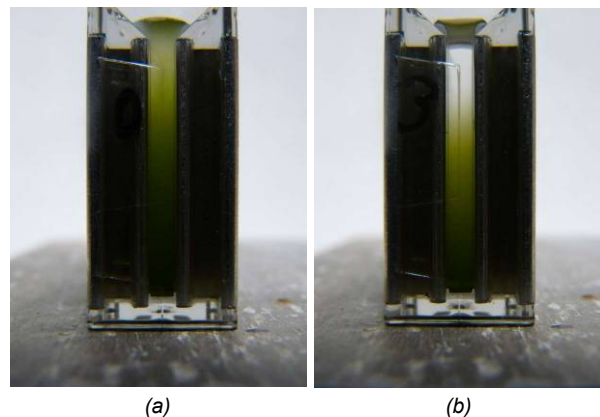
### IPP

(Greifswald/Garching)

B. Berndt  
Dr. H. Braune  
Dr. V. Erckmann (PMW)  
F. Hollmann  
L. Jonitz  
Dr. H. Laqua  
G. Michel  
F. Noke  
F. Purps  
T. Schulz  
P. Uhren  
M. Weißgerber

biomass has to be separated from culture medium. Conventional methods like centrifugation or filtration combined with flocculants or coagulants are expensive, time-consuming and energy-intensive. Basic idea of this work was to compensate ionic surface charges on microalgae cells by PEF treatment. Surface charges counteract densification due to repelling coulomb forces. After membrane electro-permeabilization charges can equilibrate.

First experiments, made on *Auxenochlorella protothecoides* (A.p.), revealed, that PEF- treated algae bodies showed different settling behaviour, depending on the applied pulse duration  $t_{imp}$ , electrical conductivity K and the amount of energy W delivered to the microalgae suspension. In all cases the electric field strength was  $E = 5 \text{ kV/cm}$ .

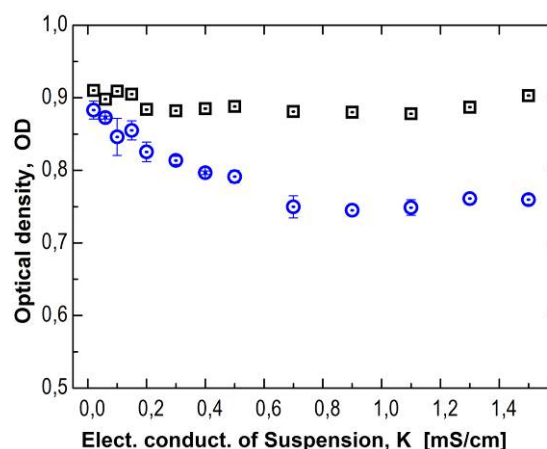


*Sedimentation: Untreated (a) an PEF- treated (b) microalgae suspensions from Auxenochlorella protothecoides (A.p.),  $K = 0.008 \text{ mS/cm}$ .*

Compared to the control sample, the application of short PEFs within a pulse length range of  $1 \mu\text{s}$  to  $10 \mu\text{s}$  showed no significant improvement of the sedimentation behaviour of microalgae suspensions.

Contrary, MA processing with longer pulse duration,  $t_{imp} = 1 \text{ ms}$ , results in a different behaviour. As shown on the images above, the long-pulse-treated sample exhibits a more efficient settling behaviour as the untreated control.

Furthermore, the electrical conductivity K affects the settling speed of MA. For demonstration, MA were suspended in buffer agents with electrical conductivities ranging from  $K = 0.02$ - $1.5 \text{ mS/cm}$ . The results of K-variation experiments with A.p. are shown in the following diagram.



*Optical density (OD) as a function of the electrical conductivity (K) of A.p. MA suspension processed with PEF,  $t_{imp} = 1 \text{ ms}$ .*

Funded by BMBF project 03FUS0010

## HGF Program: ENERGY

### Renewable Energies (EE)

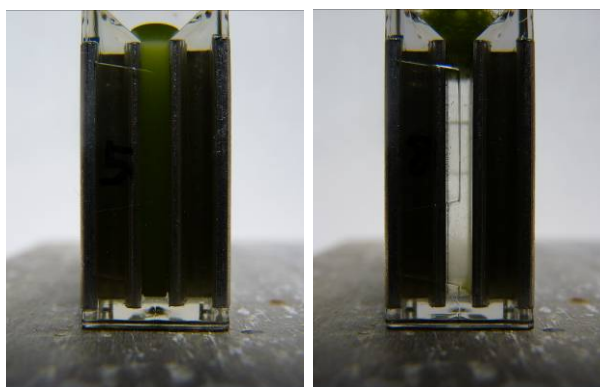
#### – Conditioning of Biomass by Pulsed Power Techniques –

This year's work mainly focussed on pulsed electric field (PEF) assisted downstream processing of microalgae. Emphasis was laid on biomass harvesting from culture medium and on cell component extraction by continuous flow processing. PEF treatment of microalgae proved to be an efficient method for cell component extraction. After treatment, water-soluble components efficiently emerge from the cells. The residual biomass still contains lipid droplets, which can be extracted at higher efficiency due to initial PEF treatment by solvent extraction. In all cases, the yield of extracted cell components could be improved by a factor of 3-4.

#### Pulsed Electric Field (PEF) assisted harvesting of microalgae (MA) from culture suspension

The concentration of microalgae biomass in culture medium is typically 0.01 % to 0.2 % by weight. Regardless of subsequent use, such as for pharmaceutical purposes, as food supplement or feedstock for biofuels, microalgae

For low buffer conductivities,  $K = 0.02\text{-}0.05$  mS/cm, the OD, measured approximately at half height of the liquid column, showed no significant differences. Consequently, the settling characteristic of treated and untreated samples is identical. When increasing  $K$ , the settling behaviour of the treated MA suspension clearly improves up to an optimum at  $K = 0.7$  mS/cm, most probably resulting from shortening of the membrane charging time due to increasing buffer conductivity. From that point, the sedimentation velocity of the algae bodies remained constant up to a conductivity of  $K = 1.5$  mS/cm. In case of a constant number of pulses delivered to the suspension, the applied energy linearly correlates with the electrical conductivity. A treatment energy of  $W = 437.5$  kJ/kg is required at the most advantageous conductivity of  $K = 0.7$  mS/cm. At the current state of work it can be concluded, that this is not a competitive value for algae harvesting.



(a)

(b)

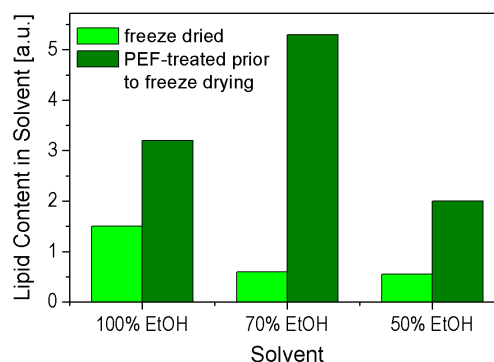
*Flotation: Untreated (a) and PEF- treated (b) microalgae suspensions from Auxenochlorella protothecoides (A.p.).  $K = 2.0$  mS/cm.*

When working at a conductivity of  $K = 2.0$  mS/cm and processing the samples with 20-25 pulses, another effect can be observed. By applying energies on the order of  $W = 1$  MJ/kg water is dissociated into  $H_2$  and  $O_2$ , bubbling up inside the cuvette and transporting algae bodies from the MA suspension to the surface. In this way algal cells are separated from the culture medium to a high degree. This so called 'flotation-process' clears the suspension, as shown on the images.

#### **Pulsed electric field (PEF) assisted extraction of lipids from microalgae**

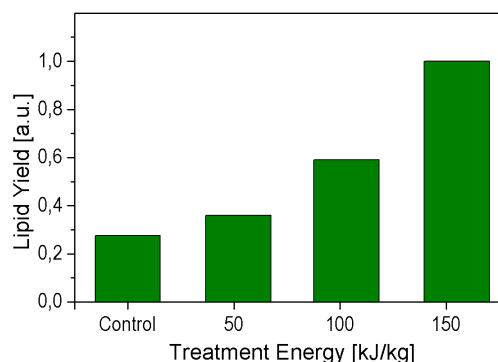
After establishing the Sulfo-Phospho-Vanillin-Reaction last year, a fast and reliable quantification of the lipid content in solvent extracts was available.

Conventionally, for extraction of lipids from plant cells and tissue freeze-dried source material is required, since remaining intracellular water impedes solvent access to the hydrophobic cellular content. By admixing of solvents of different concentrations to samples of freeze dried microalgae, it was found that ethanol in a final concentration of 70% results in maximum lipid yield. The application of PEFs to microalgae suspension prior to freeze drying clearly improves the extraction efficiency as shown below.



*Lipid content in the algae-extract with and without PEF pre-treatment. The concentration of ethanol in the solvent was varied. Electric field strength was 35 kV/cm, the applied specific energy was 180 kJ/kg. The lipid content was determined by the Sulfo-Phospho-Vanillin-Reaction.*

Freeze drying is a very energy-consuming process, which is only reasonable for laboratory scale experiments or for the production of high valuable substances, not for the extraction of lipids as feedstock for biofuel synthesis. The possibility of lipid extraction from wet microalgae biomass would considerably contribute to a reduction of process costs. For extraction experiments from wet biomass, the microalgae suspension was concentrated to 100 g dry weight per litre prior to PEF treatment. The pulse duration was  $T = 1$   $\mu$ s.



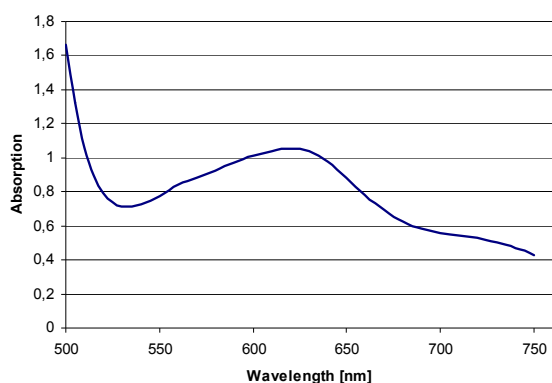
*Lipid extraction from wet algae biomass with 100% ethanol and variation of the applied specific energy. Electric field strength was 35 kV/cm. The lipid content was detected with the Sulfo-Phospho-Vanillin-Reaction.*

For extraction from wet biomass, the amount of remnant water in the algae pellet after centrifugation was determined. Successive addition of 100% Ethanol resulted in a final solvent concentration of 70% during the extraction process, which was found to provide best results. Furthermore, the results show a clear dependence of the lipid yield from the applied specific energy. When applying a treatment energy of  $W = 150$  kJ/kg a 4 fold increase of extractable lipids could be obtained. At the chosen treatment energy parameters the value pattern still does not show saturation behaviour. Future experiments will clarify whether lipid yield can be enhanced at higher treatment energies.

#### **Fast diagnostics for sugars and polysaccharides extracted from microalgae**

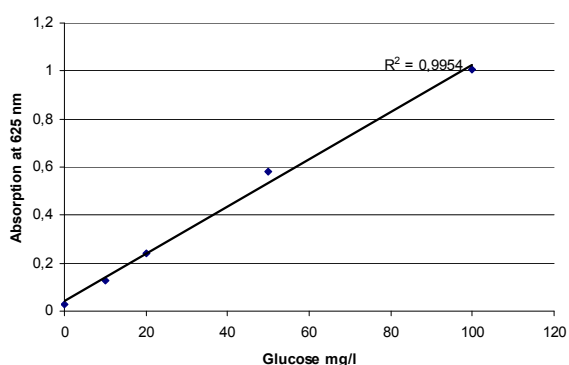
Colorimetric assays for lipid (Sulfo-Phospho-Vanillin-Reaction) and protein (Bradford) diagnostics have been established in laboratory routine and have proved to perform reproducibly and reliably. As a possible candidate for sugar and polysaccharide diagnostics, the reaction of sugars with the organic reagent anthrone was tested for applicability for quantification of saccharides extracted from microalgae.

The test is based on the reaction between carbohydrates and anthrone, a tricyclic aromatic ketone, in concentrated sulphuric acid, in final state exhibiting a green-blue colour. During heating, the strong acid hydrolyses the carbohydrates to monosaccharides, which are dehydrated to furfural derivatives that finally react with anthrone.



Absorption spectra of anthrone after reaction with carbohydrates from microalgae. The absorption of 1,06 at 625 nm corresponds to a concentration of carbohydrates of 110 mg/l.

The absorption spectra of the complex formed shows a maximum at 625 nm and is determined spectrophotometrically. Analogous to the lipid- and protein-tests, the increase of absorbance is proportional to the amount of formed complex, and thus to the amount of carbohydrates dissolved in the extract.



Calibration curve of the anthrone test using glucose as standard.

For evaluation, the measured absorbance at 625 nm is compared to a calibration curve, obtained from the analysis of glucose at different concentrations as a standard. After several modifications the test was improved to work reproducibly with carbohydrates extracted from microalgae at concentrations in the range from 0.5 mg/l up to 200 mg/l. The anthrone-test has proven satisfactory sensitivity for analysis of microalgae extracts. Samples derived from extraction experiments even require a dilution of 20- to 30-fold.

### Reproducible production of algae biomass for pulsed electric field treatment experiments

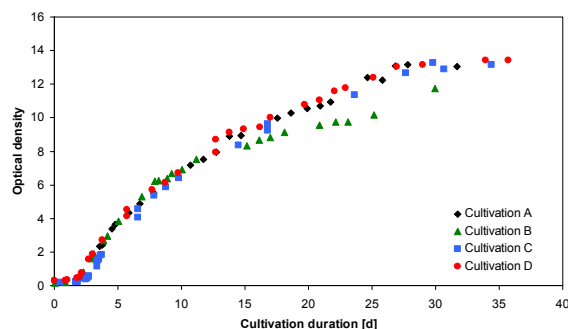
Many interesting compounds produced by microalgae are stored intracellularly. Cell walls and cell membranes are veritable barriers for the extraction of valuables. Therefore in most cases disintegration of the algae cells is necessary. Although a lot of research is currently going on in the field of algae cell disintegration, a method suitable for all microalgae species has not been found yet. The effectiveness of a certain method not only depends on the algae species but also on cultivation conditions and the cultivation status. Hence, for reproducible cell disintegration experiments it is necessary to

use “defined” algae biomass grown under controlled conditions.

Cultivations of the green fresh-water microalgae *Auxenochlorella protothecoides* were performed in a closed 26 l photo-bioreactor to provide defined biomass for the pulsed electric field treatment experiments. The algae were grown mixotrophically and axenically in TAP-medium. The batch-cultivations were carried out with continuous illumination at 25°C. The culture was aerated at a rate of 1000 cm<sup>3</sup>/min with an air carbon dioxide mixture containing 2.5% CO<sub>2</sub>.

The maximum biomass productivity was 0.6 g algae/l/day (dry weight (dw)). After 30 – 35 days of cultivation the algae were harvested at a biomass concentration of 4.5±0.5 g/kg (dw) and a lipid content of 15 – 20%. The harvested algae had a volatile solid content of 95 % and an upper heating value of 21 MJ/kg<sub>dw</sub> (measured from a concentrated algae suspension with a biomass content of 100 g/l (dw)).

The growth of the algae was monitored by optical density measurement of the suspension. A comparison of the growth curves of different cultivations of *Auxenochlorella p.* revealed a good reproducibility of successive cultivation runs. Hence, using the cultivation protocol described above defined biomass for PEF experiments can be produced in the annular photo-bioreactor.



Growth curves of cultivations of *Auxenochlorella protothecoides* in a closed annular photo-bioreactor.

### Pulsed electric field (PEF) treatment of *Auxenochlorella protothecoides* for cell content extraction (water-soluble components)

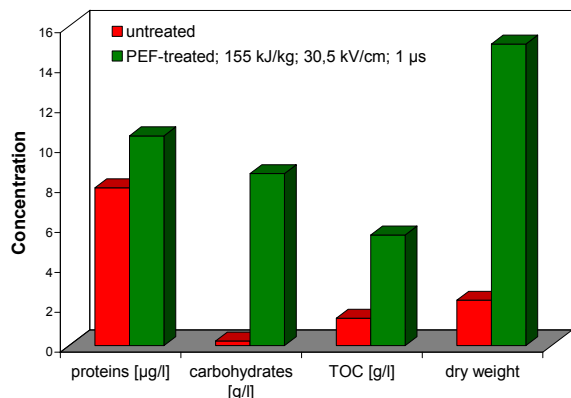
Experiments on cell disintegration of microalgae by PEF-treatment were performed on the fresh-water species *Auxenochlorella protothecoides*. Screening PEF treatment experiments were carried out in batch-mode using 800 µl electroporation cuvettes as treatment chamber. However, for profound analysis larger amounts of treated algae suspension were required. Therefore, a flow cell with a treatment volume of 2 ml and an electrode distance of 4 mm for the PEF treatment of suspensions was designed and manufactured.

For PEF treatment concentrated algae suspension containing 100 g/l biomass (dry weight) was delivered to the treatment chamber at a constant flow-rate of 6 ml/min. In order to detect the temperature change of the suspension due to PEF treatment the temperature at the inlet and outlet of the treatment chamber was measured. The treatment chamber was driven by a transmission line pulse generator, which delivered square pulses with a voltage amplitude between 8 kV and 20 kV, corresponding to an electric field strength of 20 kV/cm and 50 kV/cm. All energy data given in the following are related to concentrated algae suspension.

The influence of electric field strength and specific energy input on cell disintegration was investigated first. In all experiments the pulse duration was fixed to 1 µs. For a constant specific energy delivery of 160 ± 2 kJ/kg at different electric field strengths (23 – 43 kV/cm) the pulse repetition

frequency appropriately was adjusted between 1.0 and 5.5 Hz. The same procedure was used for variation of the specific energy input (52 - 211 kJ/kg) at a constant electric field strength ( $33.5 \pm 4.5$  kV/cm).

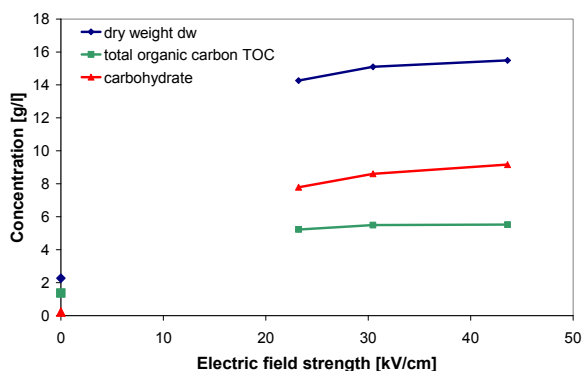
For all algae suspensions sham treatment cycles were performed identical to the PEF treatment procedure but without applying electric field pulses. After PEF treatment the samples were stored in the dark at 25°C for 40 min. Then conductivity and pH of the suspensions were measured. Subsequently, suspensions were centrifuged and the supernatant was used for further analysis.



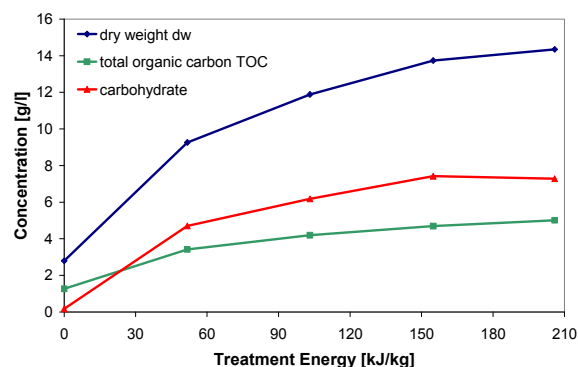
Spontaneous release of intracellular components after PEF treatment of *Auxenochlorella protothecoides*, TOC (total organic carbon).

Irrespective of the applied pulse parameters the conductivity of treated samples was always higher than that of the control samples, whereas the pH dropped slightly after PEF treatment. According to dry mass analysis of supernatant and pellet, 10 - 15% of the initial biomass remained in the supernatant. Inorganic compounds made up to 15 % of the supernatant dry mass. Besides inorganic ionic compounds that were responsible for the rise of the conductivity of the suspension organic matter leaked out of the cells. Compared to control samples the total organic carbon content (TOC) of the supernatant was up to 4 times higher after PEF-treatment. 60 - 70 % of the TOC of the treated samples can be ascribed to carbohydrates. The pH drop is most probably caused by low molecular weight acids that diffuse out of the cells. Lipids could not be detected in the supernatant.

In the range investigated the variation of electric field strength hardly changed the cell disintegration of *Auxenochlorella protothecoides*. Whereas the specific energy input had a large influence. Up to energy values of 100 kJ/kg the cell disintegration improved considerably with increasing specific energy input. Above this value the disintegration still improved at higher specific energy input but the influence diminished.



Influence of electric field strength, pulse duration: 1 μs, treatment energy: 155 kJ/kg, biomass density: 100 g<sub>dw</sub>/l.



Influence of specific treatment energy, pulse duration: 1 μs, electric field strength: 30 - 38 kV/cm, biomass: 100 g<sub>dw</sub>/l.

The electroporation of *Auxenochlorella protothecoides* results in a spontaneous release of intracellular soluble compounds into the liquid. Most of the organic compounds that leaked out of the cell were carbohydrates. In the range investigated the degree of cell disintegration was influenced by the specific energy input. In comparison, the influence of the electric field strength is low. This opens the possibility to go for semiconductor-switched lower-output-voltage pulse generator concepts for future applications, which are easier to operate and maintain.

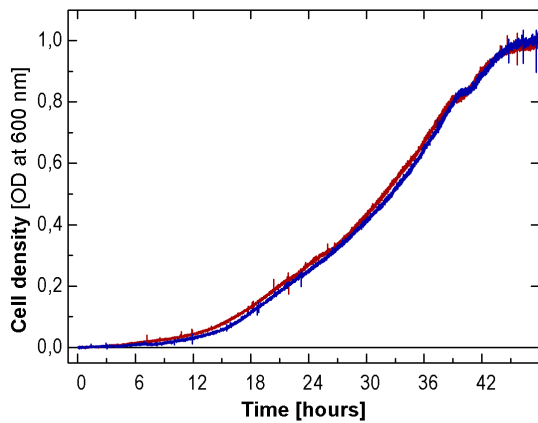
#### Stimulation of algal growth by nanosecond pulsed electric field (nsPEF) treatment

Previous work revealed, that nanosecond pulsed electric field (nsPEF) treatment of plant seedlings and fungi can stimulate their growth. Based on these results, at the beginning of 2011, a study focusing on stimulation of algal growth by nsPEF treatment was started. This study is funded by the Baden-Württemberg Foundation.

#### Determination of the optimal pulse parameters for ns PEF treatment of inoculum

In the first step PEF treated microalgal suspension was used as inoculum for subsequent cultivation in culture flask on an orbital shaker. The set-up consists of illumination (fluorescent lamps), shakers, peristaltic pump and two spectrometers with automatic data acquisition and storage. The nsPEF treatment of inoculum was performed in disposable electroporation cuvettes using an existing transmission line pulse generator. The size of culture flasks and volume of medium and inoculum was adjusted for reaching the stationary growth phase within 3-5 days. Optical density (OD) values (at 600 nm) of the algae suspension were measured at 600 nm, continuously recorded by two spectrometers and stored digitally. The treatment field strength was varied between 5 and 20 kV/cm, pulse duration between 25 ns and 100 ns and the number of pulses ranged from 10 to 40. Quite unexpected, in all cases the growth rate of cultures starting from treated and untreated inoculum showed no significant difference and was  $\mu = 0,07 \pm 0,02$  h<sup>-1</sup>.

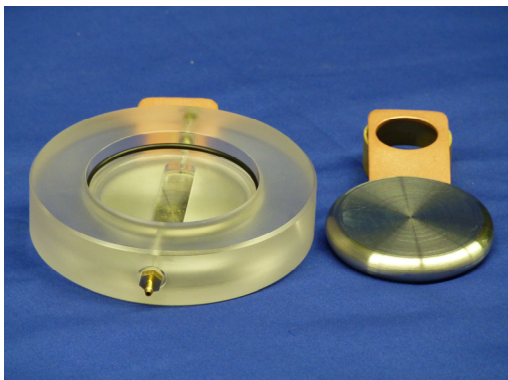




Algae culture growth, *auxenochlorella protothecoides*, with nsPEF treated inoculum (blue) compared to control (red).

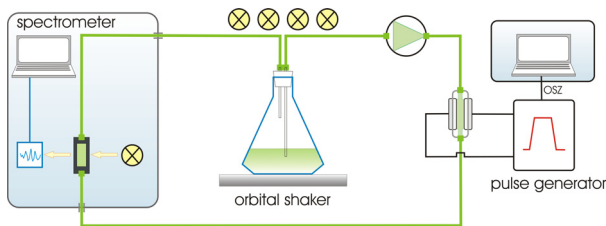
**Design of a continuous flow treatment cell and method evaluation**

Since PEF-treatment of inoculum didn't result in accelerated growth, four continuous-flow treatment cells were designed by electrostatic field calculation. The housings are manufactured of autoclavable polycarbonate. The construction allows easy cleaning access and avoids unintentional opening after autoclaving and during operation.



Continuous flow treatment cell manufactured of autoclavable polycarbonate and stainless steel.

The OD values were acquired and continuously recorded as described above. A MOSFET-switched 25 Ohm Blumlein pulse generator was integrated into the experimental setup as shown in the schematic below. Accuracy and reproducibility of the online OD measurement were verified by using a third spectrometer. OD measurements of aliquots of algae suspension confirmed results of the continuous OD measurement. Furthermore, microscopic cell count and optical density of two parallel microalgae culture runs developed identically.

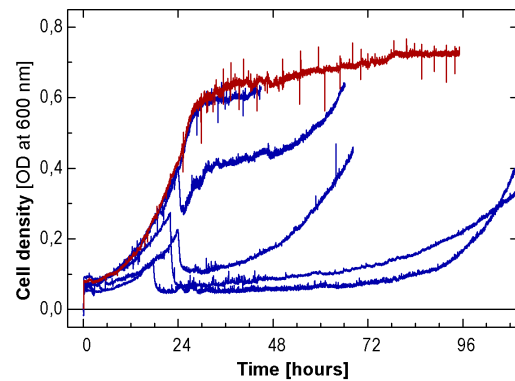


Experimental setup for continuous PEF treatment of algal suspension. Microalgae growth is detected by optical density measurement using a spectrometer enclosed into a shielding cabinet. The algae suspension was continuously exposed to electric pulses generated by a Blumlein pulse generator.

**Determination of algal lethality**

For stimulating algae growth, treatment parameters have to be chosen for not affecting lethality. At first approach, the lethal pulse parameters of PEF treatment of algae suspension were determined by colony counting on agar plates after incubation for 3 days. The algal suspension was exposed to electric pulses in disposable electroporation cuvettes. It turned out that the number of colony forming units (CFU) rather depends on the algal density of suspension than on the number of surviving cells. Hence, it was not possible to evaluate algal lethality by this method.

In the following, the algal lethality was evaluated by continuous optical density measurement using the experimental setup described before. In order to treat the algal suspension a transmission line pulse generator providing a higher treatment field strength was applied. It delivers square pulses with voltage amplitude between 8 and 20 kV and pulse duration between 10 ns and 10 μs. In order to detect the lethal energy dose of a PEF treatment of *Chlamydomonas reinhardtii*, the treatment time (15 – 180 min) and the pulse duration (25 – 400 ns) were varied.



Optical density of algal suspensions exposed to different PEF treatment parameters.

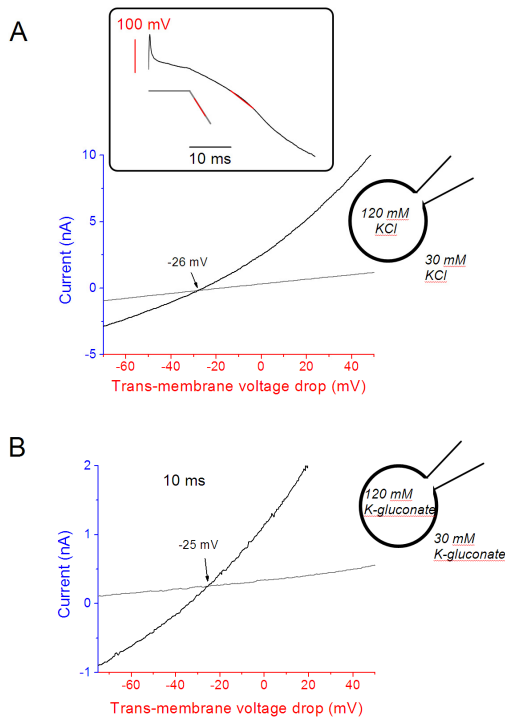
At a high treatment energy value, the optical density of the algal suspension immediately dropped after PEF treatment. Furthermore, algae cultures, which were treated with high energy doses recovered slower. Microscopic analysis of *C. reinhardtii* after PEF treatment revealed a considerable amount of destroyed cells at high treatment energy values, which could explain the sudden drop in optical density. A 30 min long PEF treatment at a field strength of 40 kV/cm and a pulse duration of 25 ns did not affect algal growth. In this case the specific energy dose was 1.4 kJ/kg. PEF treatments at specific treatment energies below this limit were considered to be non-lethal.

In summary, the experimental and diagnostic conditions for a future systematic parameter study have been developed. Optical density measurement of cell culture growth revealed to be a very sensitive diagnostic tool for determination of the lethality of pulsed electric field treatments.

**Shared Research Group (SRG 60-1)**

**Effect of strong pulsed electric fields on the plasma membrane of plant cells**

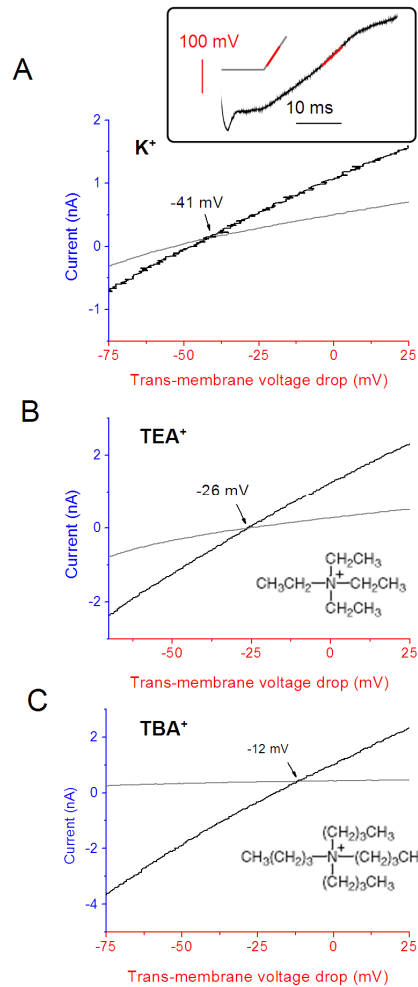
The patch clamp technique is used to study pore formation induced by pulsed electric fields in the plasma membrane of tobacco culture cells (cell-line 'bright yellow-2'). In the whole cell configuration, the cellular membrane can be charged homogeneously in a defined way to voltages that exceed by far the physiological voltage range. Polarisation beyond certain threshold levels (~ +200 mV and -275 mV,



Current-voltage curves obtained by ramp protocols after depolarizing the membrane to +100 mV (grey traces) and ~+250 mV (black traces) for 10 ms each. The exact time course of the membrane voltages for the experiment shown in A is depicted in the insert (voltage range shown in the IV curve marked in red). Note that the intersection voltage (arrows) remains unaffected when Cl<sup>-</sup> is replaced by the large monovalent organic anion gluconate, indicating that pores generated by strong membrane depolarization are highly cation selective. Further information on the solutions (in the cell/outside): pH 7.2/5.8; Ca<sup>2+</sup>: 0.1 μM (free Ca<sup>2+</sup>)/5 mM.

respectively) leads to an about 50fold increase of membrane conductance that is ascribed to the formation of aqueous pores (Wegner et al. 2011). The patch clamp technique is also well suited to analyze the selectivity of these pores to various ions. By so-called ramp protocols, currents are forced through the membrane while continuously changing the membrane voltage at a rate of 40 mV/ms; the reversal potential (i.e. the membrane voltage at which the net current passing the membrane is zero) can be used to assess the relative permeability to cations and anions, provided that an ion gradient is imposed on the membrane. The reversal potential of field-induced pores is obtained by successively imposing ramp protocols following mild polarization (±100 mV or ±150 mV, respectively; absence of pores) and strong polarization (≤-250 mV and ≥+250 mV, respectively; formation of membrane pores). From these data, current-voltage curves are calculated and superimposed for mild and strong de- or hyperpolarization. The intersection point indicates the voltage at which net current passing through the pores is zero (for a detailed description of the method, see Wegner et al. 2011). The figure above shows current-voltage relations obtained with ramp protocols using KCl concentrations of 120 mM inside and 30 mM outside the cell. An intersection potential of -26 mV indicates that field-induced pores are more permeable to K<sup>+</sup> than to Cl<sup>-</sup>. Consistently, when the small, mobile anion Cl<sup>-</sup> is replaced by a large, 'slow' monovalent organic anion (gluconate) the intersection potential remained unaffected, confirming poor permeability of the porated membrane for anions.

Subsequently, the permeability of the pores to monovalent cations of various sizes was investigated, using chloride salts of K<sup>+</sup>, and the organic cations Tetraethylammonium (TEA<sup>+</sup>) and Tetrabutylammonium (TBA<sup>+</sup>).

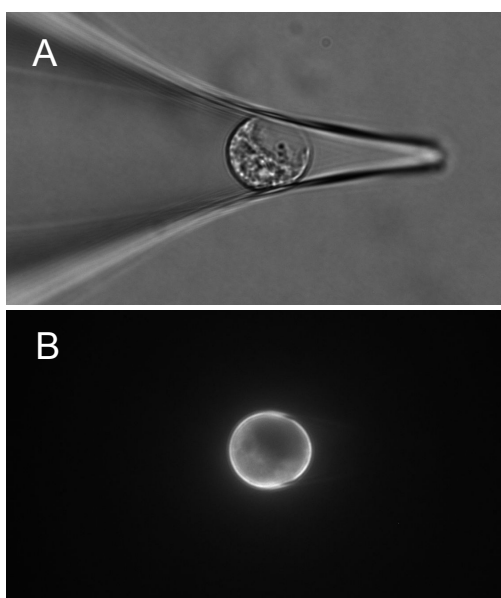


Effect of main cation on the intersection voltage of current-voltage curves following 10-ms-prepulses of -100 mV (grey traces) and ~-300 mV (black traces). TEA<sup>+</sup> = Tetraethylammonium; TBA<sup>+</sup> = Tetrabutylammonium. The insert shows the exact time course of the membrane voltages for the experiment shown in A (voltage range shown in the IV curve marked in red).

A steep gradient of 250 mM (inside) to 12.5 mM (outside) was imposed. The result is shown above for typical experiments. In the KCl media the intersection potential was fairly negative, confirming previous experiments. Interestingly, exchange of TEA<sup>+</sup> for K<sup>+</sup> led to a positive shift of the intersection potential, but the value remained clearly in the negative range, suggesting that pores are more permeable to TEA<sup>+</sup> than to Cl<sup>-</sup>. Even when K<sup>+</sup> was replaced by TBA<sup>+</sup>, the intersection potential remained slightly negative, as expected if this large cation was still more readily permeable than chloride. The selectivity sequence of field-induced pores for the main ions, as obtained from the experiments, is K<sup>+</sup> > TEA<sup>+</sup> > TBA<sup>+</sup> > Cl<sup>-</sup>. The result indicates that size of the ions does matter, but charge is the dominating factor, indicating that the majority of the pores formed by electric fields is strongly cation-selective. It is suggested that this selectivity is due to the inclusion of negative surface charges in the membrane phase forming the pore wall and/or at the mouth of the pore.

## The NIMEP project – The Non Invasive Microfluidic Electrophysiology Platform

The basic idea of the NIMEP technique is to measure current-voltage relations of individual spherical cells by imposing an external electrical field on a single cell. The current forced through the cell is measured with external electrodes, whereas the voltage drop across the membrane is recorded as a fluorescence signal by staining the cells with the voltage-sensitive dye ANNINE-6. To this end, the cell is entrapped in a conically formed borehole of a microfluidic structure. Extracellular currents that by-pass the cell have to be minimized. This configuration can be simulated by using glass micropipettes made from borosilicate glass. By mild overpressure the cell is forced into the very pipette tip where it is arrested mechanically. An example is shown below. For this experiment, a few microlitres of a protoplast suspension obtained from the tobacco cell line BY-2 was taken up by a syringe and pressed via a hollow steel needle into the shank of a micropipette that was previously filled with bath medium (as used for other patch clamp experiments). Subsequently the pipette was mounted onto the pipette holder of a patch clamp setup, and the tip was lowered into the bath containing the same medium as the pipette.



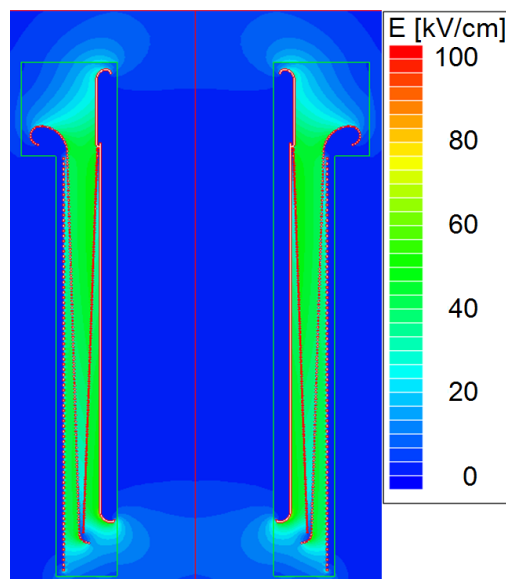
*Protoplast isolated from the tobacco culture cell line bright yellow-2 (BY-2) immobilized in a pipette tip. The protoplast had been stained with the voltage-sensitive dye ANNINE-6. DIC interference contrast picture (A) and fluorescence image (B; wavelength 475 nm, 60 ms light exposure).*

As shown above, the protoplast is slightly deformed when being entrapped in the pipette tip even if no force is applied externally, apparently due to the water column inside the capillary. This is favorable, since a considerable part of the cellular membrane is pressed against the inner wall of the glass capillary, thus increasing the extracellular resistance. Values up to 100 M $\Omega$  for the overall resistance have been obtained so far. The fluorescent image B demonstrates that the glass capillary does not affect the result (e.g. by background fluorescence). The data provide first evidence that the NIMEP approach is technically feasible. Further experiments have to be performed to substantiate this result.

## Design of Pulsed-Power Components

### Design of a Modular Trigger Generator for Over-voltage Triggering of Marx Generators

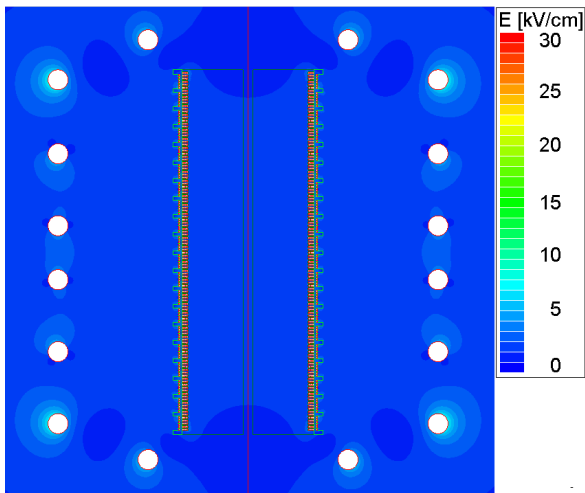
Over-voltage triggering of a spark gap enables a synchronized operation of several Marx generators in repetitive operation without an increased wear of the electrodes. In the past a compact trigger generator for over-voltage triggering of a spark gap has been built, which was designed to fit into an existing Marx generator. It consists of a semiconductor-based pulse generator in combination with a core-less pulse transformer. The Figure shows the electric field distribution in the space between primary and secondary winding.



*Electric field distribution of compact pulse transformer.*

The secondary winding consists of two layers, which are arranged in a cone-like shape. It is surrounded cylindrically by the primary winding. The distance between each turn of the secondary winding and the primary winding scales according to the increasing voltage from turn to turn in order to guarantee a good magnetic coupling between primary and secondary winding. But this design has the disadvantage, that there is a high electric field in the gap between primary and secondary winding. The magnetic coupling is limited by the insulation distance required for the total output voltage. Hence, scaling to a higher output voltage is either limited by the breakdown voltage or worse magnetic coupling. A modular design overcomes this limitation.

The modular trigger generator consists of several stacked stages, each equipped with its own power supply and pulse generator on stage potential. Each stage is supplied by the charging current of the Marx generator. As the power required for triggering depends on stage voltage and stray capacitances of the Marx generator, a modular set-up enables an easy adaptation of the trigger generator design to different types of Marx generators.

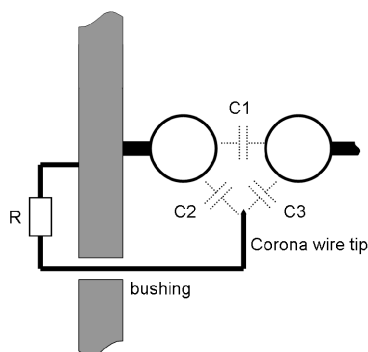


Electric field distribution of modular pulse transformer.

The figure above shows the electric field distribution of the pulse transformer for the modular design. The induced voltage increases along the whole secondary from bottom to top. But as each stage is on the same potential as the part of the secondary adjacent to it, the insulation distance between primary and secondary of each stage needs to be designed for the secondary's stage voltage only, enabling an improved magnetic coupling.

### Reduction of the Jitter of the Switching Delay during Over-Voltage Triggering of a Spark Gap

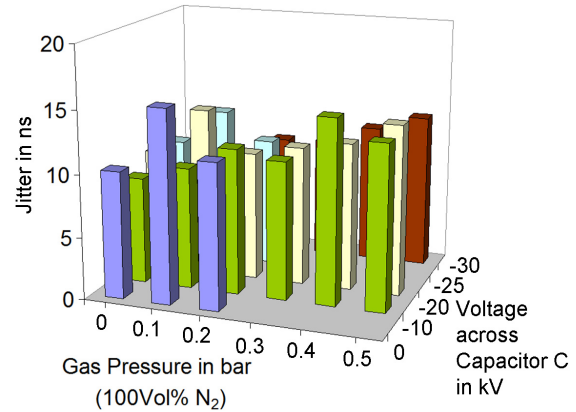
Triggering a Marx generator by applying an over-voltage to the spark gap of its first stage may involve a considerable uncertainty in switching delay due to the statistical nature of the seed electron generation. Fostering seed electron generation by means of ultra-violet light delivered by a corona discharge at the tip of a wire next to the spark gap reduces the jitter of the switching delay significantly. But in a narrow spark gap tube due to limited space a flash-over between the corona wire and a spark gap electrode may occur. In order to operate the spark gap over a wide voltage range with an appropriate seed electron generation rate, but without a flash-over to the corona wire a resistor has been switched in series to the corona wire. It limits the corona current and controls the voltage between the tip of the corona wire and the spark gap electrode of opposite polarity. The following Figure shows the equivalent schematic.



Equivalent circuit of spark gap arrangement and corona wire, including stray capacitances.

The switching behaviour of this arrangement has been tested in a test set-up comprising a single over-voltage triggered spark gap initiating the discharge of a capacitor. The pressure inside the spark gap has been adjusted to fit the static breakdown voltage to the charging voltage of the capacitor with an appropriate margin for over-voltage triggering.

According to the figure a jitter of the switching delay in the order of 15 ns has been achieved, which is sufficient for the intended use in an electroporation device. The application of the trigger voltage enables even a breakdown at zero voltage across the capacitor at low gas pressure. Hence, over-voltage triggering enables a wide operating range of the switching spark gap when adjusting the pressure or electrode distance appropriately.



Jitter depending on gas pressure and stage voltage across capacitor C.

### PEF-Treatment of Grape Mash

In cooperation with the State Institute for Viticulture and Oenology Freiburg experiments on the PEF-treatment of grape mash in laboratory scale with different pulse shapes, applied electric fields, and number of applied pulses have been performed. It is the goal of the experiments to compare the degree of cell opening depending of the way of pulse application and applied energy. Hence, the parameters have been chosen in such a way, that specific energies of 10 J/g, 20 J/g, 40 J/g and 80 J/g have been applied. A Marx generator delivering an aperiodically damped pulse shape and a LC-chain for a rectangular pulse shape have been employed. Samples of 125 cm<sup>3</sup> of mash have been processed in a homogeneous electric field. In order to determine the degree of cell opening electric impedance measurements, and an evaluation of the contents of tanning substances and pigments in the must after a 2h lasting extraction have been performed. The results are currently being evaluated and will be presented later in this year.

### PEF-treatment of Sugar Beets

In the frame of the co-operation with SÜDZUCKER on the PEF-treatment of sugar beets, in this year the research and development activities towards an industrial-scale electroporation device have been continued.

### Staff Involved

DI F. Attmann, DP T. Berghöfer, H. Brüsemeister, Dr. C. Eing, Frau Dr. B. Flickinger, J. Fleig, **Dr. W. Frey**, Dr. C. Gusbeth, Frau DI M. Göttel, Frau Dr. P. Hohenberge (KIT CS), K. Leber, E. Menesklou, Dr. G. Müller, K. Paulus, D. Quattrocchi, Frau S. Rocke, R. Stängle, DI R. Sträßner, **Dr. M. Sack**, **Dr. L. Wegner (KIT CS)**, H. Zimmermann

## HGF Program: NUCLEAR

### Safety Research for Nuclear Reactors

#### Corrosion and Wear Protection for New Reactor Technologies

To guarantee a secure future electricity supply new types of nuclear reactors are investigated in the frame of GEN IV. The development of technologies required for the safety of fast heavy metal cooled reactors like the Lead Fast Reactor (LFR) is the core area of the work performed at KIT. Especially the development of advanced materials e.g. ODS steels and the investigation and improvements of their compatibility with the proposed coolants are in the focus of this work.

Aim of the institute's contribution is the development of corrosion barriers to improve the compatibility of new structural materials with liquid Pb or PbBi. Pulsed large area electron beams (GESA - process) are used to modify surfaces such that they satisfy the demands of their targeted environment. Corrosion test facilities for specimen exposure under relevant conditions and for combined loads like fretting or erosion together with corrosion are developed, built and used at the IHM. The conditioning and control of the required oxygen level in the liquid metal is an additional task of the work.

The entire activity is integrated in European and international projects and cooperation, e.g. LEADER, GETMAT, ESFR, HELIMNET.

The ELSY project was finished in 2010 and a follow-up project for the development of a Pb cooled fast demonstration reactor LEADER was started in the FP7 frame. The main tasks there are the transfer of the GESA FeCrAl process developed for fuel claddings to heat exchanger geometry, continuing the investigation of candidate pump materials and to develop oxygen control and purification strategies for a real reactor. In the ESFR project (development of a fast Na cooled European reactor) ideas to engineer Co-free wear resistant coatings were started and will be continued. In the GETMAT project four different tasks have to be fulfilled: corrosion stability of ODS, T91 and mixed welds in Pb; procurement of 12Cr ODS steel bought in Japan, improvement of GESA FeCrAlY process and fretting investigation of fuel clad materials in Pb environment.

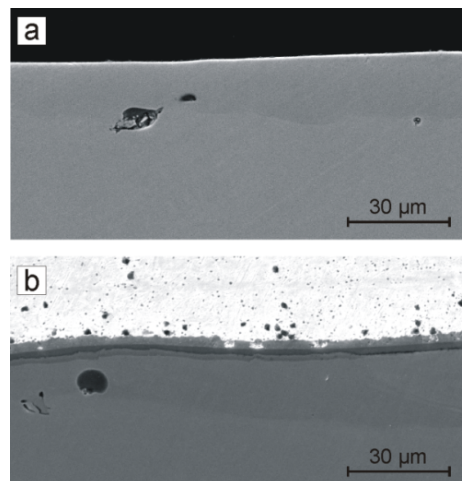
The most important results obtained in the reporting period are briefly presented:

T91 steel specimens with GESA modified FeCrAlY surface layers were investigated in detail to find an optimum composition for the formation of a thin, stable and protective oxide layer when exposed to liquid lead under reactor conditions. Respective oxidation experiments had been performed in the previous reporting period, where FeCrAlY coatings of three different compositions (Fe15Cr11.5Al0.5Y, Fe9Cr12Al0.5Y, Fe15Cr11.5Al) were re-melted using the GESA technology and exposed in the COSTA facility to liquid lead with  $10^{-6}$  and  $10^{-8}$  wt% oxygen at 400, 450, 500 and 550 °C for about 1000 h.

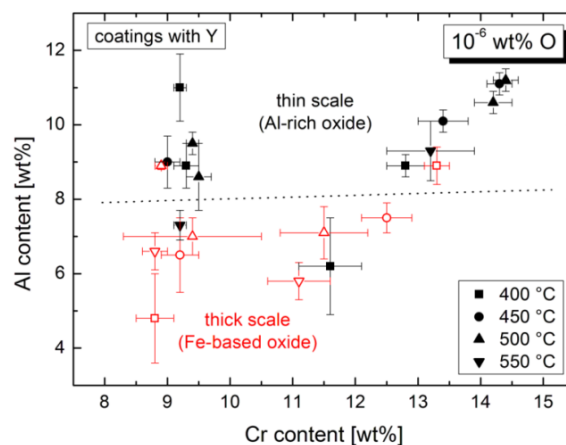
Preliminary results showed that a reduced Al and Cr content and the absence of yttrium in the modified surface layer, especially at lower temperatures, leads to the formation of thick Fe-rich oxides over substantial areas. A more detailed analysis of the exposed specimens, taking special care about the Al content, was done in the reporting period.

Due to spatially varying conditions during the re-melting process (GESA), the Al content of the modified FeCrAlY layers varies locally. It was observed that in correlation with the local Al content also the type of oxide (thick Fe-rich or thin Al-rich) found on the specimen surfaces after lead exposure

varies. EDX analyses of cross sections revealed that an Al content of at least 8 wt% is required to assure the formation of a thin protective alumina scale (Figure). This threshold is almost independent of the Cr content in the range studied (9-15 wt% Cr). For higher temperature (550 °C), the critical Al content is reduced to 7 wt%. In the absence of Y, for temperatures up to 500 °C, even above 8 wt% Al a thick Fe-rich oxide scale is formed in some places. This confirms the positive effect of small amounts of Y (<0.5 wt%) on the formation of thin protective alumina scales.



SEM images of a FeCrAl-coated specimen after exposure to lead containing  $10^{-6}$  wt% oxygen at 450 °C: (a) thin protective scale and (b) thick, Fe-rich oxide scale.

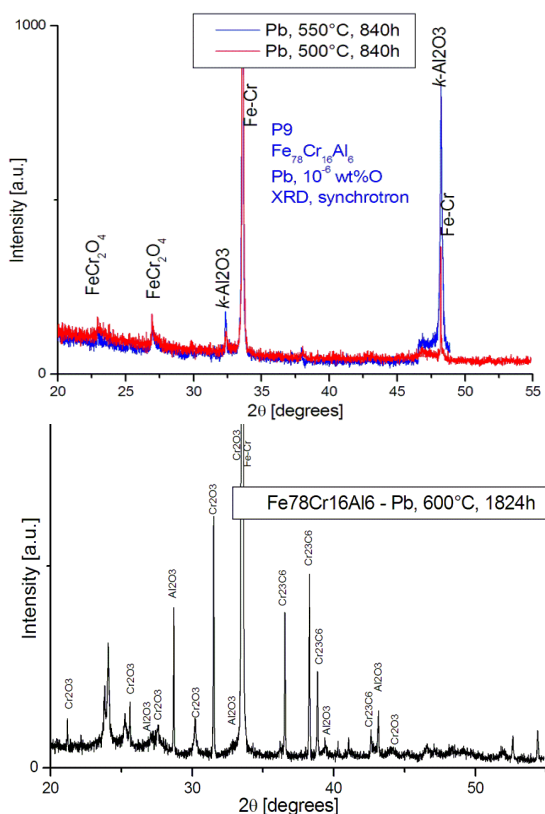


Oxide scale formation as function of Al and Cr content in liquid lead containing  $10^{-6}$  wt% oxygen.

Besides investigating an optimum composition of modified FeCrAlY layers, short-time oxidation tests of FeCrAlY-coated specimens were performed in the reporting period. For a quick quality check of modified FeCrAlY layers, the specimens were exposed to hot gaseous (Ar) environment for 72h at 450, 500 and 600 °C and at oxygen contents between  $10^{-10}$  and  $10^{-6}$  ppm. The ultimate goal of these oxidation experiments is a reliable prediction of the expected oxidation behavior in liquid lead. Under all conditions investigated, formation of Fe-rich oxide scales is observed for Al contents below 8 wt%. Above 10 wt% Al, on the other hand, an Al-rich oxide scale grows on the modified FeCrAlY layer. Compared to the thin protective alumina scales formed in liquid lead, however, the Al-rich oxide scales grown in gaseous atmosphere appear to be less homogeneous and interspersed with Fe-rich regions. For Al contents between

8 and 10 wt%, a mixed oxide scale is formed. To summarize, significantly more Al (i.e., 10 wt%) is required to form an Al-rich oxide scale in gaseous environment at  $10^{-10}$  to  $10^{-6}$  ppm (which corresponds to an oxygen content of  $10^{-1}$  to  $10^{-1}$  wt% in lead) than for the formation of thin alumina scales in lead containing only  $10^{-8}$  to  $10^{-6}$  wt% oxygen (7-8 wt%). Reduction of the Al content threshold for Al-rich oxide formation in gaseous atmosphere might be achieved by either reduction of the oxygen potential to much lower values or by using different temperatures.

To determine in detail the above described elemental composition dependent formation of oxide scales bulk FeCrAl alloys with 9 different compositions were exposed to Pb and PbBi at temperatures between 400 and 600°C. Post investigation involves beside SEM/EDX and XRD grazing incident XRD at ANKA and XPS. SEM/EDS observations were used to determine roughly the nature of the oxide scale. Similar to the above described GESA re-melted FeCrAlY layers about 6 to 8wt% Al was required to form Al-rich oxide scales at all the investigated conditions. More detailed information on the formed oxide scales was obtained by grazing incident XRD (see Figure). At 500°C  $FeCr_2O_4$  oxide is the dominating oxide scale formed, only minor  $k-Al_2O_3$  was detected. At 550°C the share of  $k-Al_2O_3$  increases clearly on the expense of the  $FeCr_2O_4$ . At 600°C  $Al_2O_3$  and  $Cr_2O_3$  are the dominating oxide scales that were formed during the exposure in Pb.



Oxide scales formed on FeCrAl specimens exposed to Pb at different temperatures, measured using grazing incident XRD (ANKA).

The qualification of welds regarding their compatibility with Pb is another task within the GETMAT project. Welds of T91 and ODS steels obtained using EB- and TIG - welding were exposed to lead with  $10^{-6}$  and  $10^{-8}$ wt% oxygen at 550°C for 2000h. Besides these, two samples manufactured using friction stir welding were exposed as well. The specimens, test conditions and exposure time are depicted in the following table. Weld 20 and 21 are friction stir welds joint using two different tools.

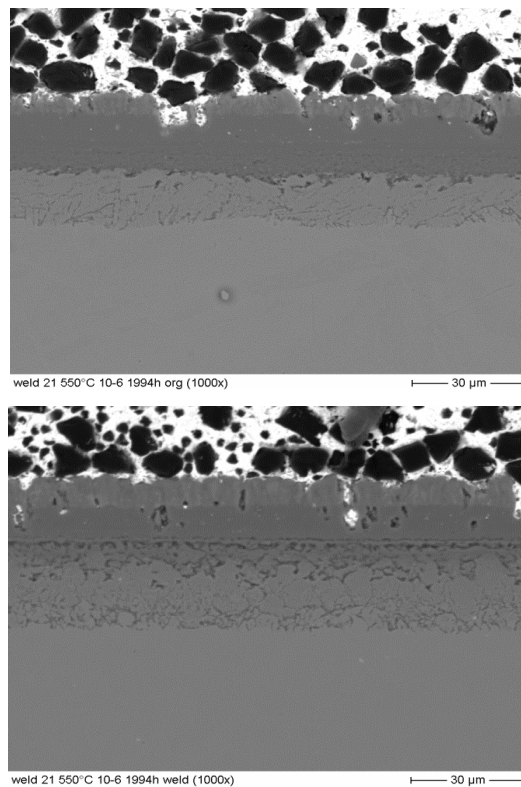
	$10^{-6}$ wt%	$10^{-8}$ wt%
P91-P91 EB		2115
P92-P92 EB	1944	2000
P92-P92 TIG	1944	2000
P91-PM2000 EB	1944	2000
PM2000-PM2000 EB	1944	2000
Weld 20 (P91-P91)	1944	2115
Weld 21 (P91-P91)	1944	2115
12Cr ODS	1944	

Specimens, test conditions, exposure time.

A post-weld heat treatment was carried out on the F/M steel specimens produced by TIG and EB welding. Therefore the welding area and the bulk material had a similar grain structure.

The friction stir joints without heat treatment exhibit smaller grains in the heat affected zone (HAZ) and the weld region. The welds of P91-PM2000 and PM2000-PM2000 specimens had large grains in the welding joint. In addition, the P91/PM2000 welds showed precipitations of elements like Al, Cr, Ti, C and O along the grain boundaries.

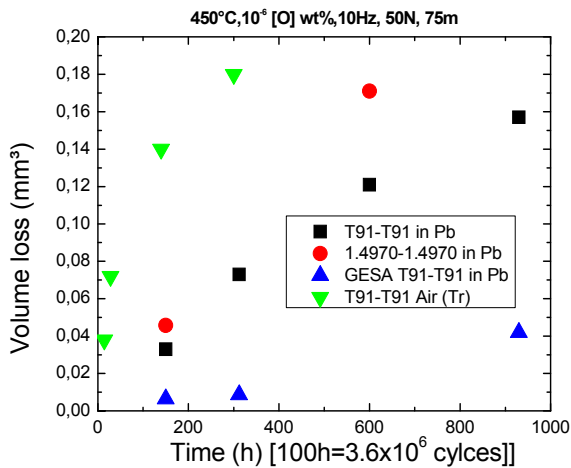
The welded areas of the 9Cr F/M steels (P91, P92) welded by EB or TIG exhibit a very similar behaviour like the bulk material due to their comparable grain sizes by the heat treatment after the welding process. At high oxygen content of  $10^{-6}$ wt% oxide scales develop, at low oxygen dissolution attack started. At high oxygen content the dissimilar welds form oxide scales at the low Al regions (P91 area and weld zone) and thin Al-rich oxides at the PM2000 surface. The oxide scales formed in the weld region are slightly thicker than in the P91 bulk. At  $10^{-8}$ wt% oxygen starting dissolution attack similar to the P91 or P92 welds, is observed. The friction stir welds without heat treatment developed larger oxide scales at areas of smaller grain sizes (in the weld region) at  $10^{-6}$ wt% oxygen containing Pb (see figure). This can result in an earlier spallation of the oxide scales in the welding region.



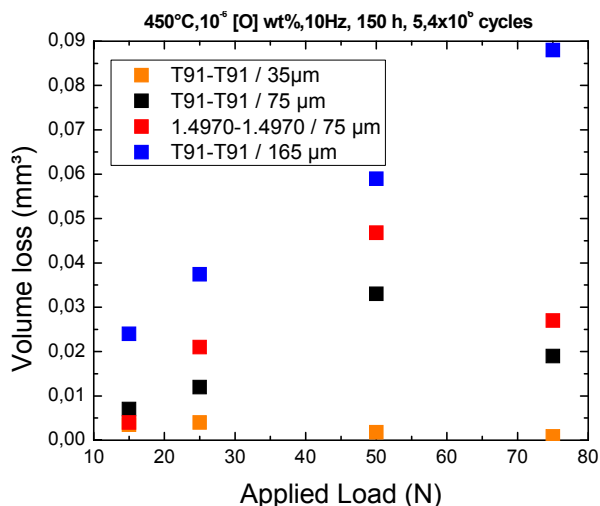
Weld 21 exposed to  $10^{-6}$ wt% oxygen containing Pb: bulk (upper), weld (lower).

In the fretting area the formation of an interposing scale made of compacted fretting debris is common. The composition of such layer depends on the materials involved in the fretting process, but generally it is made of metal debris (susceptible to Ni and Cr depletion) and oxidized debris according to the testing condition and lead. This scale, although might slow down the fretting mechanical removal, does not provide any efficient protection against dissolution. As a matter of fact the lead penetrates the scale and reaches the underlying bare steel surface where it starts dissolution.

From the results of the fretting tests carried out with different applied loads and sliding amplitudes (see figure), a close relationship between these variables was noticed. Indeed, on one hand the fretting wear increases with the amplitude regardless of the applied load; on the other hand the fretting damage increases with the load up to a turning point after which it decreases. The value of the turning points depends on the amplitude of the slip. This can be explained considering that debris retention is favored by high loads, while release of the fretting debris is more likely for larger amplitudes. Turning point and final fretting damage depends on the interplaying of these two variables.



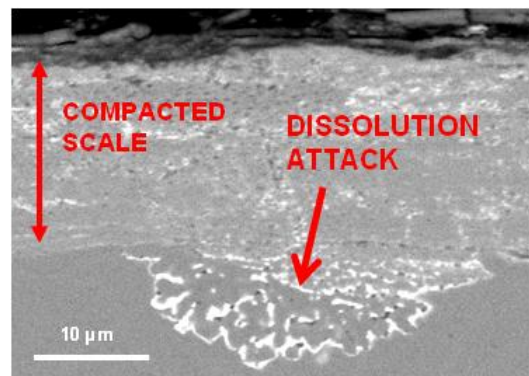
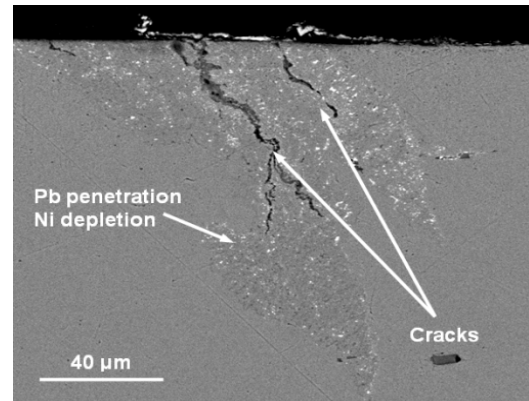
Fretting wear (volume loss) as function of the time/number of cycles in lead, in air and for different materials.



Fretting wear (volume loss) as function of the applied load, in lead and for different materials.

The experimental campaign confirmed that the fretting process at most severe conditions destabilizes, cracks and removes the protective oxide scales and parts of the corrosion barriers (e.g. FeCrAlY surface alloyed achieved by

GESA treatment), required for the use of the investigated alloys in lead cooled nuclear systems. In particular, it was observed that also in conditions in which dissolution is not expected to take places, it might be favored and triggered by the fretting process. For example, although, dissolution is not expected to occur at 450°C and 10<sup>-6</sup> wt% of oxygen in solution even after very long exposure (>10000 h), during the fretting tests dissolution was noticed already after 930 h (see figure right). Additionally, as shown in the figure left, the cyclical loading and the pits generation during the fretting action might favor the initiation of fatigue cracks, affecting the components mechanical properties and spreading in depth the dissolution attacks.

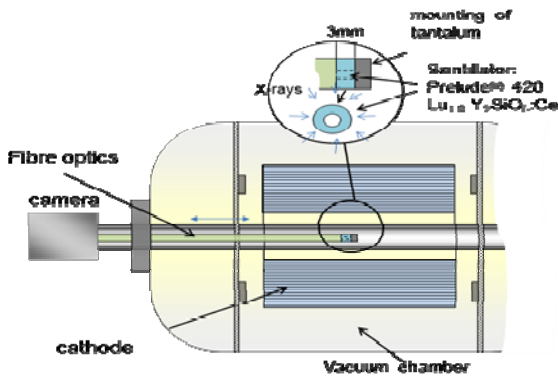


SEM picture of the 15-15Ti specimen cross-section after fretting tests in molten Pb with 10<sup>-6</sup> wt% oxygen: left) after 600h, right) after 930h.

The evaluation of heat conductivity of oxide layers formed in-situ is one of the objectives of our work related to the LEADER project. The thermal diffusivity of T91, FeCrAl bulk and a GESA surface modified FeCrAlY coated T91 was measured using laser flash calorimetry. Specimens of same kind were exposed to Pb at 550°C for 1000h and their diffusivity was measured before and after exposure to evaluate the influence of the formed oxide layers. The T91 specimen exhibits a decrease in thermal diffusivity due to the oxide scale formation. The GESA surface modified FeCrAlY instead showed even a slightly higher but definitely not reduced thermal diffusivity. The exposure and measurement will be repeated to explore in addition the influence of penetrated Pb alloy.

The measurement of the GESA IV electron beam homogeneity is one of the most important issues for GESA IV optimization. Therefore, a dedicated test set-up was developed that allows the measurement via X-ray formation using a scintillator disc mounted on glass fibre and connected to a high speed camera (see the following figure). Two of this mounted scintillators will be inserted into the target (tube), one kept at a constant position the other will be moved along the axis from pulse to pulse. So, the radial and lateral

distribution of beam energy at the target can be evaluated and used if applicable and required for cathode optimization.



GESA IV – Scheme of beam homogeneity measurement.

## Reduction of Radiotoxicity

### Corrosion Protection in Heavy Liquid Metal Cooled Sub-critical Systems

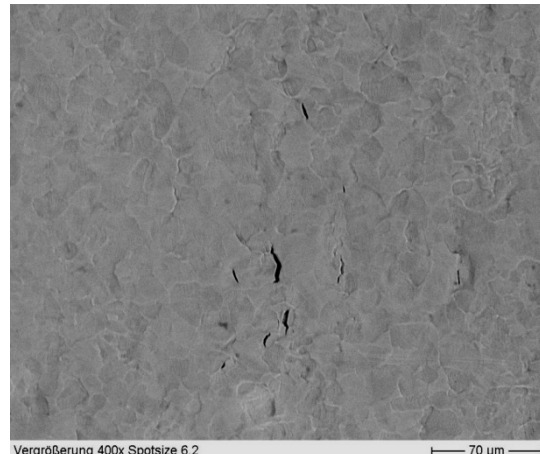
Long-living high-level radioactive waste from existing nuclear power reactors should be transmuted in short-living radio nuclides using fast neutrons provided by a spallation target in an accelerator driven subcritical system or by a fast nuclear reactor. The objective is to reduce the final disposal time of high-level radioactive waste (plutonium, minor actinides) from some  $10^6$  years down to about 1000 years. Lead (Pb) and lead-bismuth (PbBi) are foreseen as spallation-target and coolant of such devices.

The aim of the institute's contribution is the development of a suitable corrosion protection especially for parts under high loads like fuel claddings or pump materials in contact with liquid Pb or PbBi. Pulsed large area electron beams (GESA) are used to modify the surface of steels such that they fulfill the requirements of their surrounding environment. Corrosion test stands for exposure of specimens under relevant conditions are developed and operated. Test facilities for combined loads like erosion corrosions and fretting corrosion were developed, built and operated. Conditioning the lead with regard to its oxygen concentration and the transport of oxygen in PbBi are additional aspects of the work.

All tasks are embedded in European and international projects and cooperation e.g. MATTER, ADRIANA, SEARCH.

### The most relevant results obtained in the reporting period are briefly presented:

Austenitic steel with Al containing surface layers, e.g. made using the GESA process, might undergo mechanical deformation during the component production. Therefore the maximum strain that such layers can withstand without crack formation was investigated using a three point bending test placed under a microscope. Different aluminisation routes including diffusion and surface alloying were used. Al surface alloyed steels applying the GESA with an Al content of about 6 to 8 wt% Al could be strained up to 10% if a short heat treatment of 3h at 400°C was performed. Without heat treatment already a remaining strain of about 7% leads to crack formation (see figure).



Above: bending test under microscope; below: crack appearance at surface.

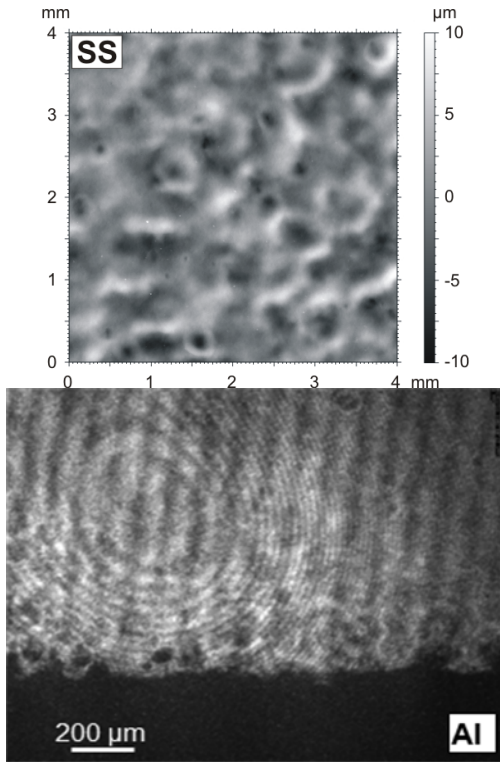
Al-rich, brittle surface layers are easily formed on top of materials aluminized via a diffusion controlled process. Such layers already show at strain levels of about 0.4% crack formation and have to be avoided or removed. If the outer layer contains Al in the order of 6 to 8 wt% (like the GESA surface alloyed specimens) similar strain levels of 10% are tolerated without crack formation. In short term exposure tests no change in oxidation even at 10% strain was detected. Detailed investigation on long term behaviour is an objective for future investigations.

### Optimisation of the GESA process:

The remelting of metallic specimens using large area pulsed electron beams (GESA) results in a more or less pronounced waviness of the surface (see next figure), which may be disadvantageous for some applications. To control the surface topography, basic understanding of the involved physical processes is required. Preliminary work in this area showed that plasma is ignited during beam treatment in the space above the target. In the reporting period, this target plasma was investigated in more detail by time-resolved spectroscopy. It was found that the vapor cloud with density  $\sim 10^{19} \text{ cm}^{-3}$ , generated by substantial evaporation of target material, is partially ionized by beam electrons via impact ionization. Fast decay of the plasma after beam termination is observed. Because of the low plasma density ( $10^{14} \text{ cm}^{-3}$ ) and its low temperature ( $< 1\text{eV}$ ), electric fields in the plasma sheath are not large enough to cause an electrohydrodynamic instability of the liquid target surface. However, substantial evaporation and the interaction between the vapor and the free liquid surface might cause the growth of unstable surface undulations. These effects are most pronounced for the largest surface temperatures, which occur around beam termination. In an earlier stage of the treatment, shortly after melting of the surface layer, bubbles appear on the target



surface (mainly on Al targets, see figure). These bubbles can grow up to 300  $\mu\text{m}$  in diameter and disappear prior to beam termination. They were observed by high-resolution imaging during treatment of fresh samples; pre-treated samples showed only very occasionally the appearance of a bubble.



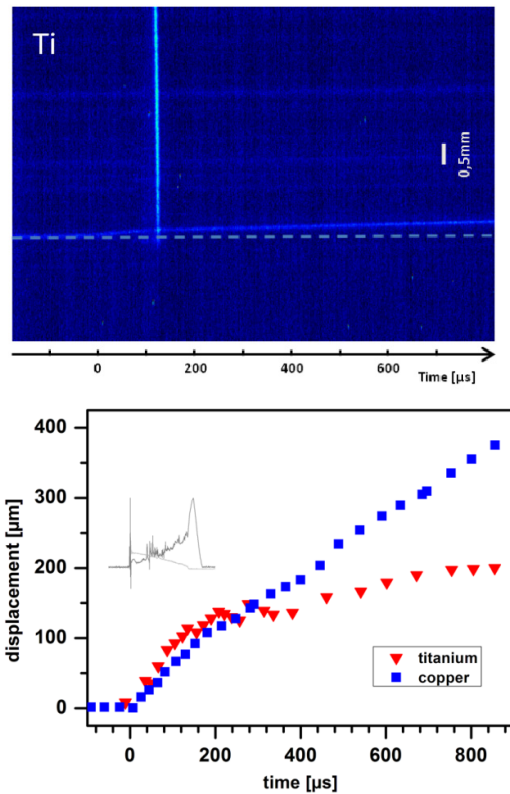
Left: Topography of stainless steel after electron beam treatment. Right: High resolution photograph of a fresh Al target during treatment.

Small targets not clued properly to the target holder are observed to fly away during application of a pulsed electron beam. Using time resolved side view imaging of the target surface, this process was studied more closely. As shown in the figure on next page, the target gets accelerated towards the incoming electron beam at the moment when the beam hits the target. The exact source of the recoil force is still unclear. Around beam termination, i.e., 150 to 200  $\mu\text{s}$  later, the target surface temperature reaches its maximum and substantial evaporation occurs. At that time, the vertical motion of the target is decelerated by the vapor recoil pressure. Deceleration is less pronounced for copper, where less material is evaporated. This experiment demonstrates clearly the effect of vapor recoil, which might also be responsible for the development of surface waviness.

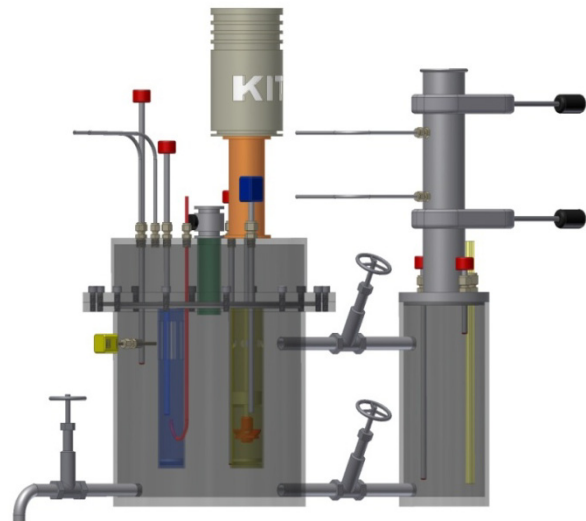
All processes involved in pulsed electron beam treatment investigated so far (bubbles, plasma, evaporation, vapor flow and recoil) are absent or cease after beam termination. However, the surface layer stays liquid for at least another 100  $\mu\text{s}$  before re-solidification (life time determined by simulations and confirmed by streak images of target specular reflectivity). During that time, in first approximation, surface tension is expected to cause relaxation of most surface features that have developed until beam termination. Effects and processes that could hinder this relaxation will be further investigated.

Within the SEARCH project a dedicated facility (next figure) to measure adsorption, entrainment of oxides in heavy liquid metals and mass transport phenomena in liquid metals will be designed. This includes the transport of oxygen and of metal(oxide) particles. This work will accompanied by CFD

calculations performed by colleagues of the IKET already in the design face. The measurement results finally will be used to qualify and optimize the CFD codes with respect to particle (oxide) transport into and in the liquid PbBi.



Above: Side view streak image to detect the surface position of a titanium target during GESA treatment. Below: Position of titanium and copper targets, synchronized with the respective current and acceleration voltage of the applied electron beam.



Scheme of oxygen and particle transport test facility.

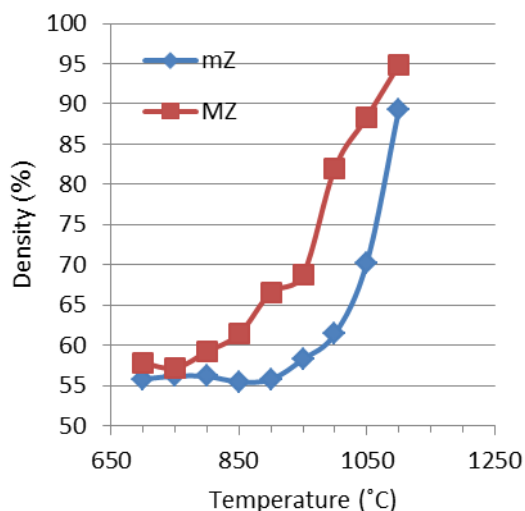
**Involved staff:**

DP. W. An, R. Beckers, M. Eing, M. DelGiacco (Doktorand), Fr. Dr. R. Fetzer, Fr. Dr. A. Heinzl, Prof. Y. Krasik (visiting scientist), DI (FH) F. Lang, Dr. A. Jianu, Dr. G. Müller, Dr. G. Schumacher (visiting scientist), A. Sivkovich, DI P. Spieler, **Dr. A. Weisenburger**, DI (FH) F. Zimmermann

## HGF Program: NANOMIKRO

### High Temperature Microwave Processing

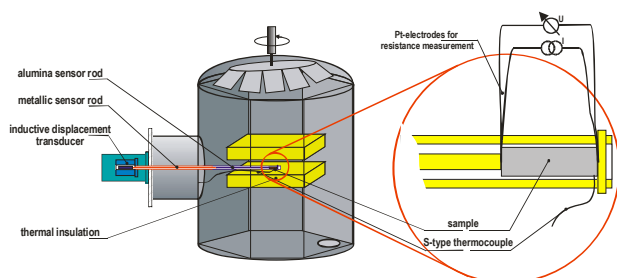
In collaboration with the Federal University of Sao Carlos, Brazil detailed investigations on microwave sintering of doped and undoped, nanokristalline varistor ceramics ZnO and of the catalyst in the system  $\text{La}_2\text{Ni}_{1-x}\text{Co}_x\text{O}_4$  were performed. Systematic variation of process parameters and measurement in a mm-wave heated dilatometer were used to optimize the sintering process with respect to the achievable density and grain size. The comparative sintering study at two different microwave frequencies as they were 2.45 GHz and 30 GHz revealed more enhanced densification for the later one as exemplary can be seen in the following graph for undoped nano-ZnO.



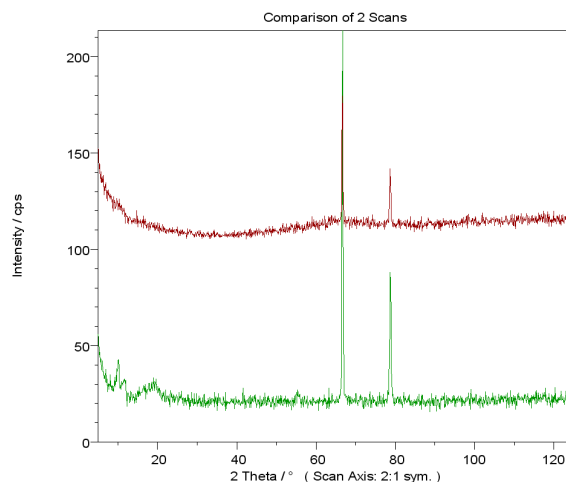
Densification behaviour of nano-ZnO at 2.45 GHz (mZ) and 30 GHz (MZ).

Within the DFG funded project on microwave processing of metal powder compacts, in collaboration with the Indian Institute of Technology, Department of Electrical Engineering, Kanpur, selected metal powders such as Copper (Cu) have been characterized using XRD and SEM before the sintering process.

The high frequency microwave sintering experiments were done in combination of in-situ electrical resistivity measurements using the four-wire method as well as using a modified dilatometer set-up for monitoring the sintering kinetics as a function of temperature. This setup gives important information about microstructural changes with respect to the inter-particle electrical contacts during the sintering process.



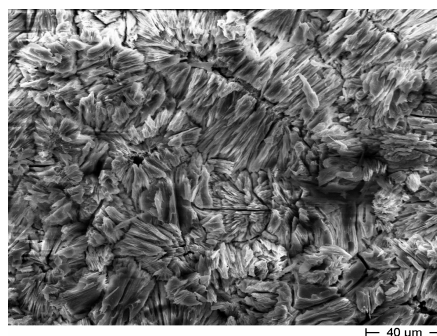
The In-Situ electric resistivity and dilatometer setup.



XRD & SEM micrographs of the as received Copper metal powder samples (bottom). XRD of the 30 GHz microwave sintered sample under inert atmosphere (top).

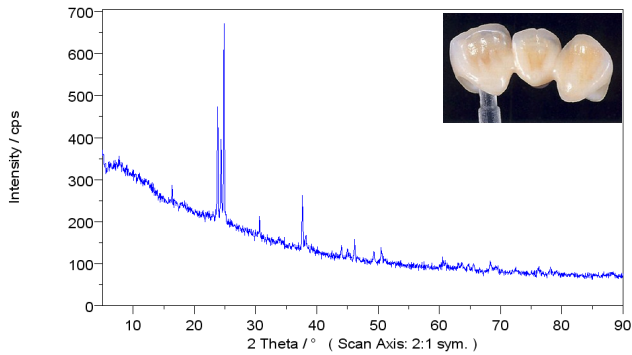
The 30 GHz microwave sintered metal samples were characterized using X-ray diffraction (XRD).

A project on the possibility of using high frequency, 30 GHz, microwave processing to crystallize lithium disilicate stoichiometric glass (LS2) composition into glass-ceramic material has been started. The experiments show that in a relatively short time, low temperature and without the aid of hybrid heating, 30 GHz microwave processing was used successfully to crystallize lithium disilicate glass using one stage heat treatment. This study also shows that the microwave absorption in lithium disilicate glass is highly dependent on the microwave frequency.



SEM micrograph of the 30GHz microwave crystallized LS2 glass sample 600°C- 1 min.

In collaboration with of Ivoclar Vivadent AG, Principality of Liechtenstein a study has been done to use 30 GHz microwave processing to LS2 based dental glass composition. The investigated commercial glass was related to the  $\text{SiO}_2\text{-Li}_2\text{O-P}_2\text{O}_5\text{-ZnO-Al}_2\text{O}_3\text{-K}_2\text{O}$  glass system. The results show that high frequency microwave processing could be a good candidate in the processing and in the crystallization of these dental crowns materials in a relatively short time and without the aid of hybrid heating using one stage heat treatment.



XRD of the 30 GHz microwave crystallized dental glass composition at 850°C-10 min.

**Staff Involved:**

Dr. M. Ahmed, H. Brüsemeister, **Dr. G. Link**, S. Miksch, D. Quattrocchi, K.-T. Schäfer, Prof. M. Thumm

**HGF Program: Energy**

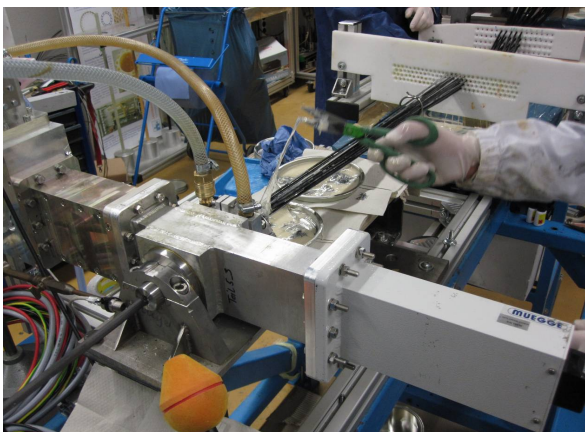
**– Rational Energy Conversion (REUN) –**

**Material Processing Using Microwaves**

Major activities in 2011 were related to different BMBF funded joint projects.

The first of it under the topic "innovative, modular microwave technology for production of fibre composite structures" was successfully finished. Different microwave systems for application in carbon fibre reinforced plastic (CFRP) production were designed and the feasibility was demonstrated.

For example a microwave heated tool for pultrusion of simple CFRP profiles, such a round profiles with 9 mm in diameter was developed. The production of several 10 m was demonstrated in collaboration with the Institute of Textile Technology (ITV) in Denckendorf.



Running experiment for microwave assisted pultrusion of CFRP.

As a result of the mentioned project one of the industrial project partners purchased a large HEPHAISTOS system and is engaged in development and certification vacuum assisted processes (VAP) for avionic CFRP structures.

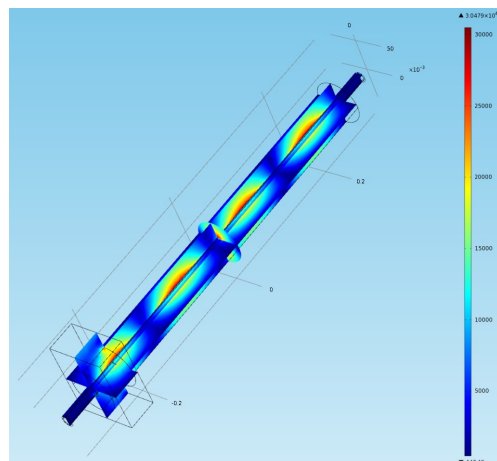
A microwave integrated tool for the fabrication of cast blanks for the manufacture of ceramic brake discs has successfully used for feasibility studies. For further investigations and process optimization the tool has been integrated into the production environment of the corresponding industrial project partner.



First prototype setup for microwave ablation of concrete.

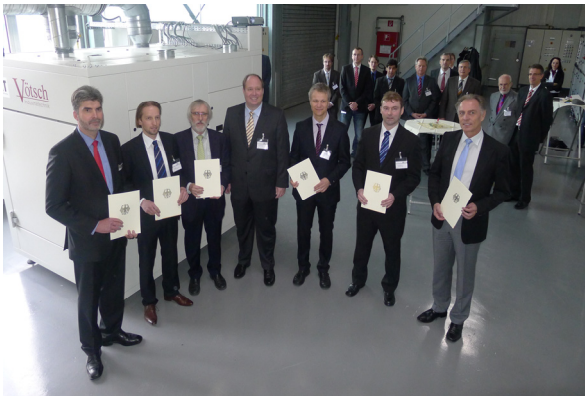
Within the second BMBF funded joint project called MACOS „Microwave Assisted Ablation of Contaminated Concrete Surfaces“, a first design for a microwave instrument has been built up and successfully tested in collaboration with the IMB of CS. This technology may be used for the ablation of contaminated surfaced in nuclear power plants. A method for systematic dielectric characterization of various concrete samples has been developed.

For the third BMBF funded joint project called "Recovery of CO<sub>2</sub> as a carbon brick by use of mainly renewable energy sources" (CO<sub>2</sub>RRECT) the task of KIT is design and testing of a microwave heated reactor. A first small scale prototype has been designed and its microwave performance was successfully tested.



Numerical field simulation for the microwave heated chemical reactor

The application and detailed project plans for a new BMBF funded joint project on microwave processing of CFRP materials called FLAME were finalized mid of 2011 and approved. The official Kick-off of the project was in October which was valued by a visit of the state secretary Dr. Helge Braun when he handed over the approval letters. The main topics of this project with KIT as project co-ordinator are a prolongation of the microwave pultrusion development of the first project and further optimization of the HEPHAISTOS technology for microwave assisted curing of CFRP winding forms.



*Visit of FLAME project kick-off by state secretary Dr. Helge Braun.*

**Staff Involved:**

J. Dittrich, Prof. H. Gemmeke, Prof. J. Jelonnek, Dr. T. Kayser, S. Layer, **Dr. G. Link**, Dr. A. Melcher, V. Nuß, Chr. Ott, T. Seitz, Dr. S. Soldatov, F. Steinhauser, Chr. Zöller

## List of Publications

### HGF Program: FUSION

#### *Publications at cross-referenced journals:*

Arnoux, G., Bazylev, B., Lehnen, M., Loarte, A., Riccardo, V., Bozhenkov, S., Devaux, S., Eich, T., Fundamenski, W., Hender, T., Huber, A., Jachmich, S., Kruezi, U., Sergienko, G., Thomsen, H., JET EFDA Contributors  
Heat load measurement on the JET first wall during disruptions.  
Journal of Nuclear Materials, 415(2011) S.S817-S820  
DOI:10.1016/j.jnuc.mat.2010.11.042

Bazylev, B., Igitkhanov, Yu., Landman, I., Pestchanyi, S., Loarte, A.  
Erosion simulation of first wall beryllium armour after ITER transient heat loads and runaway electrons action.  
Journal of Nuclear Materials, 417(2011) S.655-658  
DOI:10.1016/j.jnucmat.2011.01.074

Bazylev, B., Arnoux, G., Fundamenski, W., Igitkhanov, Yu., Lehnen, M., JET EFDA Contributors  
Modeling of runaway electron beams for JET and ITER.  
Journal of Nuclear Materials, 415(2011) S.S841-S844  
DOI:10.1016/j.jnucmat.2010.11.086

Coenen, J.W., Bazylev, B., Brezinsek, S., Philipps, V., Hirai, T., Kreter, A., Linke, J., Sergienko, G., Pospieszczyk, A., Tanabe, T., Ueda, Y., Samm, U., TEXTOR-Team  
Tungsten melt layer motion and splashing on castellated tungsten surfaces at the Tokamak TEXTOR.  
Journal of Nuclear Materials, 415(2011) Suppl. 1, S.S78-S82  
DOI:10.1016/j.jnucmat.2010.09.046

Flamm, J.H., Jin, J., Thumm, M.K.  
Wave propagation in advanced gyrotron output couplers.  
Journal of Infrared, Millimeter, and Terahertz Waves, 32(2011) S.887-896. DOI:10.1007/s10762-011-9800-y

Gantenbein, G., Erckmann, V., Illy, S., Kern, S., Kasperek, W., Lechte, C., Leonhardt, W., Lievin, C., Samartsev, A., Schlaich, A., Schmid, M., Thumm, M.  
140 GHz, 1 MW CW gyrotron development for fusion applications. Progress and recent results.  
Journal of Infrared, Millimeter, and Terahertz Waves, 32(2011) S.320-328.  
DOI:10.1007/s10762-010-9749-2

Garkusha, I.E., Landman, I., Linke, J., Makhlay, V.A., Medvedev, A.V., Malykhin, S.V., Peschanyi, S., Pintsuk, G., Pugachev, A.T., Tereshin, V.I.  
Performance of deformed tungsten under ELM-like plasma exposures in QSPA Kh-50.  
Journal of Nuclear Materials, 415(2011) S.S65-S69  
DOI:10.1016/j.jnucmat.2010.11.047

Igitkhanov, Y., Bazylev, B.  
Electric field and hot spots formation on divertor plates.  
Journal of Modern Physics, 2(2011) S.131-135  
DOI:10.4236/jmp.2011.23020

Igitkhanov, Y., Bazylev, B.  
The PFC erosion in DEMO due to runaway electrons.  
Fusion Science and Technology, 60(2011) S.349-353

Igitkhanov, Yu., Bazylev, B., Landman, I.  
Calculation of runaway electrons stopping power in ITER.  
Journal of Nuclear Materials, 415(2011) S.S845-S848  
DOI:10.1016/j.jnucmat.2010.11.071

Jin, J., Rzesnicki, T., Kern, S., Thumm, M.  
High-efficiency quasi-optical mode converter for the coaxial cavity gyrotron.  
Fusion Science and Technology, 59(2011) S.742-748

Klimov, N., Podkovyrov, V., Zhitlukhin, A., Kovalenko, D., Linke, J., Pintsuk, G., Landman, I., Pestchanyi, S., Bazylev, B., Janeschitz, G., Loarte, A., Merola, M., Hirai, T., Federici, G., Riccardi, B., Mazul, I., Giniyatulin, R., Khimchenko, L., Koidan, V.  
Experimental study of PFCs erosion and eroded material deposition under ITER-like transient loads at the plasma gun facility QSPA-T.  
Journal of Nuclear Materials, 415(2011) S.S59-S64  
DOI:10.1016/j.jnucmat.2011.01.013

Landman, I.S., Pestchanyi, S.E., Igitkhanov, Y., Pitts, R.  
Two-dimensional modelling of disruption mitigation by massive gas injection.  
Fusion Engineering and Design, 86(2011) S.1616-1619  
DOI:10.1016/j.fusengdes.2010.12.017

Litnovsky, A., Philipps, V., Wienhold, P., Kreter, A., Kirschner, A., Matveev, D., Brezinsek, S., Sergienko, G., Pospieszczyk, A., Schweer, B., Schulz, C., Schmitz, O., Coenen, J.W., Samm, U., Krieger, K., Hirai, T., Emmoth, B., Rubel, M., Bazylev, B., Breuer, U., Stärk, A., Richter, S., Komm, M., TEXTOR Team  
Overview of material migration and mixing, fuel retention and cleaning of ITER-like castellated structures in TEXTOR.  
Journal of Nuclear Materials, 415(2011) S.S289-S292  
DOI:10.1016/j.jnucmat.2010.12.018

Litvak, A., Sakamoto, K., Thumm, M.  
Innovation on high-power long-pulse gyrotrons.  
Plasma Physics and Controlled Fusion 53(2011)  
S 124002/1-14; DOI:10.1088/0741-3335/53/12/124002

Omori, T., Henderson, M.A., Albajar, F., Alberti, S., Baruah, U., Bigelow, T., Beckett, B., Bertizzolo, R., Bonicelli, T., Bruschi, A., Caughman, J., Chavan, R., Cirant, S., Collazos, A., Cox, D., Darbos, C., de Baar, M., Denisov, G., Farina, D., Gandini, F., Gassmann, T., Goodman, T.P., Heidinger, R., Hogge, J.P., Illy, S., Jean, O., Jin, J., Kajiwara, K., Kasperek, W., Kasugai, A., Kern, S., Kobayashi, N., Kumric, H., Landis, J.D. Moro, A., Nazare, C., Oda, Y., Pagonakis, I., Piosczyk, b., Platania, P., Plaum, B., Poli, E., Porte, L., Purohit, D., Ramponi, G., Rao, S.L., Rasmussen, D.A., Ronden, D.M.S., Rzesnicki, T., Saibene, G., Sakamoto, K., Sanchez, F., Scherer, T., Shapiro, M., Sozzi, C., Spaeh, P., Strauss, D., Sauter, O., Takahashi, K., Temkin, R., Thumm, M., Tran, M.Q., Udintsev, V., Zohm, H.  
Overview of the ITER ECH&CD system and its capabilities.  
Fusion Engineering and Design, 86(2011) S.951-954  
DOI:10.1016/j.fusengdes.2011.02.040

Pestchanyi, S., Garkusha, I., Landman, I.  
Simulation of residual thermostress in tungsten after repetitive ELM-like heat loads  
Fusion Engineering and Design, 86(2011), S. 1681-1684  
DOI:10.1016/j.fusengdes.2011.01.034

Schmid, M., Erckmann, V., Gantenbein, G., Illy, S., Kern, S., Lievin, Ch., Samartsev, A., Schlaich, A., Rzesnicki, T., Thumm, M.  
Technical developments at the KIT gyrotron test facility.  
Fusion Engineering and Design, 86(2011) S.518-521  
DOI:10.1016/j.fusengdes.2011.01.072

Stindl, T., Neudorfer, J., Stock, A., Auweter-Kurz, M., Munz, C.D., Roller, S., Schneider, R.  
Comparison of coupling techniques in a high-order discontinuous Galerkin-based particle-in-cell solver.  
Journal of Physics D, 44(2011) S.194004/1-9  
DOI:10.1088/0022-3727/44/19/194004

Thumm, M.  
Progress on gyrotrons for ITER and future thermonuclear fusion reactors.  
IEEE Transactions on Plasma Science, 39(2011) S.971-979  
DOI:10.1109/TPS.2010.209502

Thumm, M.K.A.  
Recent developments on high-power gyrotrons. Introduction to this special issue.  
Journal of Infrared, Millimeter and Terahertz Waves, 32(2011) S.241-252. DOI:10.1007/s10762-010-9754-5

Wagner, D., Kasperek, W., Leuterer, F., Monaco, F., Münich, M., Schütz, H., Stange, T., Stober, J., Thumm, M.  
Bragg reflection band stop filter for ECE on WEGA.  
Journal of Infrared Millimeter and Terahertz Waves, 32(2011) S.1424-1433

Wagner, D., Stober, J., Leuterer, F., Monaco, F., Münich, M., Schmid-Lorch, D., Schütz, H., Zohm, H., Thumm, M., Scherer, T., Meier, A., Gantenbein, G., Flamm, J., Kasperek, W., Höhnle, H., Lechte, C., Litvak, A.G., Denisov, G.C., Chirkov, A., Popov, L.G., Nichiporenko, V.O., Myasnikov, V.E., Tai, E.M., Solyanova, E.A., Malygin, S.A.  
Recent upgrades and extension of the ASDEX upgrade ECRH system.  
Journal of Infrared, Millimeter and Terahertz Waves, 32(2011), S.274-282. DOI:10.1007/s10762-010-9703-3

#### **Other printed publications:**

Albajar, F., Bonicelli, T., Alberti, S., Avramides, K.A., Cirant, S., Gantenbein, G., Goodman, T.P., Illy, S., Ioannidis, Z., Hogge, J.P., Jin, J., Kern, S., Latsas, G., Pagonakis, I.G., Piosczyk, B., Rzesnicki, T., Thumm, M., Tigelis, I., Tran, M.Q., Vomvoridis, J., Benin, P., Lievin, C., Darbos, C., Gassmann, T., Henderson, M.  
The European 2 MW gyrotron for ITER.  
Prater, R. [Hrsg.] Electron Cyclotron Emission and Electron Cyclotron Resonance Heating (EC-16): Proc. of the 15<sup>th</sup> Joint Workshop, Sanya, China, April 12-15, 2010. Singapore [u.a.]: World Scientific, 2011 S.331-338. Incl. CD-ROM

Behringer, M.H.  
Design studies towards a 4 MW 170 GHz coaxial-cavity gyrotron.  
Dissertation: KIT Scientific Publ., 2011 (Karlsruher Forschungs-berichte aus dem Institut für Hochleistungsimpuls- und Mikro-wellentechnik; Bd. 1)

Behringer, M., Illy, S., Jin, J., Kern, S., Thumm, M., Lievin, C.  
Physical component designs and thermo-mechanical studies towards a 4 MW 170 GHz coaxial-cavity gyrotron.  
ITG Vacuum Electronics Workshop, Bad Honnef, November 15-16, 2010; Folien auf CD-ROM

Braune, H., Erckmann, V., Laqua, H.P., Michel, G., Noke, F., Purps, F., Schulz, T., Wagner, D., W7-X ECRH Teams at IPP, IPF and KIT  
Gyrotron high power long pulse operation. Challenges and solutions.  
23<sup>rd</sup> Joint Russian-German Meeting on ECRH and Gyrotrons, Karlsruhe/Stuttgart/Garching, May 23-28, 2011.  
Folien auf CD-ROM

Erckmann, V., Kasperek, W., Petelin, M.I., Bruschi, A., Bin, W., Braune, H., van den Braber, R., Doelman, N., Gantenbein, G., Laqua, H.P., Lechte, C., Lubiako, L., Marushchenko, N.B., Michel, G., Plum, B., Thumm, M., W7-X ECRH-Teams at IPP Greifswald, IPF Stuttgart, and KIT ECRH with advanced CW systems.  
8<sup>th</sup> Int. Workshop 'Strong Microwaves and Terahertz Waves: Sources and Applications', Nizhny Novgorod, Russia, July 9-16, 2011. Proc. S. 15-16, Nizhny Novgorod: Russian Academy of Sciences, 2011

Erckmann, V., Kasperek, W., Plum, B., Lechte, C., Petelin, M.I., Bruschi, A., D'Arcangelo, O., Bin, W., Braune, H., van den Braber, R., Doelman, N., Gantenbein, G., Laqua, H.P., Lubiako, L., Marushchenko, N.B., Michel, G., Thumm, M., W7-X ECRH-Teams at IPP Greifswald, IPF Stuttgart, and KIT Large scale CW ECRH systems: meeting a challenge.  
Radio Frequency Power in Plasmas: Proc. of the 19<sup>th</sup> Topical Conf., op, Newport, R.I., June 1-3, 2011, Melville, N.Y.: American Inst. of Physics, 2011 S.165-172 (AIP Conference Proceedings, 1406)

Erckmann, V., PMW- and W7-X Teams at KIT and IPP W7-X and ECRH. Status and prospects.  
23<sup>rd</sup> Joint Russian-German Meeting on ECRH and Gyrotrons, Karlsruhe/Stuttgart/Garching, May 23-28, 2011.  
Folien auf CD-ROM

Flamm, J., Jin, J., Thumm, M.  
An FFT based spectral method for analysis of launchers in advanced gyrotron output couplers.  
ITG Vacuum Electronics Workshop, Bad Honnef, November 15-16, 2010. Folien auf CD-ROM

Flamm, J., Jin, J., Thumm, M.  
Comparison of different models of wave propagation in launchers of quasi-optical mode converters.  
23<sup>rd</sup> Joint Russian-German Meeting on ECRH and Gyrotrons, Karlsruhe/Stuttgart/Barching, May 23-28, 2011.  
Folien auf CD-ROM

Flamm, J., Jin, J., Thumm, M.  
Cylindrical wave decomposition in launchers of gyrotron quasi-optical mode converters.  
2011 IEEE Int. Vacuum Electronics Conference (IVEC 2011): Proc. of a meeting held in Bangalore, IND, February 21-24, 2011, Piscataway, N.J.: IEEE, 2011 S.111-112

Gantenbein, G., Braune, H., Dammertz, G., Erckmann, V., Illy, S., Kern, S., Kasperek, W., Lechte, C., Leonhardt, W., Lievin, C., Michel, G., Noke, F., Purps, F., Samartsev, A., Schlaich, A., Schmid, M., Thumm, M.  
New results of the 140 FHz / 1 MW series gyrotrons for W-7X.  
23<sup>rd</sup> Joint Russian-German Meeting on ECRH and Gyrotrons, Karlsruhe/Stuttgart/Garching, May 23-28, 2011.  
Folien auf CD-ROM  
US-EU-JPN RF Heating Technology Workshop, Austin, Tex., October 10-12, 2011

Gantenbein, G., Dammertz, G., Kern, S., Latsas, G., Piosczyk, B., Rzesnicki, T., Samartsev, A., Schlaich, A., Thumm, M., Tigelis, I.  
Progress in stable operation of high power gyrotrons  
Prater, R. [Hrsg.] Electron Cyclotron Emission and Electron Cyclotron Resonance Heating (EC-16): Proc. of the 16<sup>th</sup> Joint Workshop, Sanya, China, April 12-15, 2010  
Singapore [U.A.]: World Scientific, 2011 S.347-352 Incl. CD-ROM

- Gospodchikov, E.D., Shalashov, A.G., Smolyakova, O.B., Bagryansky, P.A., Malygin, V.I., Gorbatushkov, V.N., Amirov, V.Kh., Thumm, M.  
Design of auxiliary ECR heating system for the gas dynamic trap.  
23<sup>rd</sup> Joint Russian-German Meeting on ECRH and Gyrotrons, Karlsruhe/Stuttgart/Garching, May 23-28, 2011  
Folien auf CD-ROM
- Gospodchikov, E.D., Shalashov, A.G., Smolyakova, O.B., Bagryansky, P.A.; Malygin, V.I.; Gorbatushkov, V.N., Amirov, V.Kh., Thumm, M.  
Design of auxiliary ECR heating system for the gas dynamic trap.  
8<sup>th</sup> Int. Workshop 'Strong Microwaves and Terahertz Waves: Sources and Applications', Nizhny Novgorod, Russia, July 9-16, 2011, Proc. S. 175-176  
Nizhny Novgorod: Russian Academy of Sciences, 2011
- Henderson, M., Albajar, F., Alberti, S., Baruah, U., Bigelow, T., Becket, B., Bertizzolo, R., Bonicelli, T., Bruschi, A., Caughman, J., Chavan, R., Cirant, S., Darbos, C., deBaar, M., Denisov, G., Farina, D., Gandini, F., Gassmann, T., Goodman, T.P., Heidinger, R., Hogge, J.P., Kajiwara, K., Kasperek, W., Kasugai, A., Kern, S., Kobayashi, N., Landis, J.D., Li, F., Litvak, A., Moro, A., Myasnikov, V., Nazare, C., Oda, J., Omori, T., Pagonakis, I., Pamar, D., Peters, B., Platania, P., Plum, B., Poli, E., Porte, L., Piosczyk, B., Purohit, D., Ramponi, G., Rao, S.L., Rasmussen, D., Ronden, D., Saibene, G., Sakamoto, K., Sanchez, F., Scherer, T., Schreck, S., Singh, N.P., Shapiro, M., Sozzi, C., Spaeh, P., Strauss, D., Sauter, O., Tai, E., Takahashi, K., Temkin, R., Thomas, P., Thumm, M., Zohm, H.  
Present status of the 24 MW 170 GHz ITER ECH&D system.  
8<sup>th</sup> Int. Workshop 'Strong Microwaves and Terahertz Waves: Sources and Applications', Nizhny Novgorod, Russia, July 9-16, 2011. Proc. S.21-22  
Nizhny Novgorod: Russian Academy of Sciences, 2011
- Henderson, M., Becket, B., Cox, C., Darbos, C., Gandini, F., Gassmann, T., Jean, O., Nazare, C., Omori, T., Purohit, D., Tanga, A., Udintsev, V., Albajar, F., Bonicelli, T., Heidinger, R., Saibene, G., Alberti, S., Bertizzolo, R., Chavan, R., Collazos, A., Goodman, T.P., Hogge, J.P., Landis, J.D., Pagonakis, I., Porte, L., Sanchez, F., Sauter, O., Tran, M.Q., Zucca, C., Baruah, U., Kushwah, M., Singh, N.P., Rao, S.L., Bigelow, T., Caughman, J., Rasmussen, D., Bruschi, A., Cirant, S., Farina, D., Moro, A., Platania, P., Ramponi, G., Sozzi, C., DeBaar, M., Ronden, D., Denisov, G., Kajiwara, K., Kasugai, A., Kobayashi, N., Oda, Y., Sakamoto, K., Takahashi, K., Kasperek, W., Kumric, H., Plum, B., Aiello, G., Gantenbein, G., Illy, S., Jin, J., Kern, S., Meier, A., Piosczyk, B., Rzesnicki, T., Scherer, T., Schreck, S., Serikov, A., Spaeh, P., Strauss, D., Thumm, M., Vaccaro, A., Poli, E., Zohm, H., Shapiro, M., Temkin, R.  
The ITER ECH&CD system.  
Prater, R. [Hrsg.] Electron Cyclotron Emission and Electron Cyclotron Resonance Heating (EC-16): Proc. of the 16<sup>th</sup> Joint Workshop, Sanya, China, April 12-15, 2010. Singapore [u.a.]: World Scientific, 2011 S.353-363. Incl. CD-ROM
- Igitkhanov, Y.  
Modelling of multi-component plasma for TOKES.  
KIT Scientific Reports, KIT-SR 7564 (März 2011)
- Illy, S., Gantenbein, G., Schmid, M., Weggen, J.  
Design, construction and first tests of a stainless steel load for high power mm-wave radiation.  
23<sup>rd</sup> Joint Russian-German Meeting on ECRH and Gyrotrons, Karlsruhe/Stuttgart/Garching, May 23-28, 2011.  
Folien auf CD-ROM
- Jin, J., Gantenbein, G., Kern, S., Rzesnicki, T., Thumm, M.  
A matching optics unit (MOU) for coaxial-cavity ITER gyrotron.  
23<sup>rd</sup> Joint Russian-German Meeting on ECRH and Gyrotrons, Karlsruhe/Stuttgart/Garching, May 23-28, 2011  
Folien auf CD-ROM
- Jin, J., Gantenbein, G., Kern, S., Rzesnicki, T., Thumm, M.  
Design matching optics unit (MOU) for coaxial ITER gyrotron.  
2011 IEEE Int. Vacuum Electronics Conf. (IVEC 2011): Proc. of a meeting held in Bangalore, IND, February 21-24, 2011; Piscataway, N.J.: IEEE, 2011 S.271-272
- Jin, J., Flamm, J., Kern, S., Rzesnicki, T., Thumm, M.  
Theoretical and experimental investigation of a quasi-optical mode converter for a coaxial-cavity gyrotron.  
ITG Vacuum Electronics Workshop, Bad Honnef, November 15-16, 2010. Folien auf CD-ROM
- Kasperek, W., Erckmann, V., Hollmann, F., Michel, G., Noke, F., Purps, F., Plum, B., Brand, P., Lechte, C., Filipovic, E., Saliba, M., Doelmann, N., van den Braber, R., Bongers, W., Krijger, B., Petelin, M., Shchegolkov, D., Kuposova, E., Lubyako, L., Bruschi, A., Bin, W., D'Arcangelo, O., Stober, J., Wagner, D., Groups at IPF Stuttgart, IAP N. Novgorod, IPP Garching and Greifswald, IFP Milano, KIT Karlsruhe, TNO Delft and FOM Rijnhuizen  
Status of development of compact diplexers for ECRH applications  
23<sup>rd</sup> Joint Russian-German Meeting on ECRH and Gyrotrons, Karlsruhe/Stuttgart/Garching, May 23-28, 2011  
Folien auf CD-ROM
- Kern, S., Roy Choudhury, A., D'Andrea, D., Schlaich, A., Avramides, K., Alberti, S.  
Recent advances in gyrotron interaction simulations.  
23<sup>rd</sup> Joint Russian-German Meeting on ECRH and Gyrotrons, Karlsruhe/Stuttgart/Garching, May 23-28, 2011  
Folien auf CD-ROM
- Li, F., Alberti, S., Hogge, J.P., Pagonakis, I.G.  
Calculation of stray magnetic field effects on the operation of the ITER electron cyclotron system.  
38<sup>th</sup> IEEE Int. Conf. on Plasma Science (ICOPS) and 24<sup>th</sup> Symp. on Fusion Engineering (SOFE), Chicago, Ill., June 26-30, 2011  
Piscataway, N.J.: IEEE, 2011 Paper SP2-27  
Proc. also publ. online; e-ISBN 978-1-4577-0667-1  
DOI:10.1109/SOFE.2011.6052289
- Malygin, A.V., Pagonakis, I.Gr., Illy, S., Avramides, K.A., Piosczyk, B., Kern, S., Thumm, M.  
Three-dimensional numerical studies of non-uniform emission in magnetron injection guns.  
8<sup>th</sup> Int. Workshop 'Strong Microwaves and Terahertz Waves: Sources and Applications', Nizhny Novgorod, Russia, July 9-16, 2011, Proc. S. 99-100  
Nizhny Novgorod: Russian Academy of Sciences, 2011
- Neudorfer, J., Stock, A., D'Andrea, D., Illy, S., Kern, S., Munz, C.D., Schneider, R.  
High order parallel PIC simulations of microwaves devices.  
23<sup>rd</sup> Joint Russian-German Meeting on ECRH and Gyrotrons, Karlsruhe/Stuttgart/Garching, May 23-28, 2011  
Folien auf CD-ROM

- Neudorfer, J., Munz, C.D., Stindl, T., Schneider, R., Roller, S., Auweter-Kurtz, M.  
Three-dimensional particle-in-cell simulation of a pulsed plasma truster: modelling and challenges.  
32<sup>nd</sup> Int. Electric Propulsion Conference, Wiesbaden, September 11-15, 2011; Proc. publ. online  
Fairview Park, Ohio: Electric Rocket Propulsion Society, 2011 Paper 116
- Neudorfer, J., Stindl, T., Stock, A., Schneider, R., Petkow, D., Roller, S., Munz, C.D., Auweter-Kurtz, M.  
Three-dimensional simulation of rarefied plasma flows using a high order particle in cell method.  
Nagel, W. [Hrsg.] High Performance Computing in Science and Engineering '10: Transactions of the High Performance Computing Center, Stuttgart (HLRS) 2010  
Berlin [u.a.]: Springer, 2011 S. 593-604  
DOI:10.1007/978-3-642-15748-6\_43
- Pagonakis, I.Gr., Illy, S., Piosczyk, B., Kern, S., Hogge, J.P., Alberti, S.  
A new criterion for gyrotron gun design.  
23<sup>rd</sup> Joint Russian-German Meeting on ECRH and Gyrotrons, Karlsruhe/Stuttgart/Garching, May 23-28, 2011  
Folien auf CD-ROM
- Pagonakis, I.Gr., Illy, S., Piosczyk, B., Li, F., Alberti, S., Darbos, C., Henderson, M.  
The effect of the ITER stray magnetic field on the operation of the EU 2 MW coaxial cavity gyrotron.  
23<sup>rd</sup> Joint Russian-German Meeting on ECRH and Gyrotrons, Karlsruhe/Stuttgart/Garching, May 23-28, 2011  
Folien auf CD-ROM
- Pagonakis, I.Gr., Li, F., Alberti, S., Illy, S., Piosczyk, B., Hogge, J.P., Kern, S., Ferran, A., Henderson, M., Darbos, C.  
The effect of the ITER stray magnetic field on the operation of the EU 2 MW coaxial cavity gyrotron.  
8<sup>th</sup> Int. Workshop 'Strong Microwaves and Terahertz Waves: Sources and Applications', Nizhny Novgorod, Russia, July 9-16, 2011; Folien auf CD-ROM
- Roy Choudhury, A., Kern, S., D'Andrea, D., Schlaich, A., Thumm, M.  
Influence of tapered magnetic field on gyrotron interaction calculation.  
23<sup>rd</sup> Joint Russian-German Meeting on ECRH and Gyrotrons, Karlsruhe/Stuttgart/Garching, May 23-28, 2011; Folien auf CD-ROM
- Rzesnicki, T., Piosczyk, B., Illy, S., Jin, J., Kern, S., Pagonakis, I., Samartsev, A., Schlaich, A., Thumm, M.  
2 MW, 170 GHz coaxial-cavity gyrotron for ITER. Results obtained with a short pulse pre-prototype at KIT.  
8<sup>th</sup> Int Workshop 'Strong Microwaves and Terahertz Waves: Sources and Applications', Nizhny Novgorod, Russia, July 9-16, 2011; Proc. S. 121-122  
Nizhny Novgorod: Russian Academy of Sciences, 2011
- Rzesnicki, T., Piosczyk, B., Gantenbein, G., Illy, S., Jin, J., Kern, S., Pagonakis, I., Samartsev, A., Schlaich, A., Thumm, M.  
Recent experimental investigations on the 2 MW, 170 GHz coaxial cavity preprototype gyrotron for ITER.  
23<sup>rd</sup> Joint Russian-German Meeting on ECRH and Gyrotrons, Karlsruhe/Stuttgart/Garching, May 23-28, 2011  
Folien auf CD-ROM
- Rzesnicki, T., Piosczyk, B., Roy Choudhury, A., Illy, S., Jin, J., Kern, S., Samartsev, A., Schlaich, A., Thumm, M.  
Recent improvements on the 2 MW, 170 GHz coaxial-cavity pre-prototype gyrotron.  
ITG Vacuum Electronics Workshop, Bad Honnef, November 15-16, 2010; Folien auf CD-ROM
- Samartsev, A., Gantenbein, G., Dammertz, G., Illy, S., Kern, S., Schlaich, A., Thumm, M.  
Current status of multi-frequency gyrotron development.  
23<sup>rd</sup> Joint Russian-German Meeting on ECRH and Gyrotrons, Karlsruhe/Stuttgart/Garching, May 23-28, 2011  
Folien auf CD-ROM
- Samartsev, A., Gantenbein, G., Dammertz, G., Illy, S., Kern, S., Leonhardt, W., Schlaich, A., Schmid, M., Thumm, M.  
Development of frequency step tunable 1 MW gyrotron at 131 to 146.5 GHz.  
2011 IEEE Int. Vacuum Electronics Conf. (IVEC 2011): Proc. of a meeting held in Bangalore, IND, February 21-24, 2011  
Piscataway, N.J.: IEEE, 2011 S.269-270
- Schlaich, A., Flamm, J., Gantenbein, G., Kern, S., Samartsev, A., Thumm, M.  
Characterization of undesired RF oscillations in megawatt gyrotrons.  
ITG Vacuum Electronics Workshop, Bad Honnef, November 15-16, 2010; Folien auf CD-ROM
- Schlaich, A., Illy, S., Kern, S., Samartsev, A., Thumm, M.  
Recent examinations of the W7-X-SN4R gyrotron RF output spectrum.  
23<sup>rd</sup> Joint Russian-German Meeting on ECRH and Gyrotrons, Karlsruhe/Stuttgart/Garching, May 23-28, 2011  
Folien auf CD-ROM
- Stober, J., Wagner, D., Giannone, L., Leuterer, M., Maraschek, M., Mlynek, A., Monaco, F., München, M., Poli, E., Reich, M., Schmid-Lorch, D., Schütz, H., Schweinzer, J., Treutterer, W., Zohm, H., Meier, A., Scherer, T., Flamm, J., Thumm, M., Höhnle, H., Kasperek, W., Stroth, U., Chirkov, A., Denisov, G.G., Litvak, A., Malygin, S.A., Miyasnikov, V.E., Nichiporenko, V.O., Popov, L.G., Soluyanov, E.A., Tai, E.M.  
ECRH on ASDEX upgrade. System extension, new modes of operation, plasma physics results.  
Prater, R. [Hrsg.] Electron Cyclotron Emission and Electron Cyclotron Resonance Heating (EC-16): Proc. of the 16<sup>th</sup> Joint Workshop, Sanya, China, April 12-15, 2010  
Singapore [u.a.]: World Scientific, 2011 S.28-41, incl. CD-ROM
- Stober, J., Leuterer, F., Monaco, F., Müller, S., München, M., Schubert, M., Schütz, H., Wagner, D., Zohm, H., Thumm, M., Scherer, T., Meier, A., Gantenbein, G., Flamm, J., Kasperek, W., Lecht, C., Litvak, A.G., Denisov, G.G., Chirkov, A., Popov, L.G., Nichiporenko, V.O., Myasnikov, V.E., Tai, E.M., Solyanova, E.A., Malygin, S.A., Belov, Y.  
Status and plans for an extension of the ECRH systems on ASDEX upgrade.  
23<sup>rd</sup> Joint Russian-German Meeting on ECRH and Gyrotrons, Karlsruhe/Stuttgart/Garching, May 23-28, 2011  
Folien auf CD-ROM
- Stober, J., ASDEX-Upgrade Team; Gycom, IAP, KIT, IPF, IPP Greifswald  
The ECRH system of ASDEX upgrade. Status and plans.  
23<sup>rd</sup> Joint Russian-German Meeting on ECRH and Gyrotrons, Karlsruhe/Stuttgart/Garching, May 23-28, 2011  
Folien auf CD-ROM



Strauss, D., Flamm, J., Gantenbein, G., Meier, A., Scherer, T., Thumm, M., Vaccaro, A., Stober, J., Wagner, D., Denisov, G.G.  
ECH beyond ITER: broadband diamond windows.  
23<sup>rd</sup> Joint Russian-German Meeting on ECRH and Gyrotrons, Karlsruhe/Stuttgart/Garching, May 23-28, 2011  
Folien auf CD-ROM

Strauss, D., Aiello, G., Chavan, R., Cirant, S., deBaar, M., Farina, D., Gantenbein, G., Goodman, T., Henderson, M.A., Kasperek, W., Kleefeld, K., Landis, J.D., Meier, A., Moro, A., Plaum, B., Poli, E., Ramponi, G., Ronden, D., Saibene, G., Sanchez, F., Sautter, O., Scherer, T., Schreck, S., Serikov, A., Sozzi, C., Spaeh, P., Vaccaro, A., Zohm, H.  
Preliminary design of the ITER ECH upper launcher.  
38<sup>th</sup> IEEE Int. Conf. on Plasma Science (ICOPS) and 24<sup>th</sup> Symp. on Fusion Engineering (SOFE), Chicago, Ill., June 26-30, 2011  
Abstract online; DOI:10.1109/SOFE.2011.6052319

Thumm, M., Gantenbein, G., Illy, S., Kern, S., Leonhardt, W., Samartsev, A., Schlaich, A., Schmidt, M., Erckmann, V., Kasperek, W., Lechte, C., Lievin, C.  
140 GHz, 1 MW, CW gyrotron development for the ECRH system of the stellarator Wendelstein 7-X.  
2011 IEEE Int. Vacuum Electronics Conf. (IVEC 2011): Proc. of a meeting held in Bangalore, IND, February 21-24, 2011  
Piscataway, N.J.: IEEE, 2011, S. 105-106

Thumm, M., Braune, H., Dammertz, G., Gantenbein, G., Erckmann, V., Illy, S., Kern, S., Kasperek, W., Lechte, C., Leonhardt, W., Lievin, C., Michel, G., Noke, F., Purps, F., Samartsev, A., Schlaich, A., Schmid, M., Schulz, T.  
Recent progress on the 1 MW, 140 GHz, CW series gyrotrons for W7-X.  
8<sup>th</sup> Int. Workshop 'Strong Microwaves and Terahertz Waves: Sources and Applications', Nizhny Novgorod, Russia, July 9-16, 2011, Proc. S. 45-46  
Nizhny Novgorod: Russian Academy of Sciences, 2011

Thumm, M.  
State-of-the-art of high power gyro-devices and free electron masers. Update 2010.  
KIT Scientific Reports KIT-SR 7575 (April 2011)

Vaccaro, A., Aiello, G., Meier, A., Scherer, T., Schreck, S., Spaeh, P., Strauss, D., Gantenbein, G.  
Silicon oil DC200(R)5CST as an alternative coolant for CVD diamond windows.  
Prater, R. [Hrsg.] Electron Cyclotron Emission and Electron Cyclotron Resonance Heating (EC-16): Proc. of the 16<sup>th</sup> Joint Workshop, Sanya, China, April 12-15, 2010  
Singapore [u.a.]: World Scientific, 2011 S. 401-409  
Incl. CD-ROM

Wagner, D., Kasperek, W., Leuterer, F., Monaco, F., Münich, M., Schütz, H., Stange, T., Stober, J., Thumm, M.  
Band stop filter for ECE at WEGA.  
23rd Joint Russian-German Meeting on ECRH and Gyrotrons, Karlsruhe/Stuttgart/Garching, May 23-28, 2011  
Folien auf CD-ROM

**Papers or lectures, which are not available in printed form:**

Bazylev, B., Landman, I., Pitts, R.A.  
Simulations of transient heat flux damage on leading edges in the ITER alltungsten divertor.  
15<sup>th</sup> Int. Conf. on Fusion Reactor Materials, Charleston, S.C., October 16-22, 2011

Borie, E.  
Computation of RF-behavior in gyrotrons.  
10<sup>th</sup> School of Fusion Physics and Technology, Volos, GR, May 9-13, 2011

Borie, E., Gantenbein, G., Illy, S., Kern, S., Leonhardt, W., Samartsev, A., Schlaich, A., Schmid, M., Thumm, M.  
Development of 140 GHz, 1 MW, CW gyrotrons for fusion applications. Status and recent results.  
10<sup>th</sup> School of Fusion Physics and Technology, Volos, GR, May 9-13, 2011

Damyanova, M., Kern, S., Illy, S., Thumm, M., Sabchevski, S., Zhelyazkov, I., Vasileva, E., Balabanova, E.  
Simulation tools for computer aided design and numerical investigations of powerful gyrotrons.  
17<sup>th</sup> Int. Summer School on Vacuum, Electron and Ion Technologies, Sunny Beach, BG, September 19-23, 2011

Erckmann, V., Kasperek, W., Plaum, B., Lechte, C., Petelin, M.I., Bruschi, A., D'Arcangelo, O., Bin, W., Braune, H., van den Braber, R., Doelman, N., Gantenbein, G., Laqua, H.P., Lubiako, L., Marushchenko, N.B., Michel, G., Thumm, M., W7-X ECRH-Teams at IPP Greifswald, IPF Stuttgart, and KIT  
Large scale CW ECRH systems: meeting a challenge.  
Joint Meeting of the 19<sup>th</sup> Topical Conf. on Radio Frequency Power in Plasmas and the US Japan RF Physics Workshop, Newport, R.I., June 1-3, 2011

Gantenbein, G., Braune, H., Dammertz, G., Erckmann, V., Illy, S., Kern, S., Kasperek, W., Lechte, C., Leonhardt, W., Lievin, C., Michel, G., Noke, F., Purps, F., Samartsev, A., Schlaich, A., Schmid, M., Thumm, M.  
Status of 1 MW, 140 GHz series gyrotrons for W7-X.  
36<sup>th</sup> Int. Conf. on Infrared, Millimeter and Terahertz Waves (IRMMW-THz 2011), Houston, Tex., October 2-7, 2011

Igitkhanov, Yu.  
On generation of runaway electrons during massive gas injection.  
13<sup>th</sup> Int. Workshop on Plasma Edge Theory in Fusion Devices (PET 13), South Lake Tahoe, CA, September 19-21, 2011  
European Fusion Theory Conf., Frascati, I, Sept. 26-29, 2011

Igitkhanov, Yu., Bazylev, B., Pestchanyi, S., Boccaccini, L.  
Plasma facing materials lifetime in DEMO reactor.  
10<sup>th</sup> Int. Symp. on Fusion Nuclear Technology (ISFNT 2011), Portland, Oreg., September 11-16, 2011  
Abstract on CD-ROM

Illy, S., Gantenbein, G., Schmid, M., Weggen, J.  
Design, construction and first tests of a stainless steel load for high power mm-wave radiation.  
38<sup>th</sup> IEEE Int. Conf. on Plasma Science (ICOPS) and 24<sup>th</sup> Symp. on Fusion Engineering (SOFE), Chicago, Ill, June 26-30, 2011; Abstracts publ. online

Kalaria, P.C., Kartikeyan, M.V., Thumm, M.  
Design considerations of a 170 GHz, 0.5 MW, CW gyrotron.  
Int. Conf. on Microwaves, Antenna, Propagation and Remote Sensing (ICMARS), Jodhpur, IND, December 7-10, 2011

Kalaria, P.C., Kartikeyan, M.V., Thumm, M.  
Design studies of quasi-optical launcher of a 170 GHz, CW gyrotron for ECRH applications.  
Int. Conf. on Microwaves, Antenna, Propagation and Remote Sensing (ICMARS), Jodhpur, IND, December 7-10, 2011

- Kern, S., Avramides, K.A., Roy Choudhury, A., Dumbrajs, O., Gantenbein, G., Illy, S., Samartsev, A., Schlaich, A., Thumm, M.  
Simulation and experimental investigation on dynamic after cavity interaction (ACI).  
36<sup>th</sup> Int. Conf. on Infrared, Millimeter and Terahertz Waves (IRMMW-Thz 2011), Houston, Tex., October 2-7, 2011
- Litvak, A., Sakamoto, K., Thumm, M.  
Innovation on high power long pulse gyrotrons.  
38<sup>th</sup> EPS Conf. on Plasma Physics, Strasbourg, F, June 27 – July 1, 2011
- Neudorfer, J., Munz, C.D., Schneider, R.  
High order PIC simulation of high power millimeter wave sources.  
38<sup>th</sup> IEEE Int. Conf. on Plasma Science (ICOPS) and 24<sup>th</sup> Symp. on Fusion Engineering (SOFE), Chicago, Ill., June 26-30, 2011; Abstract publ. online
- Neudorfer, J., Stock, A., D'Andrea, D., Illy, S., Kern, S., Schneider, R., Roller, S., Munz, C.D.  
High-order PIC simulations of microwave sources.  
36<sup>th</sup> Int. Conf. on Infrared, Millimeter and Terahertz Waves (IRMMW-THz 2011), Houston, Tex., October 2-7, 2011
- Pestchanyi, S., Landman, I.  
Verification of TOKES simulations against the MGI experiments in JET.  
10<sup>th</sup> Int. Symp. on Fusion Nuclear Technology (ISFNT 2011), Portland, Oreg., September 11-16, 2011
- Rzesnicki, T., Piosczyk, B., Gantenbein, G., Illy, S., Jin, J., Kern, S., Losert, M., Pagonakis, I., Samartsev, A., Schlaich, A., Thumm, M.  
2 MW, 170 GHz coaxial-cavity gyrotron for ITER.  
Experimental results obtained with a short-pulse-pre-prototype tube.  
US-EU-JPN RF Heating Technology Workshop, Austin, Tex., October 10-12, 2011
- Samartsev, A., Gantenbein, G., Illy, S., Kern, S., Latsas, G., Thumm, M., Tigelis, I.  
Numerical simulation of parasitic gyro-BWO interaction in a gyrotron beam tunnel.  
36<sup>th</sup> Int. Conf. on Infrared, Millimeter and Terahertz Waves (IRMMW-THz 2011), Houston, Tex., October 2-7, 2011
- Schlaich, A., Choudhury, A.R., Gantenbein, G., Illy, S., Kern, S., Lievin, C., Samartsev, A., Thumm, M.  
Examination of parasitic after-cavity oscillations in the W7-X series gyrotron SN4R.  
US-EU-JPN RF Heating Technology Workshop, Austin, Tex., October 10-12, 2011
- Stock, A., Neudorfer, J., D'Andrea, D., Munz, C.D., Schneider, R., Roller, S.  
High-order PIC simulation of high power millimeter wave sources components.  
38<sup>th</sup> EPS Conf. on Plasma Physics, Strasbourg, F, June 27 – July 1, 2011
- Thumm, M.  
Lecture series on high-power quasi-optical mm-wave transmission and mode converters for ECRH.  
5: High-power millimetre wave quasi-optical components and mode converters.  
Vortr.: Budker Institute of Nuclear Physics, Novosibirsk, Russia, 20. April 2011
- Thumm, M.  
Lecture series on high-power quasi-optical mm-wave transmission and mode converters for ECRH.  
6: 10 MW, 140 GHz, CW gyrotron and optical transmission system for the stellarator Wendelstein 7-X (W7-X).  
Vortr.: Budker Institute of Nuclear Physics, Novosibirsk, Russia, 21. April 2011
- Thumm, M.  
Lecture series on overmoded waveguide transmission.  
1: Attenuation and mode conversion in overmoded waveguide.  
Vortr.: Budker Institute of Nuclear Physics, Novosibirsk, Russia, 10. März 2011
- Thumm, M.  
Lecture series on overmoded waveguide transmission.  
2: Diagnostics and adiabatic mode converters in overmoded waveguide.  
Vortr.: Budker Institute of Nuclear Physics, Novosibirsk, Russia, 10. März 2011
- Thumm, M.  
Lecture series on overmoded waveguide transmission.  
3: Mode converters and components in overmoded waveguides I.  
Vortr.: Budker Institute of Nuclear Physics, Novosibirsk, Russia, 11. März 2011
- Thumm, M.  
Lecture series on overmoded waveguide transmission.  
4: Mode converters and components in overmoded waveguides II.  
Vortr.: Budker Institute of Nuclear Physics, Novosibirsk, Russia, 11. März 2011
- Thumm, M.  
Progress on gyrotrons for ITER, W7-X and future magnetic confinement fusion reactors.  
Vortr.: Novosibirsk State Technical University, 06. Dezember 2011
- van't Klooster, C.G.M., Petelin, M., Aloisio, M., Thumm, M.  
Large MM-wave groundbased antenna for telecommunication and radar and associated system considerations.  
33<sup>rd</sup> ESA Antenna Workshop on Challenges for Space Antenna Systems, Noordwijk, NL, October 18-21, 2011
- Wagner, D., Kasperek, W., Leuterer, F., Monaco, F., München, M., Schütz, H., Stange, T., Stober, J., Thumm, M.  
Bragg reflection band stop filter for ECE on WEGA.  
36<sup>th</sup> Int. Conf. on Infrared, Millimeter and Terahertz Waves (IRMMW-THz 2011), Houston, Tex., October 2-7, 2011
- Wagner, D., Stober, J., Leuterer, F., Monaco, F., Müller, S., München, M., Schubert, M., Schütz, H., Zohm, H., Erckmann, V., Thumm, M., Scherer, T., Strauss, D., Meier, A., Gantenbein, G., Flamm, J., Kasperek, W., Höhnle, H., Lechte, C., Litvak, A.G., Denisov, G.G., Chirkov, A., Petelin, M.I., Popov, L.G.; Nichiporenk, V.O., Myasnikov, V.E., Tai, E.M., Solyanova, E.A., Malygin, V.E., ASDEX Upgrade Team  
Multi-frequency ECRH system at ASDEX upgrade status and activities.  
US-EU-JPN RF Heating Technology Workshop, Austin, Tex., October 10-12, 2011

Wagner, D., Stober, J., Leuterer, F., Monaco, F., München, M., Schubert, M., Schütz, H., Zohm, H., Thumm, M., Scherer, T., Meier, A., Gantenbein, G., Flamm, J., Kasperek, W., Höhnle, H., Lechte, C., Litvak, A.G., Denisov, G.G., Chirkov, A., Popov, L.G., Nichiporenko, V.O., Myasnikov, V.E., Tai, E.M., Solyanova, E.M., Malygin, S.A.

Operation of the multifrequency ECRH system at ASDEX upgrade.

36<sup>th</sup> Int. Conf. on Infrared, Millimeter and Terahertz Waves (IRMMW-THz 2011), Houston, Tex., October 2-7, 2011

Wolf, R.C., Aktaa, J., Antusch, S., Biel, W., Boccaccini, L.V., Bornschein, B., Brezinsek, S., Cismonti, F., Day, C., Demange, D., Fantz, U., Fietz, W., Franzen, P., Gantenbein, G., Ghidersa, B.E., Giegerich, Th., Gunter, S., Hauer, V., Heller, R., Hesch, K., Igitkhanov, Y., Kallenbach, A., Kern, S., Knitter, R., König, R., Konys, J., Koslowski, H.R., Lackner, K., Landman, I., Lehnen, M., Lietzow, R., Linke, J., Linsmeier, C., Meister, H., Mertens, P., Mittwollen, M., Möslang, A., Neubauer, O., Noe, M., Norajitra, P., Noterdaeme, J.M., Pautasso, G., Phillips, V., Reiter, D., Rieth, M., Roth, J., Tardini, G., Treutterer, W., Schauer, F., Schlachter, S., Strauß, D., Unterberg, B., Weiss, K., You, J.H., Zohm, H. Assessment of the physics and technology requirements for a fusion DEMO.

Integration of Fusion Science and Technology for Steady State Operation : 21<sup>st</sup> Int. Toki Conf., Toki City, Gifu, J, November 28 – December 1, 2011

## HGF Program: NANOMIKRO

### *Other printed publications:*

Arzhannikov, A.V., Burdakov, A.V., Kalinin, P.V., Kuznetsov, S.A., Makarov, M.A., Mekler, K.I., Polosatkin, S.V., Postupaev, V.V., Rovenskikh, A.F., Sinitzky, S.L., Sklyarov, V.F., Stepanov, V.D., Sulyaev, Yu.S., Thumm, M., Vyacheslavov, L.N.

Subterahertz generation by magnetized plasma at two-stream instability of high current 1-MeV REB.

8<sup>th</sup> Int. Workshop 'Strong Microwaves and Terahertz Waves: Sources and Applications', Nizhny Novgorod, Russia, July 9-16, 2011; Proc. S. 209-210  
Nizhny Novgorod: Russian Academy of Sciences, 2011

Ginzburg, N.S., Peskov, N.Yu., Sergeev, A.S., Arzhannikov, A.V., Kalinin, P.V., Sinitzky, S.L., Thumm, M.

Powerful masers and lasers with two-dimensional distributed feedback.

8<sup>th</sup> Int. Workshop 'Strong Microwaves and Terahertz Waves: Sources and Applications', Nizhny Novgorod, Russia, July 9-16, 2011, Proc. S. 57-58  
Nizhny Novgorod: Russian Academy of Sciences, 2011

Jain, C.A., Verma, A., Kumar, A., Kartikeyan, M.V., Borie, E., Thumm, M.

Design studies of a 460 GHz, 30-50 W, CW second harmonic gyrotron.

2011 IEEE Int. Vacuum Electronics Conf. (IVEC 2011): Proc. of a meeting held in Bangalore, IND, February 21-24, 2011  
Piscataway, N.J.: IEEE, 2011 S.59-60

Kartikeyan, M.V., Borie, E., Thumm, M.

Recent results in collaborative studies on the design of application specific gyrotrons.

2011 IEEE Int. Vacuum Electronics Conf. (IVEC 2011): Proc. of a meeting held in Bangalore, IND, February 21-24, 2011  
Piscataway, N.J.: IEEE, 2011 S.109-110

Krishna, P.V., Kartikeyan, M.V., Thumm, M.

Design studies of the output system of a 95 GHz, 100 kW, CW gyrotron.

2011 IEEE Int. Vacuum Electronics Conf. (IVEC 2011): Proc. of a meeting held in Bangalore, IND, February 21-24, 2011  
Piscataway, N.J.: IEEE, 2011 S.291-292

Krishna, P.V., Kartikeyan, M.V., Thumm, M.

Mode selection and resonator design studies of a 95 GHz, 100 kW, CW gyrotron.

2011 IEEE Int. Vacuum Electronics Conf. (IVEC 2011): Proc. of a meeting held in Bangalore, IND, February 21-24, 2011  
Piscataway, N.J.: IEEE, 2011 S.293-294

Link, G., Mahmoud, M.M., Thumm, M.

Investigation of millimeter-wave metal powder sintering by application of dilatometry and in-situ resistivity measurements.

8<sup>th</sup> Int. Workshop 'Strong Microwaves and Terahertz Waves: Sources and Applications', Nizhny Novgorod, Russia, July 9-16, 2011; Proc. S. 317-318  
Nizhny Novgorod: Russian Academy of Sciences, 2011

Link, G.

Measurement and modelling of intrinsic dielectric properties of ionic crystals at microwave frequencies.

13<sup>th</sup> Int. Conf. on Microwave and High Frequency Heating (AMPERE 2011), Toulouse, F, September 5-8, 2011

Tao, J. [Hrsg.] Microwave and RF Power Applications: Proc. of the 13<sup>th</sup> Int. Conf. on Microwave and High Frequency Heating (AMPERE 2011), Toulouse, F, September 5-8, 2011  
Toulouse: CEPAD, 2011 S. 115-118

Mahmoud, M.M., Link, G., Miksch, S., Thumm, M.  
30 GHz microwave crystallization of lithium disilicate based glass.  
13<sup>th</sup> Int. Conf. on Microwave and High Frequency Heating (AMPERE 2011), Toulouse, F, September 5-8, 2011  
Tao, J. [Hrsg.] Microwave and RF Power Applications: Proc. of the 13<sup>th</sup> Int. Conf. on Microwave and High Frequency Heating (AMPERE 2011), Toulouse, F, September 5-8, 2011  
Toulouse: CEPAD, 2011 S. 260-263

Sadykov, V.A., Usoltsev, V.V., Ereemeev, N.F., Salanov, A.N., Mezentseva, N.V., Kharlamova, T.S., Pavlova, S.N., Bobrenok, O.F., Ulihin, A.S., Uvarov, N.F., Smorygo, O.L., Arzhannikov, A.V., Kalinin, P.V., Thumm, M.  
Microwave sintering of functional layers in design of planar solid oxide fuel cells.  
8<sup>th</sup> Int. Workshop 'Strong Microwaves and Terahertz Waves: Sources and Applications', Nizhny Novgorod, Russia, July 9-16, 2011; Proc. S. 295-296  
Nizhny Novgorod: Russian Academy of Sciences, 2011

Sinitsky, S.L., Arzhannikov, A.V., Astrelin, V.T., Ginzburg, N.S., Kalinin, P.V., Kuznetsov, S.A., Peskov, N.Yu., Sergeev, A.S., Stepanov, V.D., Thumm, M., Zaslavsky, V.Yu.  
Planar FEM driven by two microsecond sheet E-beam.  
8<sup>th</sup> Int. Workshop 'Strong Microwaves and Terahertz Waves: Sources and Applications', Nizhny Novgorod, Russia, July 9-16, 2011; Proc. S. 131-132  
Nizhny Novgorod: Russian Academy of Sciences, 2011

Thumm, M.  
Gyro-devices and their applications.  
2011 IEEE Int. Vacuum Electronics Conf. (IVEC 2011): Proc. of a meeting held in Bangalore, IND, February 21-24, 2011  
Piscataway, N.J.: IEEE, 2011 S. 521-524

**Papers or lectures, which are not available in printed form:**

Arzhannikov, A., Kalinin, P., Sinitsky, S., Kuznetsov, S., Ginzburg, N., Malkin, A., Peskov, N., Sergeev, V., Zaslavsky, V., Thumm, M.  
Advanced Bragg structures based on coupling of propagating and cutoff waves: modeling and 'cold' tests.  
36<sup>th</sup> Int. Conf. on Infrared, Millimeter and Terahertz Waves (IRMMW-THz 2011), Houston, Tex., October 2-7, 2011

Arzhannikov, A., Burdakov, A., Kalinin, P., Kuznetsov, S., Makarov, M.A., Mekler, K.I., Popov, A.A., Postupaev, V.V., Rovenskikh, A.F., Sinitsky, S., Sklyarov, V.F., Stepanov, V.D., Sulyaev, Yu.S., Thumm, M., Vyacheslavov, L.N.  
Emission of submm-radiation by strong turbulent plasma at two-stream instability of high current REB.  
36<sup>th</sup> Int. Conf. on Infrared, Millimeter and Terahertz Waves (IRMMW-THz 2011), Houston, Tex., October 2-7, 2011

Arzhannikov, A.V., Astrelin, V.T., Ginzburg, N.S., Kalinin, P.V., Kuznetsov, S.A., Peskov, N.Yu., Sergeev, A.S., Sinitsky, S.L., Stepanov, V.D., Thumm, M., Zaslavsky, V.Yu.  
Generation of MW radiation in a two-channel planar FEM with combined electrodynamic system  
36<sup>th</sup> Int. Conf. on Infrared, Millimeter and Terahertz Waves (IRMMW-THz 2011), Houston, Tex., October 2-7, 2011

Arzhannikov, A.V., Astrelin, V.T., Ginzburg, N.S., Kalinin, P.V., Kuznetsov, S.A., Peskov, N.Yu., Sergeev, A.S., Sinitsky, S.L., Stepanov, V.D., Thumm, M., Zaslavsky, V.Yu.  
Planar FEM driven by two microsecond sheet E-beam.  
8<sup>th</sup> Int. Workshop 'Strong Microwaves and Terahertz Waves: Sources and Applications', Nizhny Novgorod, Russia, July 9-16, 2011

Arzhannikov, A.V., Burdakov, A.V., Kalinin, P.V., Kuznetsov, S.A., Makarov, M.A., Mekler, K.I., Polosatkin, S.V., Postupaev, V.V., Rovenskikh, A.F., Sinitsky, S.L., Sklyarov, V.F., Stepanov, V.D., Sulyaev, Yu.S., Thumm, M., Vyacheslavov, L.H.  
Subterahertz emission by strong turbulent plasma at two-stream instability of high current REB.  
38<sup>th</sup> EPS Conf. on Plasma Physics, Strasbourg, F, June 27 – July 1, 2011

Betz, M., Gasior, M., Caspers, F., Thumm, M.  
Status report of the CERN light shining through the wall experiment with microwave axions and related aspects.  
7<sup>th</sup> Patras Workshop on Axion, WIMPs and WISPs, Mykonos, GR, June 26 – July 1, 2011

Coletti, A.Y., Link, G., Kiminami, R.H.G.A.  
Alumina/silicon carbide nanocomposites: microwave sintering.  
Materials Science and Technology 2011 Conf. and Exhibition (MS&T'11), Columbus, Ohio, October 16-20, 2011

Ginzburg, N.S., Peskov, N.Yu., Sergeev, A.S., Arzhannikov, A.V., Kalinin, P.V., Sinitsky, S.L., Thumm, M.  
Powerful masers and lasers with two-dimensional distributed feedback.  
36<sup>th</sup> Int. Conf. on Infrared, Millimeter and Terahertz Waves (IRMMW-THz 2011), Houston, Tex., October 2-7, 2011

Jain, C.A., Verma, A., Kumar, A., Krishna, P.V., Kartikeyan, M.V., Illy, S., Borie, E., Thumm, M.  
Design of triode-type magnetron injection gun for 460 GHz, 50-100 W gyrotron for medical spectroscopy.  
36<sup>th</sup> Int. Conf. on Infrared, Millimeter and Terahertz Waves (IRMMW-THz 2011), Houston, Tex., October 2-7, 2011

Jain, C.A., Verma, A., Kumar, A., Kartikeyan, M.V., Borie, E., Thumm, M.  
Design studies of a 460 GHz, 30-50 W, CW second harmonic gyrotron.  
2011 IEEE Int. Vacuum Electronics Conf. (IVEC 2011), Bangalore, IND, February 21-24, 2011

Konoplev, I.V., Cross, A.W., MacLachlan, A.J., Phipps, A., Robertson, C.W., Young, A.R., Thumm, M., Phelps, A.D.R.  
Study of two-dimensional periodic surface lattices for high-power mm and sub-mm wave Cherenkov devices.  
36<sup>th</sup> Int. Conf. on Infrared, Millimeter and Terahertz Waves (IRMMW-THz 2011), Houston, Tex., October 2-7, 2011

Krishna, P.V., Jain, C.A., Verma, A., Kumar, A., Kartikeyan, M.V., Thumm, M.  
Design studies of a quasi-optical mode converter and output system for a second harmonic sub terahertz gyrotron.  
36<sup>th</sup> Int. Conf. on Infrared, Millimeter and Terahertz Waves (IRMMW-THz 2011), Houston, Tex., October 2-7, 2011

Link, G.  
Die perfekte Welle. Mikrowellen für die Materialprozessstechnik.  
Vortr.: Studium Generale für junge Erwachsene, Bruchsal, 20. Mai 2011

Link, G., Mahmoud, M.M., Thumm, M.  
Dilatometric study and in situ resistivity measurements during millimeter wave sintering of metal powder compacts.  
Materials Science and Technology 2011 Conf. and Exhibition (MS&T'11), Columbus, Ohio, October 16-20, 2011

Link, G.  
Innovative, modulare Mikrowellentechnologie zur Herstellung von Faserverbundstrukturen  
Schlussbericht für das BMBF Verbundprojekt  
Förderkennzeichen: 01RI05133.-135-140, -282  
Laufzeit: 01.09.2006 – 31.05.2011  
Eggenstein-Leopoldshafen, 2011

Mahmoud, M.M., Link, G., Miksch, S., Thumm, M.  
High frequency microwave processing of lithium disilicate glass-ceramic.  
Materials Science and Technology 2011 Conf. and Exhibition (MS&T'11), Columbus, Ohio, October 16-20, 2011

Thumm, M.  
Computer engineering in radio physics at KIT. Design in high power microwave technology.  
Symp. on Computer Engineering in Physics and Geophysics, Novosibirsk, Russia, September 22-24, 2011

Thumm, M.  
Historical German contributions to physics and applications of electromagnetic oscillations and waves and relations to Russian scientists.  
Vortr.: Budker Institute of Nuclear Physics, Novosibirsk, Russia, 17. Mai 2011

Thumm, M.  
Microwave vacuum electron tubes (I).  
Vortr.: Novosibirsk State Technical University,  
2. November 2011

Thumm, M.  
Microwave vacuum electron tubes (II).  
Vortr.: Novosibirsk State Technical University,  
9. November 2011

Thumm, M.K.A., Arzhannikov, A.V., Astrelin, V.T., Burdakov, A.V., Ginzburg, N.S., Kalinin, P.V., Kuznetsov, S.A., Makarov, M.A., Mekler, K.I., Peskov, N.Yu., Polosatkin, S.V., Popov, S.A., Postupaev, V.V., Rovenskikh, A.F., Sergeev, A.S., Sinitsky, S.L., Sklyarov, V.F., Stepanov, V.D., Vyacheslavov, L.N., Zaslavsky, V.Yu.  
Generation of high power THz waves in relativistic electron beam.  
3<sup>rd</sup> Shenzhen Int. Conf. on Advanced Science and Technology – Terahertz Science and Technology (the 3<sup>rd</sup> SICAST), Shenzhen, China, November 21-26, 2011;  
Book of Abstracts S.26

## HGF Program: NUKLEAR

### *Publications at cross-referenced journals:*

An, W., Krasik, Y.E., Fetzer, R., Bazylev, B., Müller, G., Weisenburger, A.  
Characterization of high-current electron beam interaction with metal targets.  
Journal of Applied Physics, 110(2011) S.093304/1-11  
DOI:10.1063/1.3660764

An, W., Fetzer, R., Müller, G., Weisenburger, A., Engelko, V.  
In-situ diagnostics of the development of surface waviness due to treatment with an intense pulsed electron beam.  
Journal of the Korean Physical Society, 59(2011) S.3481-3484

Engelko, V., Müller, G., Rusanov, A., Markov, V., Tkachenko, K., Weisenburger, A., Kashtanov, A., Chikiryaka, A., Jianu, A.,  
Surface modification/alloying using intense pulsed electron beam as a tool for improving the corrosion resistance of steels exposed to heavy liquid metals.  
Journal of Nuclear Materials, 415(2011) S.270-275  
DOI:10.1016/j.jnucmat.2011.04.030

Gorse, D., Auger, T., Vogt, J.B., Serre, I., Weisenburger, A., Gessi, A., Agostini, P., Fazio, C., Hojna, A., DiGabriele, F., Van den Bosch, J., Coen, G., Almazouzi, A., Serrano, M.  
Influence of liquid lead and lead-bismuth eutectic on tensile, fatigue and creep properties of ferritic/martensitic and austenitic steels for transmutation systems.  
Journal of Nuclear Materials, 415(2011) S.284-292  
DOI:10.1016/j.jnucmat.2011.04.07

Van den Bosch, J., Almazouzi, A., Müller, G., Rusanov, A.  
Production and preliminary characterization of ferritic-martensitic steel T91 cladding tubes for LBE and Pb cooled nuclear systems.  
Journal of Nuclear Materials, 415(2011) S.276-283  
DOI:10.1016/j.jnucmat.2011.04.052

Weisenburger, A., Müller, G., Heinzl, A., Jianu, A., Muscher, H., Kieser, M.  
Corrosion, Al containing corrosion barriers and mechanical properties of steels foreseen as structural materials in liquid lead alloy cooled nuclear systems.  
Nuclear Engineering and Design, 241(2011) S.1329-1334  
DOI:10.1016/j.nucengdes.2010.08.005

Weisenburger, A., Schroer, C., Jianu, A., Heinzl, A., Konys, J., Steiner, H., Müller, G., Fazio, C., Gessi, A., Babayan, S., Kobzova, A., Martinelli, L., Ginestar, K., Balbaud-Celerier, F., Martin-Munoz, F.J., Soler Crespo, L.  
Long-term corrosion on T91 and AISI1316L steel in flowing lead alloy and corrosion protection barrier development: experiments and models.  
Journal of Nuclear Materials, 415(2011) S.260-269  
DOI:10.1016/j.jnucmat.2011.04.028

### **Other printed publications:**

Fazio, C., Van den Bosch, J., Munoz, F., Henry, J., Roelofs, F., Turroni, P., Mansani, L., Weisenburger, A., Gorse, D., Abella, J., Brissonneau, L., Dai, Y., Magielsen, L., Neuhasen, J., Vladimirov, P., Class, A., Jeanmart, H., Ciampichetto, A., Gerbeth, G., Wetzels, T., Karbojian, A., Litfin, K., Tarantino, M., Zanini, L.

Development and assessment of structural materials and heavy liquid metal technologies for transmutation systems (DEMETRA): highlights on major results.

Technology and Components of Accelerator-Driven Systems: Workshop Proceedings, Karlsruhe, March 15-17, 2010  
Paris: OECD/NEA, 2011 S. 81-106 (Nuclear Science)

### **Papers or lectures, which are not available in printed form:**

DelGiacco, M.

Fretting corrosion behavior of candidate materials for advanced lead alloys cooled nuclear reactor. Test equipment and first results.

Friction, Wear and Wear Protection: European Symp., Karlsruhe, October 26-28, 2011

Engelko, V., Müller, G., Rusanov, A., Markov, V., Tkachenko, K., Weisenburger, A., Kashtanov, A., Chikiryaka, A., Jinan, A. Surface modification/alloying using intense pulsed electron beam as a tool for improving the corrosion resistance of steels exposed to heavy liquid metals.

Int. DEMETRA Workshop on Development and Assessment of Structural Materials and Heavy Liquid Metal Technologies for Transmutation Systems, Berlin, March 2-4, 2010

Gorse, D., Auger, T., Vogt, J.B., Serre, I., Weisenburger, A., Gessi, A., Agostini, P., Fazio, C., Hojna, A., DiGabriele, F., Van den Bosch, J., Coen, G., Almazouzi, A., Serrano, M. Influence of liquid lead and lead-bismuth eutectic on tensile, fatigue and creep properties of ferritic/martensitic and austenitic steels for transmutation systems.

Int. DEMETRA Workshop on Development and Assessment of Structural Materials and Heavy Liquid Metal Technologies for Transmutation Systems, Berlin, March 2-4, 2010

Heinzel, A.

Aktuelle Arbeiten der Nuklearen Sicherheitsforschung am Karlsruher Institut für Technologie (KIT).  
Kolloquium zur Berufsorientierung, Deutsches Atomforum, Köln, 18. Oktober 2011

Jianu, A., Weisenburger, A., An, W., Fetzer, R., DelGiacco, M., Heinzel, A., Müller, G., Markov, V.G., Kashtanov, A.D. Improving the corrosion resistance and creep strength of steels exposed to heavy liquid metals by surface modification using pulsed E-beams.

NUCLEAR 2011: 4th Int. Conf. on Sustainable Development through Nuclear Research and Education, Pitesti, R, May 25-27, 2011

Van den Bosch, J., Almazouzi, A., Müller, G., Rusanov, A. Production and preliminary characterization of ferritic-martensitic steel T91 cladding tubes for LBE of Pb cooled nuclear systems.

Int. DEMETRA Workshop on Development and Assessment of Structural Materials and Heavy Liquid Metal Technologies for Transmutation Systems, Berlin, March 2-4, 2010

Weisenburger, A.

Structural materials in LFR.

Internat. Workshop on Liquid Metal Fast Reactors: Issues and Synergies, Aix-en-Provence, F., October 4, 2011

## **HGF Program: ENERGY (EE)**

### **Publications at cross-referenced journals:**

Hohenberger, P., Eing, C., Straessner, R., Durst, S., Frey, W., Nick, P.

Plant actin controls membrane permeability.

Biochimica et Biophysica Acta, 1808(2011) S.2304-2312  
DOI:10.1016/j.bbamem.2011.05.019

Müller, G., An, W., Berghöfer, T., DelGiacco, M., Eing, C., Fetzer, R., Flickinger, B., Frey, W., Giese, H., Göttel, M., Gusbeth, C., Heinzel, A., Hoppe, P., Jianu, A., Lang, F., Leber, K., Sack, M., Schumacher, G., Singer, J., Straessner, R., Wegner, L., Weisenburger, A., Zimmermann, F., Engelko, V.

Progress in high power-particle beams and pulsed power applications at Karlsruhe Institute of Technology.  
Journal of the Korean Physical Society, 59(2011) S.3588-3593

Sack, M., Stängle, R., Müller, G.

Over-voltage trigger device for Marx generators.  
Journal of the Korean Physical Society, 59(2011) S.3602-3607

Wegner, L.H., Flickinger, B., Eing, C., Berghöfer, T., Hohenberger, P., Frey, W., Nick, P.

A patch clamp study on the electro-permeabilization of higher plant cells: Supra-physiological voltages induce a high-conductance, K<sup>+</sup> selective state of the plasma membrane.  
Biochimica et Biophysica Acta, 1808 (2011) S. 1728-1736  
DOI:10.1016/j.bbamem.2011.01.016

Wegner, L.H., Stefano, G., Shabala, L., Rossi, M., Mancuso, S., Shabala, S.

Sequential depolarization of root cortical and stelar cells induced by an acute salt shock – implications for Na<sup>+</sup> and K<sup>+</sup> transport into xylem vessels.

Plant, Cell and Environment, 34(2011) S.859-869  
DOI:10.1111/j.1365-3040.2011.02291.x

### **Other printed publications:**

Thumm, M. [Hrsg.]

Annual report 2010 Institute for Pulsed Power and Microwave Technology  
KIT Scientific Reports, KIT-SR 7590 (Juli 2011)

### **Papers or lectures, which are not available in printed form:**

Attmann, F., Sack, M., Müller, G.

Experiments for reducing the jitter of an over-voltage triggered spark gap.

18<sup>th</sup> Int. Pulsed Power Conference, Chicago, Ill, June 19-23, 2011. Book of Abstracts publ. online S.87

Frey, W., Flickinger, B., Berghöfer, T., Eing, C., Liu, Q., Nick, P.

Electropermeabilization versus nsPEF-simulation – pulsed electric fields can stimulate the growth of plants and fungi.

10<sup>th</sup> Int. Conf. of the European Bioelectromagnetic Association, Roma, I, February 21-24, 2011

Frey, W.

Konditionierung von Algen mit gepulsten elektrischen Feldern für die energetische Nutzung.

5. Kolloquium Sustainable BioEconomy, KIT, Karlsruhe, 1.-2. Dezember 2011

Göttel, M., Eing, C., Gusbeth, C., Frey, W.  
Outflow of intracellular compounds from microalgae after pulsed electric field treatment.  
19<sup>th</sup> European Biomass Conf. and Exhibition, Berlin, June 6-10, 2011

Göttel, M., Eing, C., Gusbeth, C., Frey, W.  
Pulsed electric field treatment of microalgae for cell ingredients extraction.  
1<sup>st</sup> European Congress of Applied Biotechnology together with 29<sup>th</sup> DECHEMA's Biotechnology Annual Meeting, Berlin, September 25-29, 2011

Gusbeth, C., Eing, C., Sträßner, R., Göttel, M., Frey, W.  
Microalgae to energy. Conditioning of microalgae by pulsed electric fields (PEF).  
2011 Int. Bioelectrics Symposium, Toulouse, F., May 4-6, 2011

Müller, G.  
Pulsed power applications at Karlsruhe Institute of Technology (KIT).  
Pulsed Power Symposium 2011, Loughborough, GB, September 20, 2011

Müller, G., An, W., Berghöfer, T., DelGiaccio, M., Eing, C., Fetzer, R., Flickinger, B., Frey, W., Giese, H., Göttel, M., Gusbeth, C., Heinzl, A., Hoppe, P., Jianu, A., Lang, F., Leber, K., Sack, M., Schumacher, G., Singer, S.J., Straessner, R., Wenger, L., Weisenburger, A., Zimmermann, F., Engelko, V.  
Status and recent progress in pulsed power applications at Karlsruhe Institute of Technology.  
18<sup>th</sup> Int. Pulsed Power Conference, Chicago, Ill, June 19-23, 2011. Book of Abstracts publ. online S.75

Sack, M., Sigler, J., Schmidt, O., Stukenbrock, L., Schick, A., Müller, G.  
Comparison of phenolic extraction from grape mash and impedance measurements.  
Nonthermal Processing Division Workshop 2011, Osnabrück, October 12-14, 2011

Sack, M., Müller, G.  
Modular trigger generator for over-voltage triggering of Marx generators.  
18<sup>th</sup> Int. Pulsed Power Conference, Chicago, Ill., June 19-23, 2011. Book of Abstracts publ. online S.88

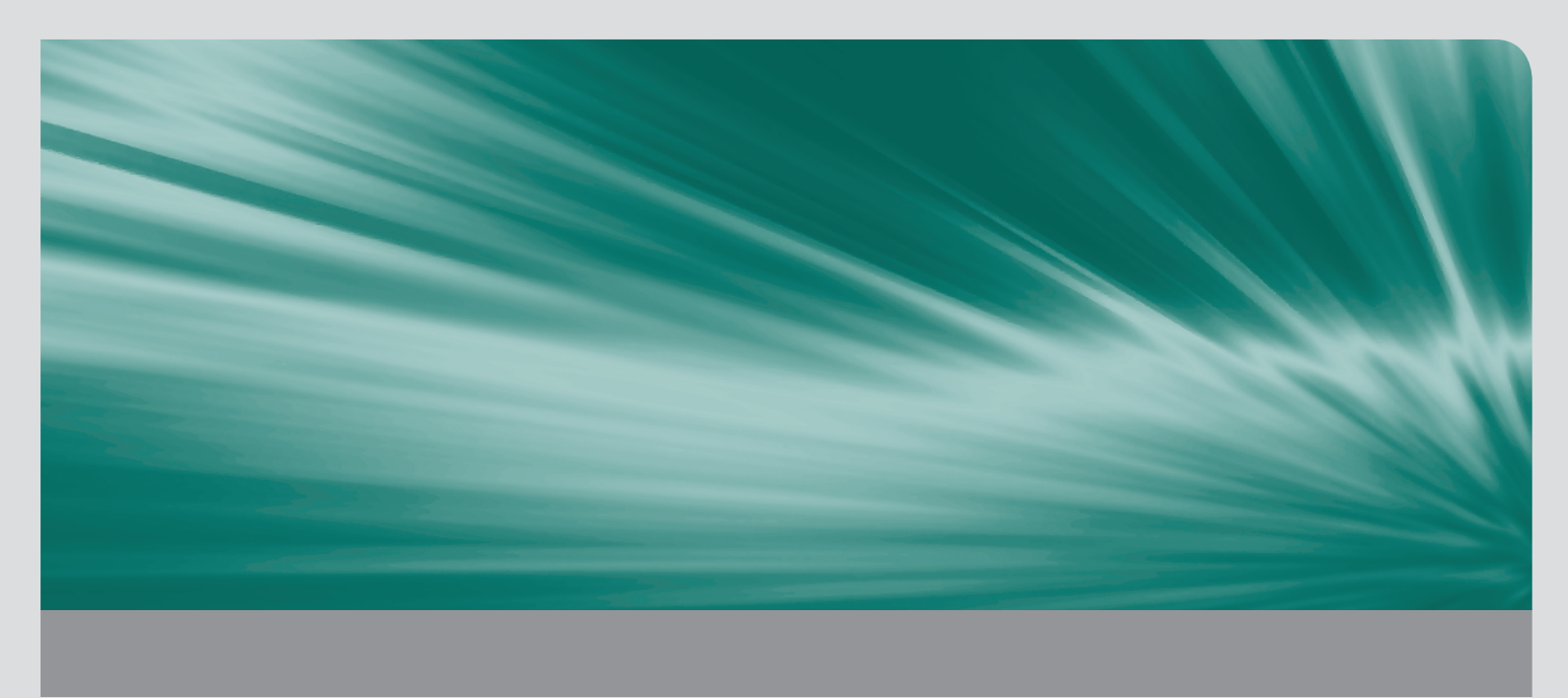
Wegner, L.H., Flickinger, b., Eing, C., Berghöfer, T., Hohenberger, P., Frey, W., Nick, P.  
Supra-physiological voltages induce a K<sup>+</sup> selective state of the plasma membrane: a patch clamp study.  
2011 Int. Bioelectrics Symposium, Toulouse, F., May 4-6, 2011

## HGF-Program: Efficient Energy Use and Conversion (REUN)

### *Papers or lectures, which are not available in printed form:*

Link, G.  
Mikrowellen und deren Potential in der Materialprozesstechnik.  
Symp. 'Mikrowellen zur thermischen Behandlung von Faserverbundwerkstoffen', Reiskirchen-Lindenstruth, 4. Mai 2011

Prastiyanto, D., Link, G., Thumm, M.  
Dielectric measurements using transmission line method and different sample geometries in a WR340 standard waveguide.  
Advances in Modeling of Microwave Sintering: 13<sup>th</sup> Seminar Computer Modeling in Microwave Engineering and Applications, Thun, CH, March 7-8, 2011



The Institute for Pulsed Power and Microwave Technology (IHM) is doing research in the areas of pulsed power technologies for material processing and biological applications as well as microwave technologies for plasma heating and material processing. It is doing research, development, academic education, and, in collaboration with the KIT Division IMA and industrial partners, the technology transfer. Projects have been conducted within six HGF Programs: Renewable Energies (EE), FUSION, NUKLEAR, NANOMIKRO, Efficient Energy Conversion and Use (REUN) and Technology-Innovation and Society (TIG).

R&D work has been done in the following topics: fundamental theoretical and experimental research on the generation of intense electron beams, strong electromagnetic fields and their interaction with plants, materials and plasmas; application of these methods in the areas of generation of energy through controlled thermonuclear fusion in magnetically confined plasmas, in materials processing and in energy technology. Research in both divisions of the IHM require the application of modern electron beam optics, high voltage technology and high voltage measurement techniques.

By October 2011, Prof. Dr.-Ing. John Jelonnek started as new appointed Director of IHM and Professor for High-Power Microwaves at the Institute of High Frequency Techniques and Electronics in the Faculty of Electrical Engineering and Information Technology of KIT.

At the 3rd Euro-Asian Pulsed Power Conference (EAPPC), Dr. Georg Müller, Deputy Director of IHM, has been elected for the International Organizing Committee. He will be the General Chair of the next EAPPC at Karlsruhe in 2012. The EAPPC 2012 conference will be in combination with the 19th International Conference on High-Power Particle Beams (BEAMS). Preparation of that conference started in 2011 with high importance.

Prof. Manfred Thumm received "EPS Plasma Physics Innovation Prize 2011" for his outstanding contributions to the realization of high power gyrotrons for multi-megawatt long-pulse electron cyclotron heating and current drive in magnetic confinement nuclear plasma devices.

The list of 172 publications in 2011 is enclosed at the end of this report.